Optimal Management of Flexible Resources in Multi-Energy Systems

Xi, Yufei

DOI (link to publication from Publisher):
10.54337/aau460285470

Publication date:
2021

Document Version
Publisher's PDF, also known as Version of record

OPTIMAL MANAGEMENT OF FLEXIBLE RESOURCES IN MULTI-ENERGY SYSTEMS

BY
YUFEI XI

DISSERTATION SUBMITTED 2021

AALBORG UNIVERSITY
DENMARK

Optimal Management of Flexible Resources in Multi-Energy Systems

Ph.D. Dissertation

Yufei Xi

Dissertation submitted October 13, 2021

Dissertation submitted: October 13, 2021

PhD supervisor: Prof. Zhe Chen
Aalborg University

Assistant PhD supervisor: Prof. Henrik Lund
Aalborg University

PhD committee: Associate Professor Mads Pagh Nielsen
Aalborg University

Professor Olav Bjarte Fosso
Norwegian University of Science and Technology

Professor Zita Maria Almeida do Vale
Polytechnic of Porto – School of Engineering

PhD Series: Faculty of Engineering and Science, Aalborg University

Department: Department of Energy Technology

ISSN (online): 2446-1636
ISBN (online): 978-87-7573-995-0

Published by:
Aalborg University Press
Kroghstræde 3
DK – 9220 Aalborg Ø
Phone: +45 99407140
aauf@forlag.aau.dk
forlag.aau.dk

Printed in Denmark by Rosendahls, 2021

CV

Yufei Xi was born in China. She received the B.S., M.S. degrees in electrical engineering from Northeast Electric Power University (NEEPU), Jinlin, China, in 2015 and 2018, respectively.

She is currently a Ph. D. student at the Department of Energy Technology, Aalborg University (AAU), Aalborg, Denmark. Her research focuses on energy integration and energy markets, specifically on the integration and optimization of flexible resources from a market perspective. Her Ph.D. project is supported by China Scholarship Council (CSC) and based on the Energy Technology Development and Demonstration Program 'Sustainable Energy Market Integration (SEMI)' (EUDP17-I: 12554).

Abstract

Climate change and the depletion of fossil fuel resources encourage the deployment of variable renewable energy sources, where the energy market is experiencing a profound transition. Accordingly, flexibility has been especially prized in the multi-energy system (MES) with higher penetration of renewable energy (e.g., solar and wind). In recent years, several measures have been implemented to increase flexibility in supply and demand such as storage installation and energy integration. Meanwhile, the optimal management issues of flexible resources (FRs) should be discussed and addressed.

From technical and economic perspectives, considering the interaction between system operation and market procedures is the key to research. On the one hand, the integration of energy networks brings broader development potential for FRs, as well as uncertainty and complexity in integrated operations. On the other hand, the liberalization of the market enables the market outcome closely related to the system operation, which means that the factors such as energy prices must be considered in the decision-making for the optimal management of FRs. Therefore, this Ph.D. project focuses on rationally utilizing and dispatching various FRs, as well as discusses solutions to provide the operation of the MES in an efficient and economical way.

Firstly, various FRs in MESs have been identified and studied including the investigation of their characteristics and mathematical models. They have been appropriately combined and used in the integrated gas, electricity and district heating system. This part lays the foundation for the subsequent optimization of the operation and management of FRs.

Secondly, this thesis has contributed to the aspect of quantifying FRs. A multi-objective optimization model for coordinating the operation of FRs has been proposed. The model allows the MES to intelligently select and employ FRs based on day-ahead market price signals. An illustrative case has been simulated to demonstrate the potential of the proposed strategy in improving social welfare and reducing the curtailment of renewable energy.

In terms of market design, the mutual influence of the real-time market and system operation has been further considered. Throughout the project, two solutions to optimize the MES with FRs according to the different market modes have been proposed:

- In the case of centralized operation and management of the MES, a bi-level programming model for integrating flexible demand has been developed. In this model, an integrated gas, electricity and district heating system with aggregated smart buildings is described. These smart buildings use photovoltaic power generation, electric vehicles with storage, electric heating and other technologies, and they are managed and operated by the aggregator considering real-time energy prices.
- Taking into account the limited communication with existing energy operators, an equilibrium model for optimally scheduling the MES with FRs has been developed. In this model, each energy subsystem has an independent operator to pursues its maximum benefits and coordinates with each other for a satisfying equilibrium.

The effectiveness of the models has been demonstrated in their corresponding illustrative cases. Meanwhile, the proposed models can optimally allocate the resources and reflect the price and quantity of the energy transaction in the MES.

Furthermore, the impact of the coordination and optimization of FRs on the MES, specifically the demand response (DR) participation level, is also analyzed in this project. The simulation results show that: 1) The MES's social welfare and wind power curtailment are greatly improved as the number of coordinated FRs is increased; 2) The Bi-directional feedback between the consumption of power systems and the real-time electricity prices of the market achieved by DR management has positive impacts on both system and market, such as improving abnormal peak-prices and reducing the investment for the storage capacity.

Dansk Resumé

Klimaændringer og udtømning af fossile brændstofressourcer har tilskyndet til indførelse af variable vedvarende energikilder, og energimarkedet gennemgår en gennemgribende forandring. Som følge heraf er fleksibilitet særlig vigtig i multienergisystemer med højere gennemtrængelighed fra vedvarende energikilder som sol og vind. I de senere år er der gennemført en række foranstaltninger for at øge fleksibiliteten i udbud og efterspørgsel, såsom lagringsanlæg og energiintegration. Samtidig bør problemet med optimal forvaltning af fleksible ressourcer drøftes og løses.

Ud fra et teknisk og økonomisk synspunkt er det vigtigt for forskningen at overveje samspillet mellem systemdrift og markedsprocedurer. På den ene side har integrationen af energinettene skabt et bredere potentiale for fleksible ressourcer, men også skabt usikkerhed og kompleksitet i integrerede operationer. På den anden side gør markedsåbningen markedsresultaterne tæt forbundet med systemdrift, hvilket betyder, at energipriser og andre faktorer skal overvejes i beslutningstagningen for at opnå optimal forvaltning af fleksible ressourcer. Derfor fokuserer dette Ph.D.-projekt på at rationalisere brugen og planlægningen af fleksible ressourcer og diskutere løsninger til at levere multienergisystemer til at fungere effektivt og omkostningseffektivt.

For det første er forskellige fleksible ressourcer i flerenergisystemer blevet identificeret og undersøgt, herunder undersøgelsen af deres egenskaber og matematiske modeller. De kombineres korrekt og anvendes i integrerede gas-, el- og regionalvarmeanlæg. Denne del lægger grunden til den efterfølgende optimering af drift og styring af fleksible ressourcer.

For det andet bidrager dette dokument til kvantificeringen af fleksible ressourcer. Der foreslås en multimålsoptimeringsmodel til koordinering af fleksible ressourceoperationer. Modellen gør det muligt for multienergisystemer intelligent at vælge og bruge fleksible ressourcer baseret på de seneste markedsprissignaler. Et illustrativt tilfælde blev simuleret for at demonstrere potentialet i den foreslåede strategi med hensyn til at forbedre den sociale velfærd og reducere reduktionen af vedvarende energi.

I markedsdesignet overvejes samspillet mellem realtidsmarked og systemdrift yderligere. Gennem hele projektet blev der foreslået to løsninger

til optimering af flerenergisystemer ved hjælp af fleksible ressourcer baseret på forskellige markedsmodeller:

• Der er udviklet en todelt programmeringsmodel med integrerede fleksible krav med centraliseret drift og styring af multienergisystemer. I denne model beskrives integrerede gas-, el- og regionalvarmeanlæg med aggregerede intelligente bygninger. Disse intelligente bygninger bruger teknologier som fotovoltaisk elproduktion, energilagring af elbiler og elvarme og styres og drives af nyhedslæsere baseret på energipriser i realtid.

• Under hensyntagen til begrænset kommunikation med eksisterende energioperatører er der udviklet en afbalanceret model for at optimere planlægningen af multienergisystemer med fleksible ressourcer. I denne model har hvert delsystem for energi en separat operatør til at forfølge sine bedste interesser og koordinere med hinanden for at opnå en tilfredsstillende balance.

Modellens gyldighed er blevet påvist i de tilsvarende illustrative tilfælde. Samtidig kan den foreslåede model optimere ressourceallokeringen og afspejle prisen og mængden af energitransaktioner i flerenergisystemer.

Under hensyntagen til begrænset kommunikation med eksisterende energioperatører er der udviklet en afbalanceret model for at optimere planlægningen af multienergisystemer med fleksible ressourcer. I denne model har hvert delsystem for energi en separat operatør til at forfølge sine bedste interesser og koordinere med hinanden for at opnå en tilfredsstillende balance..

Preface

The work reported in this dissertation is an outcome summary of the Ph.D. project "Optimal Management of Flexible Resources in Multi-Energy Systems", which was carried out at the Department of Energy Technology, Aalborg University, Denmark. This Ph.D. project is supported by China Scholarship Council and relies on the Energy Technology Development and Demonstration Program 'Sustainable Energy Market Integration (SEMI)' (EUDP17-I: 12554) through the assistance of the Danish engineering company Rambøll and Danish Gas Technology Centre. The authors are very grateful for the above-mentioned institutions.

First, Professor Zhe Chen, my supervisor, deserves my sincere appreciation for his tireless guidance, kindness, and patience during the study. He and his wife are such amiable people that they have left me beautiful memories and made me feel the family warmth. I would also like to thank my co-supervisor Professor Henrik Lund for his guidance and help during the entire period of the Ph.D. project. It has been a great experience to work under your supervision. I am also grateful to Professor Thomas Hamacher for providing me an opportunity to visit the Technical University of Munich, Germany during my study abroad and broaden my knowledge in combined smart energy systems. Furthermore, special thanks go to all my colleagues and secretaries at Aalborg University for their dependable support and fruitful discussion.

Secondly, my thanks would go to my beloved family and friends for their encouragement, care and confidence in me all through three years. Their support and company have been the main drivers for me to complete the Ph.D. study.

Finally yet importantly, I would like to extend my deepest gratitude towards my dear motherland who is friendly, peaceful and growing stronger. I sincerely hope that more and more people will enjoy the Chinese beautiful culture and magnificent landscape.

Yufei Xi
Aalborg University, August 15, 2021

Contents

Table of Figures

Table of Tables

List of Acronyms & Abbreviations

AC/DC	**Alternating current/Direct current**
ADN	Active distribution network
ASM	Ancillary service market
BIM	Bilateral monopoly
CAES	Compressed air energy storage
CFCT	Constant flow constant temperature
CFP	Coal-fired power
CFVT	Constant flow variable temperature
CHP	Combined heat and power
CM	Capacity market
CO	Centralized optimization
COP	Coefficient of performance
COSES	Combined smart energy system
CPP	Critical peak pricing
DB	Demand bidding
DH	District heating
DLC	Direct load control
DR	Demand response
DSM	Demand side management
EB	Electric boiler
EDR	Emergency demand response
EO	Equilibrium optimization
EPEC	Equilibrium problem with equilibrium constraints
EV	Electric vehicle
FR	Flexible resource
GB	Gas boiler
GFCHP	Gas-fired combined heat and power
GN	Gas node
GOG	Gas-on-gas competition

GS	Gas storage
GS	Gas subsystem
HN	Heat node
HP	Heat pump
HS	Heat storage
HVAC	Ventilation, and air conditioning
I/C	Interruptible/curtailable
IGU	International Natural Gas Union
IRRE	Insufficient ramping resource expectation
ISO	Independent system operator
KKT	Karush–Kuhn–Tucker
LBNL	Lawrence Berkeley National Laboratory
LNG	Liquefied natural gas
LPF	Load participation factor
MEPC	Mathematical programs with equilibrium constraints
MES	Multi-energy system
NET	Netback from the final product
NLP	Non-linear programming
OPE	Oil price escalation
P2G	Power to gas
P2H	Power to heat
PL	Power load
PS	Power subsystem
PV	Photovoltaics
RTP	Real-time pricing
SMES	Superconducting magnetic energy storage
SN	Source node
SOC	State of charge
SW	Social welfare
TOU	Time-of-use

V2G	Vehicle-to-grid
VFCT	Variable flow constant temperature
VFVT	Variable flow and variable temperature
VPP	Virtual power plant
WC	Wind curtailment
WT	Wind turbine

Chapter 1

Introduction

1.1. Background

With the increase in cost efficiency and competitiveness, renewable energy technologies have gradually become important producers to modern electricity demand instead of conventional power plants [1]. In terms of the Danish Energy Agency's statistics [2, 3], Fig 1.1 and Fig 1.2. show the gross energy consumption in Demark as of 2020 and the pie chart of the Danish electricity production by energy sources in 2020, respectively. It can be seen that renewable energy generation even accounts for 81% of the Danish electricity production in 2020, in which 60% of total electricity production is generated by wind and solar power. Therefore, electricity production from renewable energy may well be higher in real situations. The data reflects several typical trends in the future power system:

- Large central power plants are gradually decommissioned, mothballed, or converted to biomass power plants with reduced power capacity.
- Wind farms and photovoltaics (PV) gradually replace conventional power plants.
- Heat pumps and electric boilers increase to enable more flexible electricity consumption.
- The electrification of the transportation sector is in urgent need of development

At the same time, emerging information technology and power electronics technology have enabled power system operators to track changes in demand and control flows of power in time. In order to integrate more renewable resources in an efficient and economical way, power system operators must establish a flexible and adaptable grid to balance supply and demand. In brief, they must strive to develop, use, and optimize flexible resources (FRs).

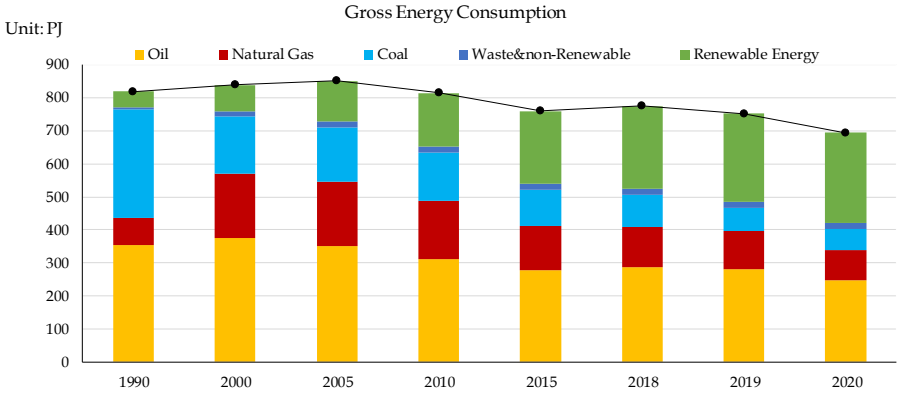

Fig. 1.1: Gross Energy Consumption in Denmark as of 2020. Source: [3]

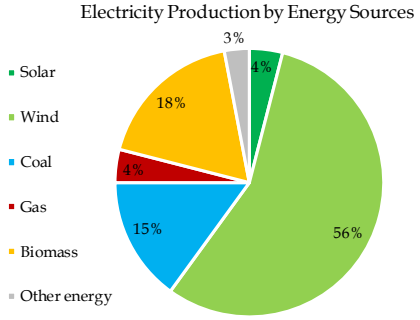

Fig. 1.2: Danish electricity production by energy sources in 2020. Source: [2]

FR is a conceptual generalization that represents those available measures for enhancing the energy system's flexibility. In the power system, the capacity of a system to adapt to variations in net demand is defined as flexibility [4, 5]. It is also considered a system facility to overcome uncertainties and maintain reliability [6]. In recent years, most studies have extensively investigated and developed the FRs of power systems, which consist of mainly two types: 1) Physical FR, which has the physical capacity to respond to the changes in supply and demand. They are required, but not sufficient, for the power system to operate in a flexible manner; 2) Structural FR, which may use proper operational approaches and market procedures to choose and combine physical FRs. More specifically, the physical FR is a technology or a certain device, while the structural FR is the mean of using those technologies and the mode of operating those devices. In the current research, there have been some popular flexibility concepts proposed in the power system, which can be described in Fig. 1.3.

Concept	Physical FR	Structural FR
• Flexible conventional units	✡	
• Power storage	✡	
• Inverter-based auxiliary services	✡	✡
• Demand response	✡	✡
• Interconnection networks	✡	✡
• Advanced market mechanism		✡
• Smart grid		✡

Fig. 1.3: Flexible resources of the power system.

- Conventional units with quick startup and high ramp capabilities, such as reciprocating engine or combustion turbine.
- Power storage, such as pumped hydroelectric storage, batteries and electric vehicles (EVs).
- Inverter-based auxiliary services: Better control of variable energy resources including disturbance ride-through [7], inertial response [8, 9], frequency regulation [10, 11], reactive and voltage support [12, 13] and business reserve [14, 15], etc.
- Demand response (DR): Adjustment in the power consumption of customers to better match for electricity supply.
- Interconnection networks: A physical connection among power grids in nearby areas or cross borders to increase access to energy production and demand.
- Advanced market mechanism: A market design with perfect competition, high frequency, and information sharing.
- Smart grid: An integration operation of advanced metering infrastructure, DR, power storage, distributed renewable energy generation and intelligent control and distribution.

From a technical perspective, FRs compensate for the deviation between uncertainty and electricity demand. From an economic perspective, the utilization of FRs requires additional investment and charges. Thus, for the power system, the essence of optimal management of FRs is seeking the satisfying compromise between flexibility and cost.

While for the multi-energy system (MES), the combination of different energy systems further expands the diversity and coverage of FRs. On the one hand, the integrated gas, heat, and electricity system allows energy conversion via conversion technologies, such as power-gas (P2G), combined heat and power (CHP) units and heat pumps, etc.), to increase the diversity and flexibility of

energy supply options. On the other hand, the flexibility provided by FRs is no longer confined to the single energy system to which they belong, but can be accessed by other energy systems. For example, in an integrated heat-electricity system, heat can be provided by using heat pumps or electric boilers to consumer surplus electricity. The thermal system can be regarded as a storage system of the power system, whereby the power system will benefit from the flexibility provided by those FRs installed in the thermal system. Therefore, the integration and optimization of FRs in MESs are also facing technical and economic challenges.

1.1.1. Integration of energy systems

The integration of FRs is achieved through the integration of energy systems (electricity, gas and heating/cooling, etc.). Fig. 1.4 shows the simplified scheme of integrated gas, electricity, district heating/cooling systems including the energy flows, supply infrastructure and its corresponding participants. The coupled energy systems aim at unified modeling. The connection between multiple energy systems is completed by different energy conversion technologies. For consistency reasons, these technologies shall be summarized as gas-to-power (gas-fired power plants), gas-to-heat (gas boilers), gas-to-power and heat (gas-fired CHP plants), power-to-gas (P2G units) and power-to-heat/cooling (heat pumps and electric boilers/air conditioning), respectively. Both power-to-gas and power-to-heat technologies have been verified in studies, that they contribute to the accommodation and increase in renewable energy power generation in the future [16-20]. From the modeling perspective, the main challenge of integration is the difference between different energy systems caused by the characteristics of different energy carriers.

First, there are some differences between electricity, heating and gas infrastructure. To a certain extent, energy can be stored in pipelines of heating and gas systems, whereas there is almost no capacity available for energy storage in power transmission lines. As a result, demand and supply in the power system must be equal at all times, which should be considered in the modeling. Moreover, power systems in cities and even in countries are not isolated. In contrast, heating systems usually supply an urban or a district. The heat is supplied by local (combined) heat (and power) plants according to local demand. The gas production is affected by the local resources (biogas and hydrogen supply), and sometimes is highly dependent on market trade (imports from other countries). Thus, heating and gas systems can be modeled with mass transfer and local sources and sinks.

Second, there are also differences between the changes in demand for electricity, heating and gas systems. The physical characteristics of different energy carriers lead to different transfer processes in time and space. These differences will be reflected on the demand sides, such as the inertia of the thermal buildings [21-22]. More specifically, in the power system, changes in demand are instant and obvious, while changes in demand in heating and gas systems take a certain time to be noticed because the water flow is relatively slow and gas is compressible. Therefore, the integrated model of the multi-energy system needs to consider these different time constants and energy losses.

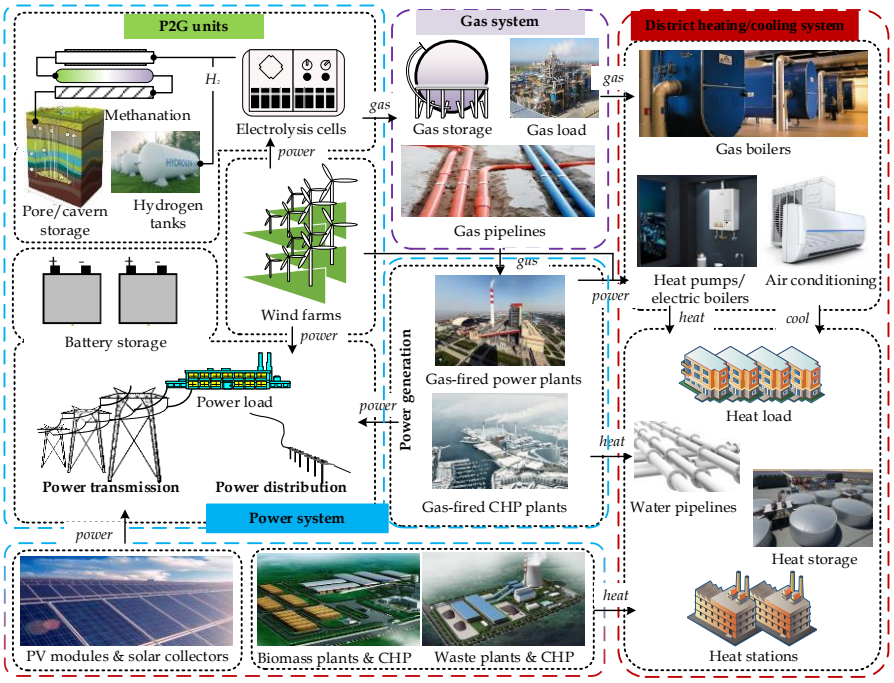

Fig. 1.4: Scheme of integrated gas, electricity, district heating systems including their corresponding producers, consumers, and storage systems. Source: [C3].

Facing these issues, the finite element method [23], the nodal method [24] and the function method [25] have been successively proposed to simulate the temperature dynamics, time delay and heat loss in the district heating network. The coupled time constraint is formulated as a charging and discharging process to represent the storage effect of the heating pipeline [26]. Based on the time-varying network theory, the heat-electricity analogy method has been proposed in [27], in which the dissipation, inertia and elasticity phenomena of heat transfer were equivalent to resistive elements by

the lumped parameter method. It is worth noting that, different from the above physical models, there was a black-box method introduced in [28], where the internal topology of the heating network was ignored and only the law of transformation between input and output was emphasized. However, this method needs to test multiple times, and it is only effective in a specific test system.

On the other hand, the Navier-Stokes equation, material-balance equation and state equation have been used to describe the pressure-driven gas dynamics and time delay along the gas pipeline [29, 30]. The steady-state model of the gas flow has been proposed in [31]. The gas system, as previously stated, requires a response time in order to restore a new steady-state. In practice, the gas system may always be in a transient-state, because the gas demand changes over time. Considering that, An integrated model combining the transient gas flow and steady power flow has been proposed, in which the linepack reflects the storage effect of the gas pipeline [32]. The above modeling is mostly applied to integrated electricity-heat and electricity-gas systems. In contrast, the unified model for the integrated gas-electricity-heat system is rarely discussed. Therefore, in order to ensure the accurate deployment and rational scheduling of FRs, the modeling of MES is required.

1.1.2. Liberalization of energy markets

In order to efficiently and economically use and allocate FRs, the coordinated operation of FRs across multiple energy systems needs to be addressed. The corresponding system operator is required to be able to intelligently access, allocate and operate its FRs to balance supply and demand and adapt to grid-connected renewable energy changes.

An open and liberalized market environment is the basis for the coordination and deployment of FRs. In the past, energy supply was a natural monopoly, including production, transmission, distribution, and trading. The so-called 'liberalization' separates these components, designs corresponding regulation schemes for activities that have to be retained by monopolies (such as transmission and distribution), and creates a competitive market for energy trading [33]. This is friendly enough for new energy suppliers to enter the market. The liberalization of energy markets provides a competitive environment that allows reducing energy prices and improving the quality of services.

The liberalization of the electricity market has been widely discussed in [34-36]. Meanwhile, countries around the world have never stopped reforming their natural gas markets. According to the annual survey report of the

International Natural Gas Union (IGU) on the evolution of global natural gas pricing mechanisms, the natural gas pricing mechanism is changing from 'regulated pricing' to 'market-based pricing' [37]. Here, the regulated gas price (covering the cost of service) is determined and approved by the regulatory agency. In the regulated pricing mechanism, some gas prices are fixed as subsidies below the average costs of producing and delivering, or the gas is supplied free as a by-product of chemical feedstock or oil refining. The market-based pricing mainly includes oil price escalation (OPE), gas-on-gas competition (GOG), bilateral monopoly (BIM) and netback from the final product (NET) [37].

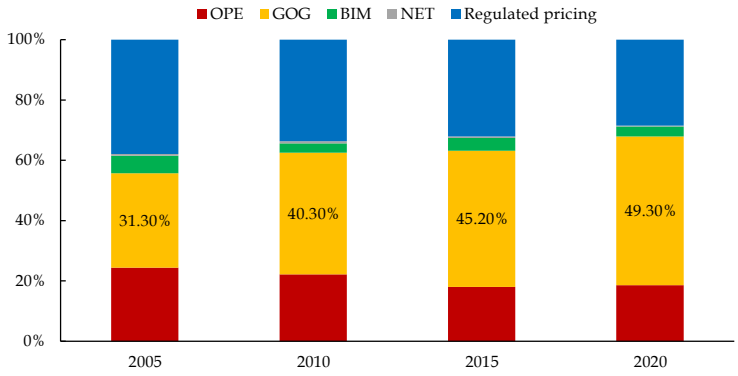

Source: IGU (2021), Wholesale Gas Price Survey 2021 Edition.

Fig. 1.5: Pricing formation for world gas consumption (2005 - 2010).

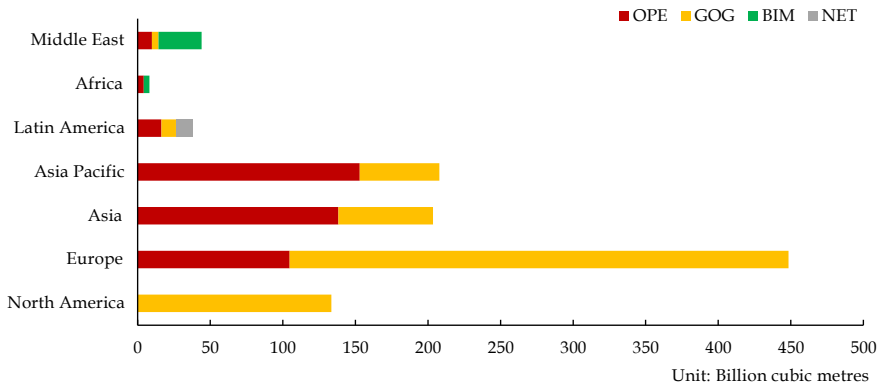

Source: IGU (2021), Wholesale Gas Price Survey 2021 Edition.

Fig. 1.6: total gas imports for market pricing mechanisms by regions in 2020.

Fig. 1.5 shows the pricing formation for world gas consumption (2005 - 2010), in which the proportion of GOG consumption in global gas consumption increases from 31.3% in 2005 to 49.3% in 2020. Fig. 1.6 shows total gas imports for market pricing mechanisms by regions in 2020. It can be seen that except for Africa and the Middle East, the GOG pricing mechanism occupies an important share of the gas market in various countries. North America even fully adopts GOG pricing. These trends shows that the gas price might depend more on the interaction of supply and demand, especially in Europe and North America. Although not all gas can be traded at a fixed price in a short-term (daily), real-time pricing might be implemented in the future, such as in the peer-to-peer market.

The liberalization of the electricity and gas markets enables FRs to be unlocked in a cost-effective way. Because the price signals they provide can incentive their system operators to make the corresponding positive actions, thereby increasing the flexibility of the system and pursuing maximum benefits.

1.1.3. Optimization of the MES with FRs

Using a large number of FRs has brought challenges to the operation of the MES and its market. From the perspective of system operation, it is necessary to promote the management of multiple FRs in the MES, reduce the operational burden and improve the efficiency of the overall system. From the perspective of the market operation, the market participants are reluctant to exploit and deploy those FRs which have high costs. Therefore, the stimulus market mechanism to attract investors and encourage the participation of FRs is demanded.

In the existing academic literature, the research subjects of the MES can be categorized into: 1) system operators or managers, including independent system operators, integrated system operators, resource aggregators, etc.; 2) market participants, including network operators, virtual power plants (VPPs), distributed generations, storage suppliers, load aggregators, and even grid-connected microgrids [38-40]. Fig. 1.7 shows the coordination process of system operation and market procedures. Market participants need to submit their integrated external features to the system operator, such as cost functions, operation constraints, conversion efficiencies, network parameters, etc.) Then, the system operator calculates the optimal operational decision and transmits the dispatch commands to the market participants taking into account the network loss and bid outcomes [39]. However, there will be conflicts of interest when the different energy systems with FRs have different owners or operators. Considering various FR models and their economic

objectives and operational constraints in different energy systems is very important for formulating the optimal strategy of the MES. In order to improve the overall economic performance of the MES, the market operator promotes the participation of FRs through appropriate energy pricing. As a result, it is necessary to build collaborative optimization models of the MES with FRs.

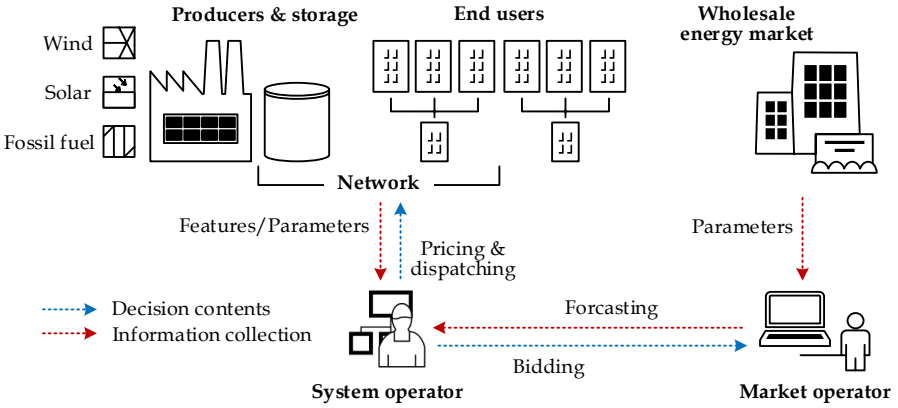

Fig. 1.7: Coordination process of system operation and market procedures.

Generally, different optimization levels can be considered in terms of the application scenarios and the research subjects of the formulated problems. This makes collaborative optimization problems mainly have two types: 1) If the upper-level problem describes the market participation while the lower-level problem represents the system operation, a multi-leader-follower optimization model will be formed as illustrated in [41-45]. Essentially, this type of optimization problem is a competitive game. The resulting model focuses on solving the cooperative bidding and transaction management among multiple market participants until reaching a Nash equilibrium that all participants in the system are satisfied. 2) If the upper-level problem describes the system operation whereas lower-level problem considers the market paricipation, a one-leader and multi-follower optimization model will be formed as demonstrated in [46-50]. This type of model focuses on solving the optimal pricing between system operations and market procedures, which aims at encouraging FRs at the lower-level to deliver services on their own initiative and improving the economic effectiveness of the MES.

In summary, there are still several pressing issues to be addressed: 1) Market procedures should be considered in order to promote the participation of FRs by acceptable transaction prices; 2) To ensure the economic operation of the

MES, the coordination among the bidding plan, the scheduling of controllable resources and the market pricing needs to be analyzed; 3) For different scenarios, the collaborative optimization models of the MES with FRs need to be developed and proposed as well as the corresponding solutions and optimal strategies. Therefore, in combination with market procedures, addressing the optimal management of the MES with FRs is of great significance for maintaining flexible and efficient system operation and improving overall economic benefits.

1.2. Project Motivation

As mentioned above, several problems still need to be overcome in order to fully use FRs to achieve a flexible, efficient and economical MES to accommodate more renewable energy. The research activities of this Ph.D. project are summarized in Fig. 1.8.

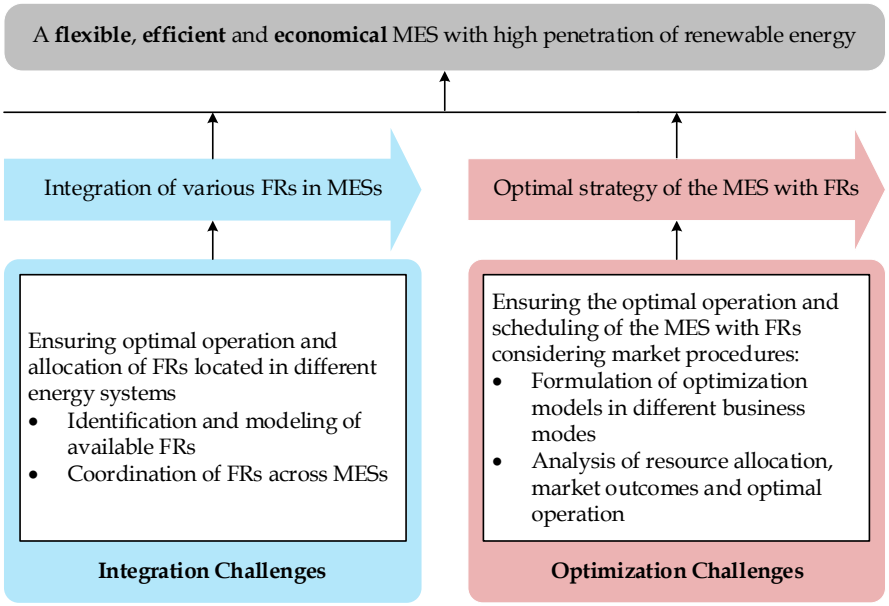

Fig. 1.8: Research activities in the Ph.D. project: Optimal Management of Flexible Resources in Multi-Energy Systems.

From the technical perspective, the integration of various FRs in MESs to ensure optimal operation and allocation of FRs in different energy systems is the primary issue of research. This includes the identification and modeling of available FRs in the MES and the coordination of FRs across multiple energy systems. Different FRs located in different energy systems need to be

properly allocated and utilized to cope with the changes in supply and demand because of the fluctuation of renewable energy. Thus, the unified modeling of the MES is firstly required, where the differences between different energy systems in terms of infrastructure and supply and demand must be considered. Then, system operators must consider economic costs to ensure optimal operation of various FRs and maintain a balance between supply and demand. This puts forward a demand for the model formulation of the coordinated operation of FRs in the MES. The integration and coordination of FRs lay the foundation for the subsequent research on the collaborative operation and optimal dispatch of the MES.

From the economical perspective, the optimal strategy of the MES with FRs is important for ensuring the economic cost and optimal allocation of resources, where the impact of market procedures cannot be ignored. In order to encourage the economic operation of FRs, each system operator is obliged to issue dispatching commands to its own controllable resources by considering its market bidding. Hence, analyzing the interaction among optimal operation of FRs, market outcomes (energy pricing) and the dispatch of controllable resources are demanded. Generally, one business mode is that there is an entity, the integrated system operator is responsible for collaborating and operating the centralized scheduling model to optimize the entire MES. The other business mode is that each energy system and its corresponding FRs have their own system operator. They operate their controllable resources to pursue their own profits in the market environment, which leads to a competitive game. As a result, the optimal strategies according to different business modes are demanded to promote the utilization of FRs and improve the overall economic benefit of the MES. Particularly, different business modes lead to different collaborative optimization problems.

1.3. State of Art

Energy systems require flexibility in order to maintain the balance between supply and demand over time. This requirement is especially important today when there is a large-scale implementation of renewable energy. This section reviews the research on FRs in MESs. The state of art involving the development, quantification, management of FRs based on market procedures is summarized as follows.

1.3.1. Development of FRs

The first topic is the development of FRs, which categorizes and analyzes the resources that can provide flexibility to the energy system. Originally, those research work only explored and developed the FRs available in decoupled

energy systems (ie, electricity, gas or heating/cooling systems). The integrated energy system with the power system as a core provides a new prospect for the development of FRs. As a result, the integrated energy system can use a series of FRs from the supply-side to the demand-side, even the coupled subsystems can access the FRs of each other.

The variety of FRs based on the energy carrier integration is broad, as well as the classification. Take the power system as an example, FRs can be categorized according to physical and structural features in [51]. In [52], FRs are categorized according to their located position in the chain of the energy system, including supply-side, conversion, storage, and demand-side. Another classification method is mentioned in [53], in which FRs are classified by their impact on the system and the required response time. Chapter 2 of this Ph.D. thesis uniformly classifies the common FRs in MESs and introduces their principles and mathematical models in detail.

1.3.2. Quantification of FRs

The second focus is the quantification of FRs - an indicator for defining and measuring FRs. In the existing literature, most metrics used to evaluate FRs are from the perspective of power systems. In [54], based on the metric of power generation adequacy rate, the insufficient ramping resource expectation (IRRE) is proposed to identify the time when the system lacks FRs, and to measure the impact of changes in operating strategies and additional resources. In [55], the metric for operational FRs including ramping ability, storage ability, and upward/downward adjustment ability is introduced to evaluate the role of operational FRs in power curtailment. In [56], three metrics of ramp magnitude, ramp frequency and response time are proposed to evaluate the flexibility requirements of the power system on different time and space scales. In [57], a metric is expressed as a ramp rate to define location flexibility, and then, a reserve procurement strategy is used in transmission operation to achieve the optimal system response to the uncertainty. In [58], an approach for quantifying FR services is proposed. It can be applied to the scenarios of local power generation, thermal storage and heating, ventilation, and air conditioning (HVAC) services. Factors such as time, weather, building use, and comfort all have impacts on the metric of FRs.

These examples show that different FRs have their own clear measurement metrics for different application scenarios. Thus, it might not be appropriate to use a single metric to evaluate and measure different FRs. The following subsection presents various applications of FRs in MESs.

1.3.3. Management of FRs

The third focus theme is the management of FRs, the related literature review on which started from two aspects: coordinated operation and market design.

Coordinated operation

For the integrated electricity-gas system, effective solutions to its coordinated operation and dispatch have been investigated [59, 60]. Particularly, an integrated stochastic day-ahead scheduling model to deploy various FRs has been proposed in [61], where the coordinated FRs involve dispatchable generation units, DR and energy storage. Several reports focus on the positive effects brought by the bidirectional feedback of the electricity and gas systems [62-64]. In [65], a real-time subsidy-based robust scheduling scheme for the integrated electricity-gas system is proposed, in which bidirectional energy conversion is controlled by the dynamic variation of energy prices. Actually, work [61] and [65] put forward a new idea that power system operators can coordinate and optimize FRs through price signals to satisfy load and flexibility requirements.

For the integrated electricity-heat system, various conventional optimization techniques have been effectively used to carry out the collaborative dispatch of cogeneration systems with CHP units and heat storage [66, 67]. However, a new perspective to observe interactions between integrated systems, and to coordinate the flexible generators, energy storage and integrated electricity-heat DR and has been proposed in [68]. This so-called integrated electricity-heat demand-side management has gradually become a new type of FR and has been applied in the integrated electricity-heat system with the thermal building as a unit [69, 70]. More specifically, electricity demand is adjusted by controlling the heating demand in buildings to respond to supply changes. Besides conventional thermal storage, the thermal inertia of buildings has also been considered [71].

Although several studies have made interesting discussions on the coordination of FRs in the integrated gas, electricity and district heating system, the discussions are limited within coordinated operating, siting and sizing of multiple storage facilities [72]. Therefore, an economical solution to coordinate and optimize multiple FRs in MESs with an in-depth analysis of their impacts is still missing.

Market design

From existing studies, the challenges of management FRs are mainly from two directions: 1) Lack of information and communication technology infrastructure/systems to provide or deliver timely information of prices, energy flows and benefits [73]; 2) Lack of the related market design and regulation strategy to incentive supplier investment and consumer participation [74].

To address these problems, several effective solutions have been proposed, such as virtual power plant (VPP) technology [75] and smart buildings/communities [76, 77]. Through the aggregation and scheduling of the uncontrollable resources (such as renewable energy generation [78], inelastic load [79], etc.) and flexible controllable resources (such as elastic load, controllable heat demand, storage equipment and fast-ramp products [80], etc.), these technologies transformed various FRs into easy-to-handle and service-centric aggregators, which facilitate the management of system operators or market operators and provide flexible services for the MES.

To further explore the interaction between market outcomes, system operation, and resource allocation, many effective optimization models have been developed. As introduced in Section 1.1.3, these models are formulated into different collaborative optimization problems according to various application scenarios and research objectives.

Some models focus on exploring the market game of multi-leaders with followers [41-45]. For example, in [81], a Stackelberg game model for the integrated energy system and its end-users is proposed. In this model, the integrated system operator plays a leader by deciding energy supply and jointly pricing, while the end-users follow it to make consumption and pursue their own benefits. In [82], A monotone generalized Nash game model for autonomous energy management is proposed, in which each energy hub of residential is considered as a self-interested market participant. Some models emphasize the driving effect of upper market procedures on the lower system operation, which forms a collaborative optimization of a single leader with followers [46-50]. This type of optimization is especially applicable to solve the strategic interconnection of VPPs and the active distribution network (ADN). For example, a bi-level energy management model is proposed in [75], in which the upper level aims at minimizing the operating cost of ADN considering the market bid, while the lower level maximizes the benefits of VPPs. Compared with this, the model developed in [83] sets the minimum operating cost of ADN as the upper-level objective, while VPPs bid for the market is completed in the lower-level.

Another challenge is to solve these collaborative optimization problems. Generally, the more subsystems a MES has, the more complexity, nonlinearity, and calculational difficulty the resulting optimization model will have. In order to deal with the nonlinearity or non-convexity of the optimization model, several heuristic methods have been developed in [45] and [84], including simulated annealing algorithm, genetic algorithm, and differential evolution algorithm, particle swarm algorithm, etc. Single-loop distributed algorithm has been used to solve the variational inequality problem [82]. Several nonlinear optimization issues have been solved using second-order cone programming [85-87]. For the bi-level programming problem, some mathematical tools have been adopted to transform it into an equivalent single-level optimization problem with equilibrium constraints. The detailed examples include Karush–Kuhn–Tucker (KKT) conditions [41], strong duality theory, binary expansion approach [46], big-M method [50], Fortuny-Amat transformation [75], etc.

1.4. Project Objectives and Contributions

1.4.1. Research questions and objectives

Based on the above motivation, the final purpose of this Ph.D. project is to optimally manage FRs to achieve a flexible, efficient and economical MES with more renewable energy. In order to do this, the technical challenges of integrating and coordinating multiple FRs across MESs need to be solved. Meanwhile, considering market procedures and business modes, the optimal strategies of the MES with FRs to improve economic performance and optimize resource allocation are also demanded. Accordingly, the specific research questions are as follows.

- What FRs are available in the MES and how to describe their mathematical models?
- How to integrate and coordinate various FRs in different energy systems to ensure proper allocation and utilization?
- Is it possible to further propose optimal strategies for the MES with FRs according to different business modes?

With those research questions, the objectives of this Ph.D. project are summarized as follows.

Identification and modeling of available FRs in MESs

As mentioned previously, the identification and modeling of FRs in MESs is the basis of the follow-up research. In this Ph.D. project, various FRs will be

pre-investigated to determine what FRs are available in multiple energy systems. Then, their corresponding mathematical models and operating characteristics will be studied.

Integration and coordination of FRs in the MES

To ensure optimal operation and allocation of FRs located in different energy systems, a unified model of MES with FRs will be described and an optimal scheduling model for coordinating FRs will be formulated in this Ph.D. project. The expected outcome of the scheduling model is to enable each energy system operator to intelligently use and dispatch FRs according to day-ahead market energy prices, allowing the MES to accomodate more renewable energy while improving economics.

Optimal strategies for the MES with FRs under the market environment

Based on the above research contents, the collaborative optimization problems according to different application scenarios will be formulated in order to ensure a flexible, efficient and economical operation of the MES with FRs. The proposed optimal strategies involve the aspects of generation schedule, energy loss, resource allocation, as well as real-time market pricing. The impacts of different wind power levels will be also considered in which the corresponding optimal schedule of the MES and its controllable resources including FRs will be analyzed. The interaction between system operation and market pricing will also be discussed. Furthermore, the impacts of integrated FRs on social welfare and wind curtailment of the MES, especially the DR participation level, are analyzed in this project.

1.4.2. Project contributions

The harmonized integration of gas, electricity and heat systems that has various FRs under the market environment has been studied in this Ph.D. project. The main contributions based on the research outcomes are summarized as follows:

Identification and modeling of FRs in the MES

This Ph.D. study has comprehensively investigated and summarized FRs related to supply, conversion, storage and demand located in different energy systems. Several typical and common FRs have been introduced invovling their operating principle, mathematical modeling and technological development including:

- Supply-side flexibility
- Energy storage
- Conversion technology
- Demand side management

The mathematical modeling and flexible features of the considered FRs have been applied in the formulation of the follow-up optimization problems.

Multi-objective model for coordinating FRs in the MES

The problem of the integration and coordination of FRs across gas, electricity, and district heating systems has been investigated. For coordinating FRs and improving resource allocation, a multi-objective day-ahead dispatch model was developed. This model enables the MES to access and allocate available FRs depending on day-ahead market price signals. As a test case, an improved MES referring to the energy supply options in Aalborg, Denmark has been considered. The positive impacts of the coordination of FRs on the MES have been also discussed.

Bi-level programming model for the MES with flexible demand

Regarding smart buildings as flexible demand of the MES, a bi-level programming model has been proposed. These smart buildings integrated and managed by the aggregator have PV generation, EV chargers, storage, and electric heaters. The proposed model allows searching for optimal energy prurchase prices for the downstream customers so that the lower-level aggregator spontaneously provides services to improve the economic performance of the whole MES. The build-in flexibility of smart buildings on the demand side has been discussed in the illustrative cases.

Nash equilibrium market model for the MES with multiple FRs

Considering the limited communication between energy subsystem operators, a Nash equilibrium market model has been developed, in which each subsystem operator pursues its maximum profits. The used FRs include conversion technologies (such as P2G, CHP, gas boilers and electric boilers), DR and multiple energy storage. This model can address resource allocation and market pricing by simulating the game process between those subsystem operators in the real-time market.

1.5. Project Limitation

As a flexible resource, district cooling and its storage are crucial for demand side managment. There is a unique synergy between district heating and cooling systems since pumps can supply heat and cold energy. In most cases, the district cooling system is considered to be a component of the district heating system. In Denmark, different from the non-profit district heating market, the cooling market makes a profit by setting the cooling price. This further complicates the interaction and dispatch of multi-energy markets, making it difficult to formulate the modeling of collaborative optimization. In this Ph.D. project, only the integration of gas, electricity, and heat systems is considered and described as an application scenario for multiple FRs where:

In the simulation, the scheduling time is limited to 24h. The MES with FRs and its corresponding market procedures are considered in short-term operation. The short-term operation involves the management of the FR that has a response time of hours, hourly generation unit combination and resource allocation, and hourly market pricing, etc. Long-term planning such as energy policies, consumption patterns, network expansion, etc., are not taken into consideration.

The inputs of renewable energy involving wind and solar are mainly considered in this study. While this consideration may not be 100 % consistent with the real energy system, its simulation results have representative and reference values because wind power and photovoltaic power are widely applied, and they occupy an important share of the energy supply in renewable energy.

1.6. Thesis Outline

This Ph.D. thesis is documented as a monographic report. The report has a comprehensive record of the research work during the Ph.D. time including study problem, method, outcomes and their corresponding introduction, discussion and analysis. The thesis consists of six chapters and it is organized as follows:

Chapter 1 introduces the background and motivation of the Ph.D. project, and then reviews the state of the art of related topics. Based on those, the objectives, limitations and main contributions of the follow-up research are presented.

Chapter 2 identifies various FRs and classifies them according to their energy positions in MESs, involving supply-side, storage, conversion and demand-side. The operation principles and mathematical models of several typical FRs are investigated, which provides a theoretical and model basis for subsequent coordination and optimization.

Chapter 3 proposes a day-ahead scheduling model for addressing the issues of integration and coordination of FRs. The model allows using day-ahead price signals to dispatch and allocate FRs loacted in multiple energy systems. The work in this chapter involves the system construction, model formulation, simulation solution and result discussion.

Chapter 4 develops a bi-Level programming model for integrating flexible demand in the MES. The smart building clusters comprising PV generation, EV chargers with storage, and electricity-to-heat converters, are aggregated as the flexible demand-side of the MES. The proposed optimal strategy aims at searching for an optimal transaction price for the downsteam customers to enable the spontaneous service of the lower-level aggregator, as well as improving the economic performance of the whole MES. The build-in flexibility of smart buildings is also discussed based on the simulation results.

Chapter 5 develops a Nash equilibrium model for the MES with various FRs including multiple conversion technologies, storage, load shifting DR. The proposed model aims at addressing resource allocation and market pricing by simulating the game process between the subsystem operators that have limited coordination. The simulation results are analyzed and discussed in the different scenarios of wind power levels.

Finally, Chapter 6 gives the concluding remarks and presents the future research perspectives of this Ph.D. thesis.

1.7. List of Publications

The research outcomes during the Ph.D. study have been disseminated as journal papers and conference publications. They are listed as follows.

Publications in journals

J1 Y. Xi, J. Fang, Z. Chen, Q. Zeng, H. Lund, "Optimal Coordination of Flexible Resources in the Gas-Heat-Electricity Integrated Energy System," Energy, vol. 223, May 2021, Article 119729.

J2 Y. Xi, Q. Zeng, Z. Chen, H. Lund and A. J. Conejo, "A Market Equilibrium Model for Electricity, Gas and District Heating Operations," Energy, vol. 206, Sept. 2020, Article 117934.

Publications in conferences

C1 Y. Xi, T. Hamacher, V. Perić, Z. Chen, H. Lund, "Bi-Level Programming for Integrating Flexible Demand of a Combined Smart Energy System," in Proc. 2021 IEEE International Smart Cities Conference, virtual, Sept. 2021.

C2 Y. Xi, J. Fang, Z. Chen, H. Lund, S. M. Thomsen, A. Dyrelund and P. G. Kristensen, "Integration and Coordination of Flexible Resources in Multi-energy Systems," in Proc. 2019 IEEE PES General Meeting, Montreal, Canada, Aug. 2020.

C3 Y. Xi, J. Fang, Z. Chen, H. Lund, S. M. Thomsen, A. Dyrelund and P. G. Kristensen, "Integrated Flexible Resources and Energy Markets in the Danish Multi-energy System," in Proc. 2019 IEEE Innovative Smart Grid Technologies - Asia (ISGT Asia), Chengdu, China, May 2019.

The thesis structure is illustrated in Fig. 1.9, where a guideline is provided on the relation of selected publications and individual chapters in this report.

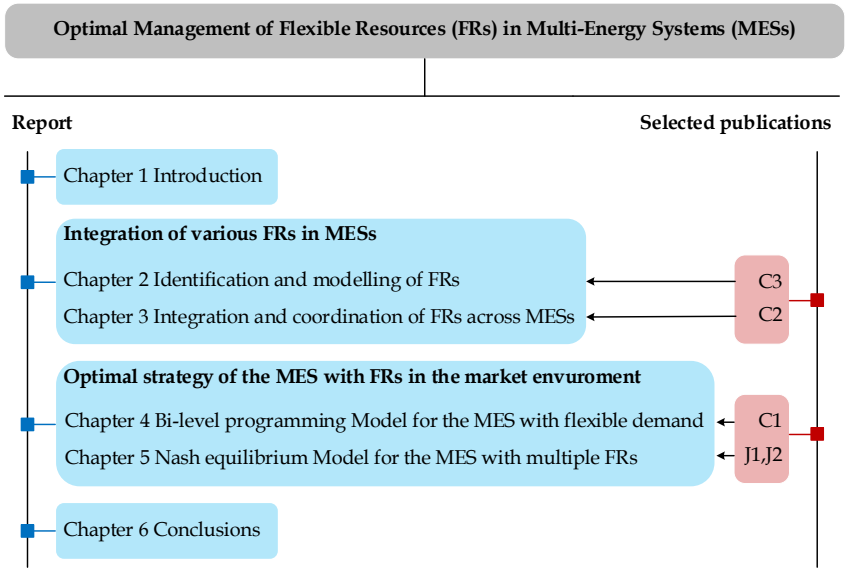

Fig. 1.9: Thesis structure and the related topic of each chapter.

Chapter 2

Identification and Modelling of FRs

2.1. FRs in Modern Energy Systems

As mentioned above, a multi-energy system (MES) with the integration of different energy carriers provides an efficient and economical approach to deal with the growing use of renewable energy. Coupled with continuous breakthroughs of emerging energy technologies, all evolutions have created conditions for the feasibility of the collaboration of flexible resources (FRs) in multiple energy systems. In Section 1.1, the FR of the power system has been introduced, including its definition and classification. From another perspective, this section provides an overview of definitions and classifications of FRs in modern energy systems, as well as the modeling of common FRs in studies.

In this Ph. D. thesis, the MES is defined as an integrated system that comprises at least two different energy subsystems and their infrastructure (such as electricity, gas, heating/cooling). The infrastructure can be centrally managed and controlled. According to scheduling instructions, the MES makes optimal resource allocation and energy production to ensure safe operation and satisfying benefits. In the last five years, most publications on MESs have shown an interest and relevance of FRs, where the range of the MES developed by researchers from small to large involves residences, communities, distribution systems and even larger-scale systems [61, 75, 77]. Tab. 1 provides commonly used FRs in current research on MESs. For the convenience of describing and analyzing various FRs in electricity, gas, heating/cooling systems, FRs are divided into four categories – supply-side, storage, conversion and demand-side. Each category includes various FRs. From Tab. 1, the FR can be a certain technology, equipment, operation mode or even control strategy. In the strict sense, these categories of FRs are not completely independent and parallel, because they are usually combined and integrated together in the practical application of the MES.

It should be emphasized that the main gas fuels injected into the gas system are natural gas, hydrogen or biogas, which can be injected directly or indirectly into the gas pipelines. Thus, the FRs in the gas system discussed

below are applicable for all these gas fuels. The following is a detailed introduction to these common FRs.

	Electricity	**Gas**	**Heating/cooling**
Supply-side	- Quick-dispatched energy generators - Increasing resource diversity and geographic coverage - Inverter-based capabilities		
Storage		Storage capacity of pipelines	
	Mechanical - Pumped hydroelectric storage - Compressed air energy storage - Flywheel **Electrical** - Superconducting magnetic energy storage - Supercapacitor **Electrochemical** - Battery - Plug-in-electric-vehicles	**Gas storage** - Hydrogen storage - Liquified natural gas (LNG) storage	**Heat storage** - Tank thermal energy storage - Pit thermal energy storage
Conversion	Power-to-X & Gas-to-X		
Demand-side	Demand side management (DSM)		

Tab. 2.1: FRs in the MES by categories.

2.2. FRs of Supply-Side

The first category is defined as the supply-side FRs.They are committed to improving the flexibility of the supply-side of the energy grid and making energy production flexible, diverse and complementary.

2.2.1. Quick-dispatched energy generators

Quick-dispatched generators can respond to slow/rapid variations in demand between night and day in an energy system, which has a high proportion of unschedulable renewable energy sources like wind and photovoltaics (because the power system needs to always maintain a balance between supply and demand). Generally, these energy generators have a fast start-up time and can be put into production within seconds or minutes in order to respond to sharp disturbances caused by intermittent renewable energy, peak periods and emergencies. In the power system, natural gas power and hydroelectric plants are the most quickly dispatched plants. For

instance, pumped storage power plants can achieve maximum production in dozens of seconds [88]. In the heating system, gas boilers and heat pumps have both short start-up time and fast response time, so that they can supply heat on demand [89]. Notably, there is a new type of CHP plant is built at Amager Ressource Center in Copenhagen, Denmark [90], called the 'bypass' CHP plant. In the so-called 'bypass' operation mode, the CHP unit is no longer subject to the rigid constraints between electricity and heat generations. Its heat production can be increased to the maximum within minutes, while the maximum power production can be reduced to the minimum within 30 minutes as required in the meantime. In summary, these quick-dispatched energy generators can smooth the changes in energy production, contribute to alleviating grid congestion, and maintain the quality and stability of the energy supply.

2.2.2. Increasing resource diversity and geographic coverage

In the MES, the combination of renewable resources is an effective way to increase flexibility. For example, wind resources (in two regions) and solar generation in Texas had different, but complementary, load capacity profiles [91]. This complementarity between wind and solar PV has also been verified in a large number of experiments of the Iberian Peninsula [92]. At the same time, expanding the geographic coverage creates an opportunity to use multiple resources. These resources can produce a smooth profile that closely approximates system demand. Cases in [93] have indicated that increasing resource and geographic diversity not only reduces curtailments but also improves price fluctuations.

2.2.3. Inverter-based capabilities

Historically, turbine generators are driven by the steam created by burning fuels to produce electricity. If there is too much load in the grid, the energy consumption is much faster than the energy supply. As a result, the spinning speed and frequency of the turbine will decrease. This resistance to changes in frequency is known as a property of inertia [94]. Different from the inertial properties of steam-based generation, smart inverter-based generation convert electricity at any frequency in order to adapt to frequency fluctuations and creat a stable grid environment.

Some advanced inverter-based technologies have been applied to renewable energy generation. These advanced inverters may even generate the signal to identify when switching will take place, resulting in a sine wave on the grid. For example, a small network with PV can assign one of the inverters to lead grid-connected operation, and the rest of the inverters will follow that. As a

consequence, a stable grid is established that is independent of turbine-based generation [95].

Therefore, the inverter-based supply-side that relies on the generation resources behind them, can provide its system with important capabilities as required, including disturbance ride-through, reactive and voltage supports, frequency regulation, dispatchability and response-ability [7].

2.3. FRs of Storage

The second category of FRs is energy storage technology. Energy storage improves the mismatch between supply and demand of the system using the time-shift of energy delivery. This feature makes storage become the optimal solution to integrate renewable energy sources [96]. The existing literature shows that there are two main approaches for combining storage systems with renewable energy generation. One is to connected to a local power plant and operates as a whole. This approach is suitable for the situation that both the generator and storage system benefit from a sharing location, such as installing thermal storage near the site of solar generation [97]. Another approach is to upgrade energy storage to a system-level FR, which is usually combined with energy conversion. For example, a P2G station converts surplus wind power into gas for energy storage or regeneration [16]. In this section, various storage technologies are introduced according to different energy carrier systems including their working principles. Then the common expressions of storage technologies in mathematical models are described.

2.3.1. Storage in power systems

Energy storage technology in the power system has been extensively developed and researched. There are relatively mature technologies such as pumped hydroelectric, compressed air and batteries [98], as well as technologies of engineering value such as flywheels, superconducting magnetics and supercapacitors. The research in this Ph. D. thesis focuses on electric vehicle (EV) technology combined with batteries.

Pumped hydroelectric

Pumped hydroelectric storage stores electricity in the form of the gravitational potential energy of water. During off-peak demand periods, low-cost surplus electricity is used to pump the water from a lower elevation reservoir to a higher elevation. While during peak demand periods, turbines release the stored water to produce electricity. As of 2020, pumped hydroelectric storage

is now the most widespread form of storage technology, which accounts for around 95% of the active storage installations worldwide [99].

Compressed air

Compressed air energy storage (CAES) stores electricity in the form of air compression. During periods of storing energy, electricity is used to run electric turbocompressors to compress air into the storage container, such as salt cavern, abandoned mine shafts, or some specific underground structures (aquifers, depleted natural gas mines, etc.) [100]. During periods of extracting energy, the stored air is expanded and mixed with fuel to drive generators to produce electricity. In terms of renewable integration, studies [100-102] show that CAES can effectively flat the fluctuation of wind power, provide reserve flexibility and improve economic benefits.

Batteries

Battery storage, here specifically refers to secondary (rechargeable) batteries, store and release energy by the bi-conversion of chemical energy and electrical energy. Three examples are lead-acid batteries applied in vehicles, lithium-ion batteries adopted in portable electronic products, and high-temperature batteries (sodium-sulfur or chlorine) used in military engineering [98]. Due to the extremely short response times, in recent years, battery technologies have been quickly developed and implemented on a massive scale. They have become active participants in electrified transportation and renewable energy grids [103]. For instance, distributed batteries used in EVs and household storage have smart metering and fast responsive ability [104, 105].

Flywheels

Flywheels stores energy in the form of rotational momentum, made of high-strength steel or composite materials [106, 107]. The advanced flywheel storage system has a rotor made of high-strength carbon-fiber composite material, with rapid response time, good temperature tolerance and low maintenance costs [108-110]. They have been widely used in the electrified transportation sector, such as in Sentinel-Oerlikon Gyro Locomotive for shunting or switching [111] and on the line side of electrified railways to help regulate line voltages and reduce energy costs [112].

Superconducting magnetic energy storage,

Superconducting magnetic energy storage (SMES) stores electricity in the magnetic field of superconducting coils and then returns the electromagnetic energy to the grid or other loads when needed. Based on the zero resistance of superconductors, SMES can not only store electrical energy in the superconductor inductors without losses but also achieve a large capacity of electricity storage, improve power supply quality and increase system capacity [113]. At the same time, it can quickly exchange active/reactive power with external systems through power electronic converters [114]. SEMS systems have been applied in maglev trains and high-rise buildings.

Supercapacitors

Supercapacitors store energy through polarized electrolytes. Unlike batteries, this storage process is reversible in which no chemical reaction occurs. As a result, supercapacitors can be repeatedly charged and discharged a few hundred thousand times. The Supercapacitor has outstanding advantages of high energy efficiency, short charging/discharging time, long cycle-life and wide operating temperature bounds [98]. However, the shortcomings of high costs and low energy density greatly restrict its development, leading to being replaced by batteries in the transportation and renewable energy industry. In the short term, the extremely low specific energy makes supercapacitors impossible to be used in an EV system alone, while they have significant benefits when used as an auxiliary source. For example, the optimal combination used for EVs is the battery-supercapacitor hybrid energy system [115]. For another example, in wind energy/solar battery systems, supercapacitors with rapid response times can replace some of the batteries to improve efficiency in spite of a high initial investment cost [116, 117].

Electric vehicles

Based on several technologies mentioned above (such as lithium-ion batteries and flywheels), EVs can provide distributed, movable storage services for their connected grid [52]. Generally, EVs can be powered by a power system with aggregators [118], or they can be powered by batteries (such as solar panels and fuel cells). If an EV is equipped with battery devices, then it can select to charge or discharge just like a traditional storage option [104, 105]. For plug-in EVs, they are charged by household sockets, taking about 4-11 hours. Using public fast charging piles might take 45-90 minutes. In particular, the charging time of the vehicle is only 7 minutes when using an ultra-high power charging pile [119].

EVs are often combined with demand-side management to provide flexibility for the energy system [120]. Firstly, EVs have excellent energy-saving benefits. According to the 2020 official US government source for fuel economy information [121], EVs convert more than 77% of the electricity from the grid into wheel power, while traditional gasoline vehicles just convert about 12%–30% of the energy stored in gasoline into wheel power. Secondly, EVs are beneficial to the environment. Because they release no pollutants from the exhaust pipes and their electricity may be generated by wind-, solar-,or hydro-power plants, which likewise emit no pollutants into the atmosphere. In addition, the driven electricity for plug-in EVs can be a domestic energy source. For example, in [122], an optimal management approach for smart houses with PV and plug-in EVs is proposed. In terms of renewable integration, studies [123, 124] show that EV services can be used to regulate wind power and provide operational reserves to reduce power curtailment and generation costs.

2.3.2. Storage in gas systems

Similar to the significance of electrical storage to the power system, gas storage is one of the key steps in the construction of building a natural gas pipeline network. It helps the gas system respond to the demand of different periods to provide the necessary flexibility. In research on MESs, gas storage is closely linked with the FRs of F2G and EV technologies [125, 126].

Hydrogen storage

Hydrogen is a clean fuel that plays an important role in modern energy systems with large amounts of renewable energy. At present, several hydrogen storage technologies are available.

First, hydrogen can be physically stored in gas or liquid form. The simplest method to store hydrogen as a gas is gas compression, which usually requires high-pressure tanks [127]. Storing hydrogen in liquid form requires a low temperature and enough insulating materials because the boiling point of hydrogen is about -252.8°C [127]. Hydrogen can also be absorbed and stored on solid surfaces or interiors such as metal-organic frameworks and porous or layered carbon materials [128, 129]. Second, hydrogen can be stored in a specific chemical through a series of chemical reactions [130], such as the reaction of hydrogen-containing materials with water or alcohols. Besides, other technologies such as automotive onboard storage and photo-chemical storage [128, 131] also receive attention.

Liquefied natural gas (LNG) storage

Generally, natural gas (predominantly methane, CH4) is cooled into liquid form for efficient and safe transport (usually ocean shipping) and storage. The LNG storage tank has a double-wall structure. The inner tank is made of low-temperature alloy and the outside tank is surrounded by insulating materials [132, 133]. Sometimes the underground tank with a more expensive cost is used for storage [132]. To ensure LNG as a liquid form, the focus is to control temperature rather than air pressure [134]. Sometimes the heat transfer might cause LNG gasification in the storage tank. The gasified natural gas is compressed and injected into the local natural gas network, or re-sent to the liquefaction plant to be cooled down and returned to the storage tank [135].

2.3.3. Storage in district heating/cooling systems

Thermal energy storage stores excess heat by specific technologies/devices for hours, days or months. The application scale ranges from an individual process, a building, a building cluster, a district or a town. Because of a high specific heat capacity, the most common storage medium - water is applied, such as heat water tanks and pits with water large reservoirs [136]. This heat storage method that only uses the temperature increase/decrease of the medium (water) is called 'sensible heat storage' [137]. This type of storage method is well received and commercialized, as the others including latent heat storage and thermochemical storage are still being research and developed [137,138].

The application of heat storage is usually closely linked to PV generation and electricity-to-heat technology. In the district heating/cooling system, the heat storage tank is usually built together with the CHP unit, which typically has an 8-hour storage size [139]. In addition, the heat storage pit is another good choice for district heating systems. It enables the storage and utilization of excess heat from PV generation or industrial processes [140]. The electrothermal storage heaters commonly used in European households can consume cheaper electricity for heating and storing at night, and then release and use the stored heat during the day. Besides, the more popular facilities in recent years use seasonal thermal energy storage, storing heat in summer for heating in winter or storing cooling in winter for air conditioning in summer [140, 141].

2.3.4. Mathematical model for storage

The realistic process of energy storage and release is complex, like distributed mass transfer in battery reactions [142], gas compression/diffusion in gas

storage [143, 144], and heat transfer of fluid in heat storage [145]. As a result, the model formulated is non-linear based on these physical and chemical principles. In the model, the power limits for energy storage and release are related to many factors such as time-varying, operating parameters and other external conditions. The detailed energy storage models are rarely applied in real-time because of their high computational requirements and large parametric identifications.

In the existing literature, the general model for energy storage has constant charge/discharge power constraints [69, 75, 146, 147, 148]. This steady-state model only considers energy loss and ignores the impact of different working conditions, which makes the analysis and calculation much easier. This simplification is acceptable and applicable in the operation and planning of MESs. Therefore, for any energy storage unit during the scheduling period T, the storage constraints can be modeled as follows:

$$SOC_{t+1} = SOC_t + Q_t \tag{2-1}$$

At each time step t, SOC_t is the state of charge (SOC), namely the volume of energy stored in the storage unit, and Q_t is the volume of energy change, in which Q_t determines the direction of energy storage flow:

$$Q_t^{\max} \geq Q_t \geq 0, \text{ injecting energy into storage unit at time } t \tag{2-2}$$

$$-Q_t^{\min} \leq Q_t \leq 0, \text{ withdrawing energy into storage unit at time } t \tag{2-3}$$

where $Q_t^{\max}$ and $Q_t^{\min}$ represent the maximum energy injection and extraction of the storage unit at time t, respectively. The SOC limits can be expressed as:

$$S_t^{\min} \leq SOC_t \leq S_t^{\max} \tag{2-4}$$

where $S_t^{\max}$ is the storage capacity. $S_t^{\min}$ is the buffer capacity of the storage unit, which sometimes can be set to 0. In some special conditions, it might maintain a certain value. For example, for the gas storage unit, $S_t^{\min}$ represents the cushioning capacity that is the gas required in storage to keep adequate pressure [146].

2.4. FRs of Conversion

The third category of FRs is energy conversion technology. As introduced in Section 2.3, energy conversion and storage technologies are usually combined

to provide flexibility for MESs. The energy conversion facility serves as the interface of different energy systems as shown in Fig. 2.1. On the one hand, it builds a bridge across different energy systems for the system operator to access various FRs. On the other hand, it provides a variety of options for energy consumption. As a result, the overall economic benefit and energy efficiency of the integrated system are improved. In the next, several conversion technologies involved in this Ph. D. thesis are presented.

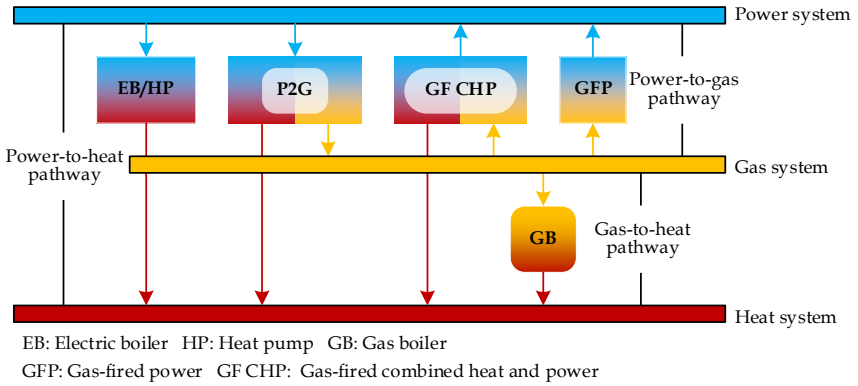

Fig. 2.1: Conversion pathway for electricity, gas and heat systems.

2.4.1. Power-to-X

Power-to-X (P2X) conversion technology allows the surplus power (possibly produced by renewable generation) to be decoupled from the power sector and used in other sectors (such as gas, heat, transport and chemicals). Typical examples include power-to-heat, power-to-gas, as well as vehicle-to-grid (V2G). In this way of converting other energy loads into the power system, P2X can reduce or even avoid the electricity waste from renewable energy curtailments [52, 149].

Power-to-heat (P2H)

In the P2H application, heat or cold energy is converted from surplus electricity for heating or cooling [150]. Since storing heat is much easier than storing electricity, P2H has a higher priority at the end of energy consumption. The main converison equipment to realize P2H includes conventional heating resistors, electric boilers and heat pumps, equipped with corresponding heat storage devices [26, 70, 71, 89]. In terms of response time, both electric boilers and heat pumps have good performances. The investment cost of electric boilers is lower than heat pumps, but the coefficient

of performance (COP) of heat pumps is 3-4 times higher than that of electric boilers. Therefore, from the perspective of energy saving, buying and installing heat pumps might be a better choice for households.

Power-to-gas (P2G)

In the P2G application, excess electricity is converted into gas fuel for chemical feedstock or power regeneration [151]. Most P2G systems use electrolysis technology to produce hydrogen that is used directly or further converted into methane. The gas produced can be fed into the local natural gas pipelines [131, 152]. Some studies have analyzed the potential of P2G technology in terms of environmental and economic operations, especially the improvement of restrictions on gas and power transmission networks [16, 17, 59, 61]. Meanwhile, the research on siting and sizing P2G plants has received attention [62, 72]. At present, it is not ready to widely implement P2G technology due to the insufficient P2G system and high investment costs.

2.4.2. Gas-to-X

Generally, most of the transported gas is used as fuel for power generation [153]. From the natural gas system side, the power system (except for P2G facilities) and the heating system can be seen as energy consumers. For this reason, gas-to-X technology mainly focuses on producers of power systems and heating systems. For example, the gas-fired power plant generates electricity by consuming gas, which is often used to provide seasonal dispatchable power generation to balance variable renewable energy [154]. A combined heat/cooling and power system can be obtained by reforming the conventional gas-fired power plant [155]. Another example is the gas boiler that uses gas fuels to provide heat for residential and commercial properties.

2.4.3. Mathematical model for conversion devices

In the existing literature, the mathematical model of conversion units (such as P2G units, heat pumps, gas boilers, etc.) is described as constant-coefficient conversion and power input/output constraints [20, 62, 63, 89]. These static models are simplified by a scheme similar to a 'black box', which focuses on the energy input and output of the unit rather than the detailed process of internal energy conversion. Again, this simplified static model is acceptable and applicable to the operation and planning of MESs.

For any conversion unit in the scheduling period T, the conversion constraints can be modeled as follows:

$$P_t^{\text{in}} = COP_t^{\Pi} \cdot P_t^{\text{out}} \tag{2-5}$$

where P_t^{in} and P_t^{out} represent the energy power consumed and the new energy power produced by the conversion, respectively. COP_t^{Π} is the coefficient of performance, which is defined as the relationship between the power input and output of conversion unit Π.

At each time step t, the energy input/output of the conversion unit is limited in its rated power bounds.

$$P_t^{\text{in/out,min}} \le P_t^{\text{in/out}} \le P_t^{\text{in/out,max}} \tag{2-6}$$

where $P_t^{\text{in/out,min}}$ and $P_t^{\text{in/out,max}}$ are the upper and lower limits of the power input/output of the conversion unit.

2.5. FRs of Demand-Side

The fourth category of FRs is summarized as demand side management (DSM), in which consumers change their consumption behaviors to reduce costs. This includes all actions where customers of the MES reduce their energy usage during peak times or shift energy usage to off-peak times, whether the overall energy consumption of the system changes or not. As an important component of DSM, demand response (DR) is only discussed for electrical loads in most studies [156]. Accordingly, a series of DR programs has been developed. These DR programs can be managed individually for each consumer or collected and centrally operated by an aggregator [157].

2.5.1. DR programs of electrical loads

Report [158] has divided DR programs of electrical loads into two basic groups - time-based DR programs and incentive-based DR programs, as shown in Fig. 2.2.

Time-based DR programs

The electricity price changes in different periods according to the cost of electricity production, such as high electricity prices in peak periods, low electricity prices in trough periods, and moderate electricity prices in off-peak periods. This group of DR programs has neither incentives nor penalties. Specifically,

- Time-of-use (TOU) program: The electricity price is calculated based on the energy cost of each period. These electricity prices change in a few hours, days or even seasons.
- Critical peak pricing (CPP) program: It is a combination of the TOU program and the unified pricing approach, as shown in Fig. 2.3. This program focuses on the implementation cost of energy in peak periods.
- Real-time pricing (RTP) program: The electricity price is calculated based on hourly energy cost, as shown in Fig. 2.4. This program links the hourly electricity price to the change in the hourly electricity cost of the day or the day ahead. it is addressed in two ways: One is called 'one-part RTP' [159], where the price is calculated on the basis of hours, the other is called 'two-part RTP' [160], which sets an upper bound for the customer's consumption. Whenever the customer's consumption is lower or higher than this bound, the corresponding electricity prices are different.

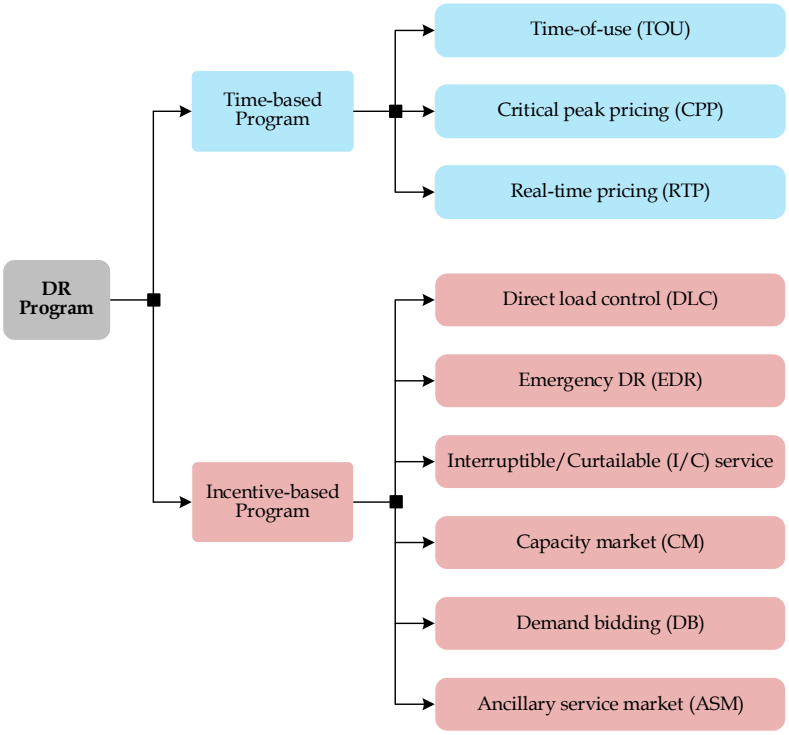

Fig. 2.2: DR programs of electrical loads by groups.

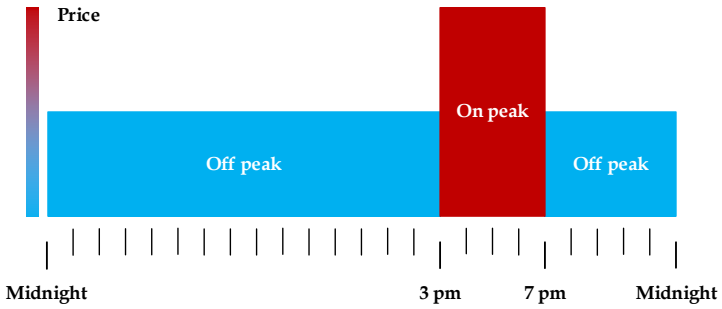

Fig. 2.3: An illustration of CPP program.

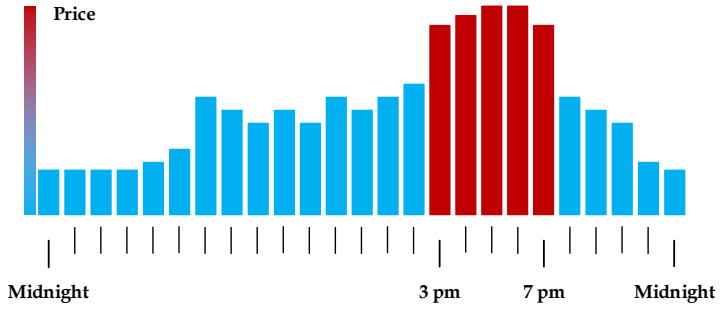

Fig. 2.4: An illustration of RTP program.

Incentive-based DR programs

When the system needs or faces pressure, customers are subsidized by the operator to reduce electricity consumption. Such group of DR programs can span long-term, medium-term, short-term, and even real-time.

- Direct load control (DLC) and emergency DR (EDR) program: Customers can participate voluntarily in these programs. The customers will not be punished whether they reduce their consumption as required or not.
- Interruptible/curtailable (I/C) service and capacity market (CM): Customers sign a mandatory agreement with the operator and get a certain discount of energy purchase, in which they will be punished once they do not reduce consumption in accordance with scheduling commands.
- Demand bidding (DB) program: A large number of customers are encouraged to help with load shedding at a payment that they are

satisfied with, or customers are willing to reduce a certain amount of loads for a published price.

- Ancillary service market (ASM): Customers can bid for load shedding in the electricity market to provide operating reserves.

Based on the above DR programs of electrical loads, several interesting points of view are found. From the supplier's perspective, an appropriate market signal is needed to trigger the desired response load. To this end, the researchers in [161] propose a DR simulation tool to maximize retailers' profits and improve the overall system efficiency. From the consumer's perspective, minimizing the customer's energy purchase cost is the main target to ensure their active participation in the DR program. The authors in [80] and [158] refer to the concept of price elasticity and customer benefit function and propose the DR economic models to simulate the behavior of customers with different incentives, punishments and elasticities. These models improve both load characteristics and customer satisfaction. In [162], a real-time DR model is proposed to maximize consumer benefits by using robust optimization and linear programming. In this model, the consumer and the supplier reach an agreement, in which the consumer can receive the corresponding hourly price several minutes prior and adjust its consumption for that hour as a response to that price. From an institutional point of view, the feasibility of DR programs depends on the market environment, including market mechanism design and market regulation. In addition, the profitability of DR programs seems to be only a certain range of energy costs, expected benefits, and load curtailments [163].

2.5.2. DR services in the MES

In the MES, DR is no longer limited to electrical loads. Because customers have their own selections of the way of energy consumption through the conversion and storage of multiple energy sources. In the MES environment, DR can respond to the demands of other power systems or other energy systems. This means that the power system can access potential demand-side flexibility from different energy systems. Accordingly, extending the DR concept to the MES will influence the outcomes of multiple energy markets (such as electricity and natural gas prices). This is also the focus of the DR application in this Ph. D. thesis.

According to the terminology elaborated in Lawrence Berkeley National Laboratory (LBNL) [164], DR services in the MES can be summarized and categorized by different periods as shown in Fig. 2.5.

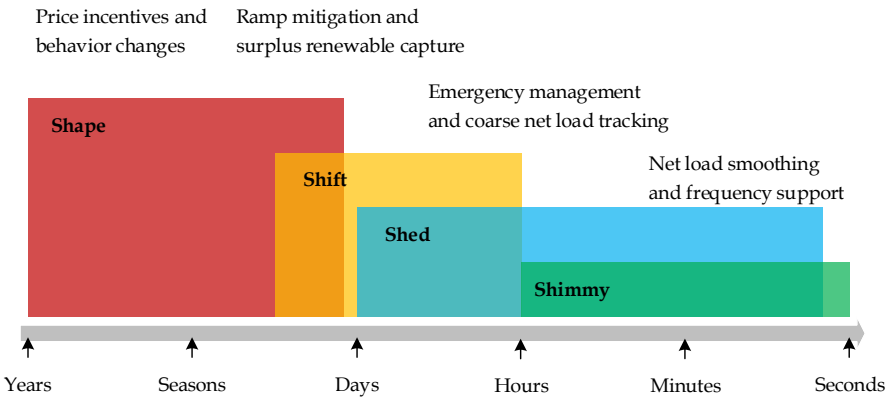

Fig. 2.5: An illustration of DR services in the MES by timeframes.

Long-term DR - load shaping

The features of a load shape represent the energy consumption patterns of an energy system. Load shaping refers to the seasonal and time-of-day changes in energy consumption via a specific technology, in which the shapes of load curves are modified through long-term price response or behavioral campaigns [165]. Currently, there are three main measures to change energy consumption patterns.

- Energy efficiency upgrades: Commercial, residential, industrial facilities use energy-efficient, dimmable and long-lifetime lighting devices, such as compact fluorescent lamps and t8 led bulbs, install chillers and boilers or stick window films.
- Time-of-use adjustments: The demand control software or building management system provides time schedules of energy equipment, such as staggering start-up times, making ice at night, installing daylight/motion sensors, and increasing thermostats.
- Curtailment capability: The load shape has access to loads curtailed on occasion to offer reduction service and peak capacity by conventional curtailable rates.

Mid-term DR – load shifting

Load shifting encourages energy consumption to shift from periods of high demand to periods of abundant renewable supply. This is comparable to the time-of-use adjustment under load shaping but is accomplished through different incentives (such as energy prices) resulting in a more flexible load shift that takes just when needed instead of a permanent load change.

Different from many energy cost-saving strategies, load shifting tackles the "when" rather than the "how much" problem. In other words, load shifting does not result in a reduction in the net quantity of energy used. For instance, electric vehicles can charge and store cheaper electricity at times of low demand or times of surplus renewable energy. Heating, ventilation and air conditioning buildings can provide heating and cooling while effective load shifting [166]. Besides, load shifting could also act as a fast-responding FR to help address net-load ramp issues of energy systems.

Short-term DR – load shedding

Load shedding is usually done as a controlled option in response to unplanned events to protect the energy system from a complete paralyzation. The load shedding is similar to the occasional curtailment capability under load shaping. Here, it is envisioned as being more adaptable, giving customers more choices in how and when to participate, including advanced lighting, interruptible appliances and air conditioning cycling among others.

Instantaneous DR – shimmy load

Shimmy load, also known as frequency regulation in the power system, is the second-by-second, minute-by-minute adjustment of loads to assist keep the supply-demand balance. For example, in 2016, a research titled 'The Hidden Battery' described how adjustable water heaters in households start up and shut down to respond almost immediately to regulate load [167].

This fast response load can shimmy back and forth to dynamically adjust demand on the system. Shimmy load can offer DR services such like frequency regulation and ramping reserves because it can relieve short-term ramps and shocks on timeframes ranging from seconds to an hour.

2.5.3. Mathematical model for hourly DR load

Since the scheduling period T for all simulations is set to one day (24 hours), the application of DR resources involved in this Ph.D. thesis is load shifting or load shedding. According to their definitions, the hourly load of the power system (P_t^{rl}) can be divided into responsive load (P_t^{rl}) and non-responsive load (P_t^{nl}), expressed as:

$$P_t^{\mathrm{l}} = P_t^{\mathrm{rl}} + P_t^{\mathrm{nl}} \tag{2-7}$$

Here, a load participation factor (LPF) is introduced to express the proportion of the responsive load to the forecasting load in unit time, which is defined as:

$$\mathrm{LPF} = \frac{P_t^{\mathrm{rl}}}{P_t^{\mathrm{l}}} = \frac{P_t^{\mathrm{rl}}}{P_t^{\mathrm{rl}} + P_t^{\mathrm{nl}}}, \mathrm{LPF} \in (0,1) \tag{2-8}$$

The value of LPF is between 0 and 1. As LPF is larger, the more customers participate in the DR service and the larger load capacity can be adjusted. Thus, the mathematical model of DR in each energy system can be expressed as:

$$P_t^{\mathrm{lDR}} = P_t^{\mathrm{l}} - P_t^{\mathrm{sl}} \tag{2-9}$$

where P_t^{lDR} is the power load improved by load shifting and P_t^{sl} is the hourly load shifting/shedding. At the same time, the amount of load shifting/shedding cannot exceed the amount of load participating in the DR service.

$$\left| P_t^{\mathrm{sl}} \right| \le \mathrm{LPF} \cdot P_t^{\mathrm{l}} \tag{2-10}$$

For the load shifting of DR, $P_t^{\mathrm{sl}}>0$ means that part of the load is shifted out to other periods, and $P_t^{\mathrm{sl}}<0$ represents that the part of the load is shifted in from other periods. It should be noted that the load change per unit time should be limited to a reasonable range for stable system operation.

$$\left| P_t^{\mathrm{lDR}} - P_{t-1}^{\mathrm{lDR}} \right| \le \left| P_t^{\mathrm{l}} - P_{t-1}^{\mathrm{l}} \right| \tag{2-11}$$

If the system requires the total load to remain unchanged during the scheduling period, the corresponding load shifting must be balanced as shown in Equation (2-12). This is consistent with the original intention of load shifting, which only changes the time of energy consumption rather than the quantity.

$$\sum_{t=0}^{24\mathrm{h}} \left(P_t^{\mathrm{sl}} \right) = 0 \tag{2-12}$$

2.6. Summary

This chapter classifies the FRs of electricity, gas and heating systems uniformly, including supply-side, storage, conversion and demand-side. The technologies involved in these common FRs (working principles and practical

applications) are introduced in turn and their mathematical models in the operation and planning problem of MESs are described.

Based on this, the following studies focus on the integration and coordination of energy storage technology, conversion technology, and demand-side management mentioned in this chapter.

Chapter 3

Integration and Coordination of FRs across MESs

3.1. Background

The integration and coordination of FRs are based on the integration and joint operation of MESs. Thus, a unified model of the MES with FRs needs to be described to connect the energy flow of different FR facilities. The next focus is to appropriately allocate and use FRs in accordance to supply and demand variations caused by renewable fluctuations. To this end, the price information of the day-ahead market can be introduced as a dispatch signal. More specifically, it is hoped that the different energy subsystems in the MES can coordinate with each other to maximize the benefits, and intelligently select and use FRs at the proper time to increase the accommodation of renewable energy.

Following the above identification of FRs in MESs, this chapter will discuss the optimal coordination of FRs based on the system interconnection. A MES integrating power, gas and district heating systems is considered in the implementation, in which the supply options of the energy system in Aalborg, Denmark are referred [168]. In this MES, wind power is the input of renewable energy and the FRs used include energy conversion units (such as P2G units, electric boilers (EBs), gas boilers (GBs), gas-fired combined heat and power (GFCHP) units, energy storage units (such as gas storage (GS) and heat storage (HS)) and load shifting of DR service. In order to coordinate these FRs in the different energy subsystems, a multi-objective scheduling model is proposed to ensure the optimal operation of the MES. In the following, the integrated framework of FRs across MESs and the formulation of the optimization model will be described, the effectiveness of the proposed model will be demonstrated through simulations, and the positive impact of DR participation on resource utilization will be discussed.

3.2. Integration of FRs Across MESs

Fig. 3.1 shows the integrated framework of FRs across MESs. The integrated system consists of power, gas and district heating subsystems. The energy supply options for each energy subsystem are determined and improved based on the current state of energy supply in Aalborg, Denmark [168]. It should be noted that the CHP unit is an important facility for district heating production in Denmark. Its fuel mainly comes from coal, natural gas, biomass, waste, as well as wood pellet or straw. In the city of Aalborg, there are two CHP plants 'Nordjyllandsværket' and 'Reno-Nord' in the back-pressure operation, in which the main fuels are coal and waste respectively. In this Ph. D. thesis, in order to emphasize the interaction with the gas system, it is assumed that all CHP units runs just on natural gas as fuel.

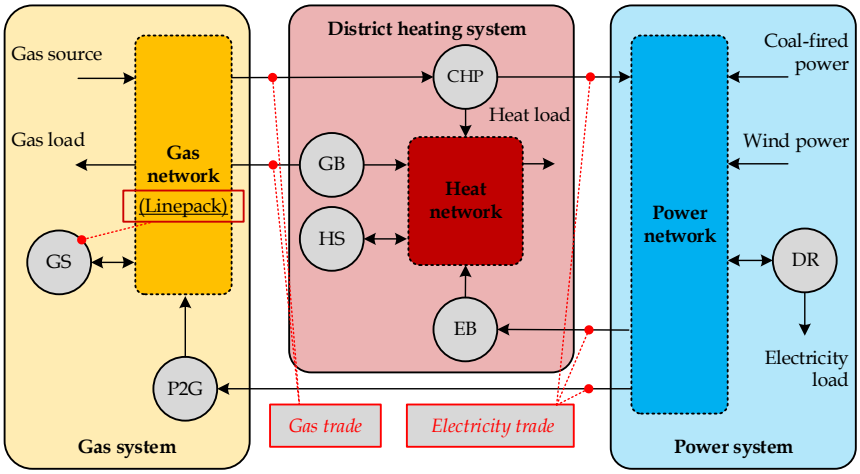

Fig. 3.1: Integrated framework of the FRs across MESs. Source: [C2].

From the perspective of energy flow, each energy subsystem has its own generation units, conversion units, transmission network and energy demand. In the gas subsystem, the gas is provided by the gas source and P2G units, and delivered to the demand-side through the gas network. The gas can be stored in a small amount in the gas pipelines, namely linepack [32], or directly stored in the gas storage device. Besides the initial gas load, the gas demand includes the gas consumption of GBs and GFCHP units. In the power subsystem, the electricity is produced by wind turbines, conventional coal-fired power (CFP) units and GFCHP units, and delivered to the demand side through the power network. Here, the electricity demand includes the electricity consumption of EBs and P2G units besides the forecasting load. It should be noted that a DR scheme is introduced into the electricity load-side,

in which the consumers participate by shifting part of their consumption to off-peak periods as required. In the district heating subsystem, the heat can be supplied by gas-fired facilities such as GFCHP units and GBs, or electricity-consumed facilities such as EBs. Through the heat network, the heat is delivered to the heat stations that directly heat local users. In this process, the heat can be stored in the heat storage device.

From the perspective of market outcomes, every energy exchange between the subsystems is accompanied by energy trading. It is assumed that each energy facility is controlled by the system operator corresponding to the energy carrier that the facility produces. For example, GFCHP units, GBs and EBs are controlled by the district heating subsystem operator because they produce heat. This framework mainly has two types of energy trades:

- Gas trade: The district heating system needs to purchase gas from the gas system to run GBs and GFCHP units to supply heat.
- Electricity trade: On the one hand, the district heating system may sell electricity (a by-product of heat production) to the power system through GFCHP units or purchase electricity from the power system to run EBs to supply heat. On the other hand, the gas system purchases electricity from the power system to operate the P2G unit to produce gas.

There is an interesting finding that the district heating system is a pure consumer from the standpoint of the gas and power systems. In this framework, different system operators can access FRs through the conversion and exchange of energy carriers.

3.2.1. Steady-state modelling of energy flow

This subsection focuses on the modeling of various components in MESs. The steady-state models of energy flow in the power, gas and district heating systems are described. Then, the models for the used energy facilities are formulated.

Power flow model

In the power system, the purpose of power flow calculation is to obtain a series of nodal electrical parameters (injected power, voltage amplitude and voltage phase angle) based on the given load and network parameters [169]. Fig. 3.2 shows a typical distribution line modeled as an equivalent π branch with corresponding electrical parameters. For a power system with N nodes, the power flow in the polar form can be expressed as:

$$\begin{cases} P_i = |V_i| \sum_{j}^{N} |V_j| \left[G_{ij} \cos\left(\theta_i - \theta_j\right) + B_{ij} \sin\left(\theta_i - \theta_j\right) \right] \\ Q_i = |V_i| \sum_{j}^{N} |V_j| \left[G_{ij} \sin\left(\theta_i - \theta_j\right) + B_{ij} \cos\left(\theta_i - \theta_j\right) \right] \end{cases} \tag{3-1}$$

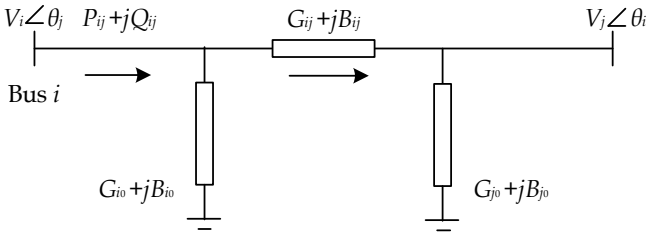

Fig. 3.2: Equivalent π circuit of balanced branch.

$$\begin{cases} P_{ij} = V_i^2 \left(G_{i0} + G_{ij}\right) - V_i V_j \left[G_{ij} \cos\left(\theta_i - \theta_j\right) + B_{ij} \sin\left(\theta_i - \theta_j\right) \right] \\ Q_{ij} = -V_i^2 \left(B_{i0} + B_{ij}\right) - V_i V_j \left[G_{ij} \cos\left(\theta_i - \theta_j\right) - B_{ij} \sin\left(\theta_i - \theta_j\right) \right] \end{cases} \tag{3-2}$$

Equation (3-1) is the power injected into node i, and Equation (3-2) is the power flow distribution of branch $i-j$. P and Q represent the active power and the reactive power, respectively. V and θ are the voltage amplitude and the voltage phase angle. G_{ij} and B_{ij} are the conductance and susceptance of branch $i-j$.

The AC power flow model is non-linear, but it can be simplified and linearized into a DC power flow model. The DC power flow model is used to calculate the active power distribution, which needs to meet the following assumptions [170]:

- The branch reactance is much larger than the branch resistance so that the branch resistance or conductance is ignored, $G_{ij} = 0$.
- The difference between the voltage phase angles of each branch is small enough, $\cos(\theta_i - \theta_j) \approx 1$, $\sin(\theta_i - \theta_j) \approx \theta_i - \theta_j$.
- All branches to the ground are ignored, $G_{i0} + jB_{i0} = 0$.
- All nodal voltage amplitude are close enough per unit, $|V_i| = 1$.

Based on the above assumptions, the updated power flow model ignores the reactive power and line losses. As a result, the DC power flow model can be expressed as:

$$P_i = \sum_{j}^{N} B_{ij} \left(\theta_i - \theta_j \right) \tag{3-3}$$

$$P_{ij} = -B_{ij} \left(\theta_i - \theta_j \right) \tag{3-4}$$

Since the DC power flow model is only composed of linear equations, the real solving process becomes simple (it can be directly calculated by the solver under the simulation platform).

Gas flow model

In the gas system, the calculation of gas flow is based on the nodal flow balance, and the nodal gas pressure is used as the state variable to formulate the Weymouth equation as follows [171, 172]:

$$G_{ij} \left| G_{ij} \right| = \frac{p_i^2 - p_j^2}{R_{i,j}^{\mathrm{T}}} \tag{3-5}$$

where p_i and p_j are the gas pressures at nodes i and j, respectively. G_{ij} is the gas flow of branch $i-j$. R_{ij}^{T} is the characteristic parameter of the high- and medium-pressure gas network. Similar to the branch impedance in the power system, R_{ij}^{T} can be regarded as the resistance coefficient of the gas pipeline. In a gas system with given network parameters, R_{ij}^{T} can be determined according to [63].

Equation (3-5) is applicable for high- and medium-pressure gas transmission networks. For a low-pressure distribution network, the gas flow model is rewritten as [172]:

$$G_{ij} \left| G_{ij} \right| = \frac{p_i - p_j}{R_{i,j}^{\mathrm{D}}} \tag{3-6}$$

where R_{ij}^{D} is the characteristic parameter of the low-pressure gas distribution pipeline. It should be noted that if there is a gas compressor on branch $i-j$, which consumes a certain amount of gas to maintain the nodal gas pressures, the following equations will be considered [173]:

$$\gamma_{ij} = \frac{p_j}{p_i} \tag{3-7}$$

$$G_{ij}^{\mathrm{GC}}=\frac{G_{ij}}{\eta_{ij}^{\mathrm{GC}}}\left(\frac{\alpha}{\alpha-1}\right)\left[\left(\frac{p_j}{p_i}\right)^{\left(\frac{\alpha}{\alpha-1}\right)}-1\right] \tag{3-8}$$

where γ_{ij} is the compression ratio. G_{ij}^{GC} is the gas power consumed by the compressor. η_{ij}^{GC} is the compressor efficiency. α is a parameter related to the adiabatic index and compressor temperature.

Since the compressor model described in Equation (3-8) is nonlinear and non-convex, it is difficult to solve the related optimization problem. The linearization method is proposed in [174], which can be used for approximate calculation. Although the temperature factor is not mentioned in the above gas flow model, it cannot be ignored for the effect of temperature on a large-scale, long-distance gas transmission network. To this end, the gas flow equations that take into account the temperature factor are proposed in [175].

In addition, the gas pipeline itself has a certain storage capacity. The amount of gas stored in the pipe is called gas linepack, which can be expressed as [176, 177]:

$$\begin{cases} LP_{ij,0}=\beta\overline{p_{ij}} \\ LP_{ij,t}=LP_{ij,0}+\sum_{h=1}^{t}\left(G_{ij,h}^{\mathrm{in}}-G_{ij,h}^{\mathrm{with}}\right) \end{cases} \tag{3-9}$$

where, $LP_{ij,0}$ is the initial linepack, which is determined by a constant β and the average gas pressure of pipeline $i-j$. $LP_{ij,t}$ is the linepack at time t, which is determined by the initial linepack and the difference between the gas injection and withdrawal of pipeline $i-j$ [63].

Similar to the operation of most storage devices, the gas linepack needs to be restored within a certain period T, which is expressed as:

$$LP_{ij,T}=LP_{ij,0} \tag{3-10}$$

Heat flow model

Fig. 3.3 shows the schematic diagram of the district heating network. Different from the power and gas systems, in the heating (or cooling) system, the heat flow model is described in the form of the boundary function method (BFM). The state variables include branch mass flow, the water temperatures in

supply and return pipes. In general, if the nodal heat load is given, the heat flow model can be expressed as [67]:

$$c_w m_{mn} \left(T_m - T_n\right) = H_{mn} \tag{3-11}$$

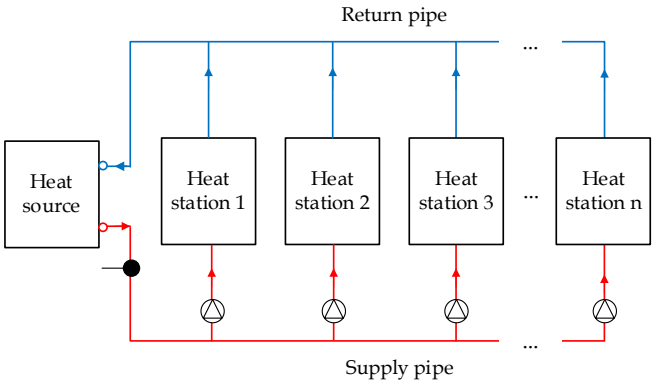

Fig. 3.3: Schematic diagram of a district heating network.

$$k_{mn} m_{mn} \left|m_{mn}\right| = p_m - p_n \tag{3-12}$$

$$T_m - T^{\mathrm{a}} = \left(T_n - T^{\mathrm{a}}\right) \mathrm{e}^{-\frac{\lambda_{mn} L_{mn}}{c_w m_{mn}}} \tag{3-13}$$

$$m_m T_m = \sum_{n=1}^{m} \left(m_n T_n\right) \tag{3-14}$$

where c_w is the specific heat capacity of water. m_{mn} is the mass flow rate through pipe $m-n$. T_m and T_n represent the temperatures of node m and n, respectively. H_{mn} is the heat power exchanged. k_{mn} is the resistance coefficient of pipe $m-n$. p_m and p_n represent the water pressures of node m and node n, respectively. T^a is the ambient temperature. λ_{mn} is the heat transfer coefficient of pipe $m-n$. L_{mn} is the length of pipe $m-n$.

Equation (3-11) represents the heat exchange, which describes the relationship between the mass flow, nodal temperatures and heat power. Equation (3-12) represents the hydraulic pressure drop, which defines the relationship between the nodal pressure and mass flow. Equation (3-13) represents the temperature drop, which describes the water temperature reduction caused by the heat loss in the pipe transmission process. Equation (3-14) represents

the fluid mixing, which describes the temperature change of the node at which the water from the connected branches is mixed.

Sometimes, the pressure provided by the heat source node may not guarantee the fluid delivery in the entire network. For this reason, the circulation pump can be added at an appropriate location of the pipe. The following equations should be considered for pipe $m-n$ with a pump [178].

$$H_{mn}^{\mathrm{CP}}=\frac{m_{mn}gp_{mn}^{\mathrm{CP}}}{\eta_{mn}^{\mathrm{CP}}} \tag{3-15}$$

where H_{mn}^{CP} is the heat power consumed by the circulating pump. g is the acceleration of gravity. p_{mn}^{CP} is the pressure output of the circulating pump; η_{mn}^{CP} is the pump efficiency.

As shown in the above heat flow model, the district heating system can control the heat supply by adjusting the fluid flow rate and water temperature. Therefore, the heat system operator can adopt four control schemes according to different given conditions: the constant flow constant temperature (CFCT) strategy, the constant flow variable temperature (CFVT) strategy, the variable flow constant temperature (VFCT) strategy and the variable flow and variable temperature (VFVT) strategy [23-26].

3.2.2. Modelling of energy facilities

GFCHP unit

In traditional power generation, the heat generated by the plant is largely wasted. CHP plants can capture this "waste" heat for beneficial use, thereby improving energy efficiency. In this work, the GFCHP unit becomes a conversion interface between the power, gas and district heating subsystems. The GFCHP units supply heat and electricity by burning natural gas. At time t, the power model of GFCHP unit i can be expressed as [23, 63]:

$$P_{i,t}^{\mathrm{CHP}}=\eta_i^{\mathrm{e}}G_{i,t}^{\mathrm{CHP}} \tag{3-16}$$

$$\gamma_i^{\mathrm{CHP}}=\frac{H_{i,t}^{\mathrm{CHP}}}{P_{i,t}^{\mathrm{CHP}}}=\frac{\eta_i^{\mathrm{h}}\left(1-\eta_i^{\mathrm{e}}-\eta_i^{\mathrm{l}}\right)}{\eta_i^{\mathrm{e}}} \tag{3-17}$$

where $G_{i,t}^{\mathrm{CHP}}$ is the gas power consumed of GFCHP unit i. $P_{i,t}^{\mathrm{CHP}}$ and $H_{i,t}^{\mathrm{CHP}}$ represent the electric power and heat power produced of GFCHP unit i,

respectively. γ_i^{CHP} is the heat-to-electricity ratio. η_i^{e}, η_i^{l} and η_i^{h} are the electricity production efficiency, heat loss coefficient and heat exchange coefficient, respectively. It should be noted that the GFCHP unit in this research adopts an operating mode that determines electricity generation by heat load. More specifically, the GFCHP unit is controlled by the operator of the district heating subsystem to satisfy the heat load first, which results in a constant electricity-to-heat ratio γ_i^{CHP}.

Storage unit

Based on the storage model mentioned in Section 2.3, the operating equation of each energy storage unit is composed of charging/discharging power limitation, energy balance, state of charge limitation (storage capacity limitation), and storage recovery constraint. During the scheduling period T, their operating constraints can be expressed as follows [69, 75].

$$\begin{cases} G_{i,t}^{\mathrm{GS,min}} \le \left| G_{i,t}^{\mathrm{GS}} \right| \le G_{i,t}^{\mathrm{GS,max}} \\ SOC_{i,t+1}^{\mathrm{GS}} = SOC_{i,t}^{\mathrm{GS}} + G_{i,t}^{\mathrm{GS}} \Delta t \\ S_{i,t}^{\mathrm{GS,min}} \le SOC_{i,t}^{\mathrm{GS}} \le S_{i,t}^{\mathrm{GS,max}} \\ SOC_{i,0}^{\mathrm{GS}} = SOC_{i,T}^{\mathrm{GS}} \end{cases} \tag{3-18}$$

where $G_{i,t}^{\mathrm{GS}}$ is the gas power change of gas storage unit i. When $G_{i,t}^{\mathrm{GS}} > 0$, the gas storage unit i is in a gas charging state, and when $G_{i,t}^{\mathrm{GS}} < 0$, it is in a gas discharging state. $SOC_{i,t}^{\mathrm{GS}}$ is the state of charge in gas storage unit i. $SOC_{i,T}^{\mathrm{GS}}$ and $SOC_{i,0}^{\mathrm{GS}}$ are the initial and final states of charge in gas storage unit i. $G_{i,t}^{\mathrm{GS,min}}$ and $G_{i,t}^{\mathrm{GS,max}}$ represent the allowable minimum and maximum charging or discharging gas power of gas storage unit i, respectively.

$$\begin{cases} H_{i,t}^{\mathrm{HS,min}} \le \left| H_{i,t}^{\mathrm{HS}} \right| \le H_{i,t}^{\mathrm{HS,max}} \\ SOC_{i,t+1}^{\mathrm{HS}} = SOC_{i,t}^{\mathrm{HS}} + \eta_i^{\mathrm{HS}} H_{i,t}^{\mathrm{HS}} \Delta t \\ S_{i,t}^{\mathrm{HS,min}} \le SOC_{i,t}^{\mathrm{HS}} \le S_{i,t}^{\mathrm{HS,max}} \\ SOC_{i,0}^{\mathrm{HS}} = SOC_{i,T}^{\mathrm{HS}} \end{cases} \tag{3-19}$$

where $H_{i,t}^{\mathrm{HS}}$ is the heat power change of heat storage unit i. When $H_{i,t}^{\mathrm{HS}} > 0$, the heat storage unit i is in a heat charging state, and when $H_{i,t}^{\mathrm{HS}} < 0$, it is in a heat discharging state. $SOC_{i,t}^{\mathrm{HS}}$ is the state of charge in heat storage unit i. η_i^{HS} is heat storage efficiency. $SOC_{i,T}^{\mathrm{HS}}$ and $SOC_{i,0}^{\mathrm{HS}}$ are the initial and final states of charge in heat storage unit i. $H_{i,t}^{\mathrm{HS,min}}$ and $H_{i,t}^{\mathrm{HS,max}}$ represent the allowable minimum

and maximum charging/discharging heat power of heat storage unit i, respectively.

P2G unit, GB and EB

Based on the Equations (2-5) and (2-6) in Section 2.5, for each time step t, the operating constraints of the P2G unit, the GB and the EB can be expressed as [63, 179]:

$$\begin{cases} G_{i,t}^{\mathrm{P2G}} = \eta_i^{\mathrm{P2G}} P_{i,t}^{\mathrm{P2G}} \\ G_{i,t}^{\mathrm{P2G,min}} \le G_{i,t}^{\mathrm{P2G}} \le G_{i,t}^{\mathrm{P2G,max}} \end{cases} \tag{3-20}$$

$$\begin{cases} H_{i,t}^{\mathrm{GB}} = \eta_i^{\mathrm{GB}} G_{i,t}^{\mathrm{GB}} \\ H_{i,t}^{\mathrm{GB,min}} \le H_{i,t}^{\mathrm{GB}} \le H_{i,t}^{\mathrm{GB,max}} \end{cases} \tag{3-21}$$

$$\begin{cases} H_{i,t}^{\mathrm{EB}} = COP_i^{\mathrm{EB}} P_{i,t}^{\mathrm{EB}} \\ H_{i,t}^{\mathrm{EB,min}} \le H_{i,t}^{\mathrm{EB}} \le H_{i,t}^{\mathrm{EB,max}} \end{cases} \tag{3-22}$$

where η_i^{P2G}, η_i^{GB}, and COP_i^{EB} are conversion efficiencies of the corresponding units. $G_{i,t}^{\mathrm{P2G}}$ and $P_{i,t}^{\mathrm{P2G}}$ are the gas power generated and electric power consumed of P2G unit i, respectively. $G_{i,t}^{\mathrm{P2G,min}}$ and $G_{i,t}^{\mathrm{P2G,max}}$ are the bounds of the gas output of P2G unit i. $H_{i,t}^{\mathrm{GB}}$ and $G_{i,t}^{\mathrm{GB}}$ are the heat power generated and gas power consumed, respectively. $H_{i,t}^{\mathrm{GB,min}}$ and $H_{i,t}^{\mathrm{GB,max}}$ are the bounds of the heat output of GB unit i. $H_{i,t}^{\mathrm{EB}}$ and $P_{i,t}^{\mathrm{EB}}$ are the heat power generated and electric power consumed of EB unit i, respectively. $H_{i,t}^{\mathrm{EB,min}}$ and $H_{i,t}^{\mathrm{EB,max}}$ are the bounds of the heat output of EB unit i.

3.3. Optimal Operation for Coordinating FRs

This section proposes a solution to coordinate and optimize FRs across MESs. A multi-objective day-ahead scheduling model is developed using information from the day-ahead market for electricity and gas pricing. The proposed model searches for the Pareto optimal solution using the IPOPT solver in GAMS software [179]. Then, the simulation results of the test system are discussed and analyzed.

3.3.1. Multi-objective day-ahead scheduling model

Before formulating the model, there are several assumptions:

- Each energy subsystem has an individual operator to pursue its social welfare maximization;
- The power and district heating subsystems are small enough not to affect the real-time energy prices in the wholesale market;
- There is smooth information dissemination between the market and systems, as well as the perfect communication between energy subsystems;
- The operating cost is replaced with the corresponding fuel cost.
- The marginal cost of wind generation is set to 0, and there is no penalty for wind power curtailment.

As a common evaluation indicator in optimization problems, social welfare is defined as the total benefits of consumers and suppliers in the energy system [157]. The consumers' welfare can be calculated by the total marginal benefits of energy consumption minus the expenses of energy purchasing. The suppliers' welfare is described as the difference between the revenues from the selling energy and the costs of energy generation. Therefore, maximum social welfare is introduced as objective function of the optimization problem, which can be expressed as:

$$\text{Max f}\left(\boldsymbol{x}\right)=\sum_{t=1}^{T}\left\{\underbrace{\left[B\left(\boldsymbol{d}\right)-\boldsymbol{fp}\cdot\boldsymbol{d}\right]}_{\text{Benefits}\quad\text{Expenses}}+\underbrace{\left[\boldsymbol{fp}\cdot\boldsymbol{g}+C\left(\boldsymbol{g}\right)\right]}_{\text{Revenues}\quad\text{Costs}}\right\} \tag{3-23}$$

where T sets time horizon as 24h. $\boldsymbol{d}$ and $\boldsymbol{g}$ are the sets of power variables related to energy demand and production, respectively. $\boldsymbol{fp}$ is the set of energy price variables.

In order to facilitate subsequent solving and programming, the objective function of each subsystem should be expressed in a minimized form. Therefore, the objective functions are transformed into minimizing negative social welfare, which are expressed as [179]:

$$\min\ \text{f}_{\text{PS}}\left(\boldsymbol{x}^{\text{PS}}\right)=\sum_{t=1}^{T}\left(\begin{array}{l}\sum_{i=1}^{N^{\text{CFP}}}c_{i}^{\text{CFP}}P_{i,t}^{\text{CFP}}+\sum_{i=1}^{N^{\text{CHP}}}fp_{t}^{\text{e}}P_{i,t}^{\text{CHP}}\\-\sum_{i=1}^{N^{\text{EB}}}fp_{t}^{\text{e}}P_{i,t}^{\text{EB}}-\sum_{i=1}^{N^{\text{P2G}}}fp_{t}^{\text{e}}P_{i,t}^{\text{P2G}}-\sum_{i=1}^{N^{\text{PL}}}B^{\text{PL}}P_{i,t}^{\text{IDR}}\end{array}\right) \tag{3-24}$$

$$\min \ \mathrm{f}_{\mathrm{GS}}\left(\boldsymbol{x}^{\mathrm{GS}}\right)=\sum_{t=1}^{T}\left(\begin{array}{l}\sum_{j=1}^{N^{\mathrm{SN}}} c_{j}^{\mathrm{SN}} G_{j,t}^{\mathrm{SN}}+\sum_{i=1}^{N^{\mathrm{P2G}}} fp_{t}^{\mathrm{e}} P_{i,t}^{\mathrm{P2G}}+\sum_{j=1}^{N^{\mathrm{GS}}} c_{j}^{\mathrm{GS}}\left|G_{j,t}^{\mathrm{GS}}\right| \\ -\sum_{j=1}^{N^{\mathrm{GB}}} fp_{t}^{\mathrm{g}} G_{j,t}^{\mathrm{GB}}-\sum_{j=1}^{N^{\mathrm{CHP}}} fp_{t}^{\mathrm{g}} G_{j,t}^{\mathrm{CHP}}-\sum_{j=1}^{N^{\mathrm{GL}}} B^{\mathrm{GL}} G_{j,t}^{\mathrm{l}}\end{array}\right) \tag{3-25}$$

$$\min \ \mathrm{f}_{\mathrm{HS}}\left(\boldsymbol{x}^{\mathrm{HS}}\right)=\sum_{t=1}^{T}\left(\begin{array}{l}\sum_{i=1}^{N^{\mathrm{EB}}} fp_{t}^{\mathrm{e}} P_{i,t}^{\mathrm{EB}}+\sum_{j=1}^{N^{\mathrm{GB}}} fp_{t}^{\mathrm{g}} G_{j,t}^{\mathrm{GB}}+\sum_{j=1}^{N^{\mathrm{CHP}}} fp_{t}^{\mathrm{g}} G_{j,t}^{\mathrm{CHP}} \\ +\sum_{m=1}^{N^{\mathrm{HS}}} c_{m}^{\mathrm{HS}}\left|H_{m,t}^{\mathrm{HS}}\right|-\sum_{i=1}^{N^{\mathrm{CHP}}} fp_{t}^{\mathrm{e}} P_{i,t}^{\mathrm{CHP}}-\sum_{m=1}^{N^{\mathrm{HL}}} B^{\mathrm{HL}} H_{m,t}^{\mathrm{l}}\end{array}\right) \tag{3-26}$$

where N is the number set of energy units or nodes. c and B represent the marginal cost and the marginal benefit, respectively. fp_t^{e} and fp_t^{g} are the hourly electricity and gas prices in the day-ahead market. At time t, $P_{i,t}^{\mathrm{IDR}}$, $G_{j,t}^{\mathrm{l}}$ and $H_{m,t}^{\mathrm{l}}$ is the nodal power load improved by load shifting of the DR service, the nodal gas load and the nodal heat load. $P_{i,t}^{\mathrm{CFP}}$ is the electric power generated by CFP unit i at time t. $G_{j,t}^{\mathrm{SN}}$ is the gas power provided by gas source node j at time t.

It is noted that the energy storage facility is a net consumer due to the storage process accompanied by energy losses [52]. Generally, social welfare consists of the benefits created by consumers and the operating costs of producers [157]. Equation (3-24) includes five components - the fuel cost of CFP units, the cost of purchasing electricity by GFCHP units, the profit of selling electricity by EBs and P2Gs, and the benefit created by power load. Equation (3-25) includes six components - the gas injection cost of the gas source node, the cost of purchasing electricity by P2G units, the operating cost of gas storage, the profit of selling gas by GBs and GFCHP units, and the benefit created by gas load. Equation (3-26) also includes six components - the cost of purchasing electricity by EBs the cost of purchasing gas by GBs and GFCHP units, the operating cost of heat storage, the profit of selling electricity by GFCHP units and the benefit created by heat load.

At each time step t, energy supply and demand should be balanced in the operation of each energy subsystem.

$$\begin{aligned}&\sum_{i=1}^{N^{\mathrm{CFP}}} P_{i,t}^{\mathrm{CFP}}+\sum_{i=1}^{N^{\mathrm{CHP}}} P_{i,t}^{\mathrm{CHP}}+\sum_{i=1}^{N^{\mathrm{WT}}}\left(P_{i,t}^{\mathrm{WT}}-P_{i,t}^{\mathrm{WC}}\right) \\ &\quad-\sum_{i=1}^{N^{\mathrm{EB}}} P_{i,t}^{\mathrm{EB}}-\sum_{i=1}^{N^{\mathrm{P2G}}} P_{i,t}^{\mathrm{P2G}}-\sum_{i=1}^{N^{\mathrm{PL}}} P_{i,t}^{\mathrm{IDR}}=0\end{aligned} \tag{3-27}$$

$$\sum_{j=1}^{N^{\mathrm{SN}}} G_{j,t}^{\mathrm{SN}} + \sum_{i=j}^{N^{\mathrm{P2G}}} G_{j,t}^{\mathrm{P2G}} - \sum_{j=1}^{N^{\mathrm{GS}}} G_{j,t}^{\mathrm{GS}} - \sum_{j=1}^{N^{\mathrm{LP}}} \left(G_{j,h}^{\mathrm{in}} - G_{j,h}^{\mathrm{with}} \right) - \sum_{j=1}^{N^{\mathrm{GB}}} G_{j,t}^{\mathrm{GB}} - \sum_{j=1}^{N^{\mathrm{CHP}}} G_{j,t}^{\mathrm{CHP}} - \sum_{j=1}^{N^{\mathrm{GL}}} G_{j,t}^{\mathrm{l}} = 0 \tag{3-28}$$

$$\sum_{m=1}^{N^{\mathrm{GB}}} H_{m,t}^{\mathrm{GB}} + \sum_{m=1}^{N^{\mathrm{EB}}} H_{m,t}^{\mathrm{EB}} + \sum_{m=1}^{N^{\mathrm{CHP}}} H_{m,t}^{\mathrm{CHP}} - \sum_{m=1}^{N^{\mathrm{HS}}} H_{m,t}^{\mathrm{HS}} - \sum_{m=1}^{N^{\mathrm{HL}}} H_{m,t}^{\mathrm{l}} = 0 \tag{3-29}$$

where $P_{i,t}^{\mathrm{WT}}$ and $P_{i,t}^{\mathrm{WC}}$ are the wind power output and the wind power curtailment of wind turbine i.

In addition, these objective functions are subject to the operating constraints of energy facilities and the transmission constraints of the networks. The constraints include Equations (2-7)-(2-12) and (3-3)-(3-22), as well as the following equations.

$$0 \le P_{i,t}^{\mathrm{WT}} \le P_{i,t}^{\mathrm{WT,max}} \tag{3-30}$$

$$0 \le G_{j,t}^{\mathrm{SN}} \le G_{j,t}^{\mathrm{SN,max}} \tag{3-31}$$

$$\begin{cases} P_{i,t}^{\mathrm{CFP,min}} \le P_{i,t}^{\mathrm{CFP}} \le P_{i,t}^{\mathrm{CFP,max}} \\ \left| P_{i,t+1}^{\mathrm{CFP}} - P_{i,t}^{\mathrm{CFP}} \right| \le RP_{i,t}^{\mathrm{CFP}} \end{cases} \tag{3-32}$$

$$\left| P_{ni,t} \right| \le P_{ni}^{\mathrm{TL}} \tag{3-33}$$

$$\left| G_{nj,t} \right| \le G_{nj}^{\mathrm{TL}} \tag{3-34}$$

$$\left| H_{nm,t} \right| \le H_{nm}^{\mathrm{TL}} \tag{3-35}$$

where $P_{i,t}^{\mathrm{WT,max}}$ and $G_{j,t}^{\mathrm{SN,max}}$ represent the maximum output power of wind turbine i and gas source node j, respectively. $P_{i,t}^{\mathrm{CFP,min}}$ and $P_{i,t}^{\mathrm{CFP,max}}$ are the minimum and maximum power output of CFP unit i. $RP_{i,t}^{\mathrm{CFP}}$ is the ramping limit of CFP unit i. $P_{ni,}^{\mathrm{TL}}$, G_{nj}^{TL} and H_{nm}^{TL} represent the maximum power allowed to pass through transmission bus $n-i$, gas pipeline $n-j$ and heating pipeline $n-m$.

As a typical method to solve multi-objective optimization, the weighted metric method can convert a multi-objective optimization problem into a single-objective optimization problem by setting weight coefficients [180]. In this MES, the priorities of all energy subsystems are considered the same. Here, the weight coefficient w is introduced and the proposed multi-objective optimization model can be summarized as:

$$\begin{aligned}
\min\ & \mathrm{F}(\boldsymbol{x}) = w_1 \mathrm{f}_{\mathrm{PS}}\left(\boldsymbol{x}^{\mathrm{PS}}\right) + w_2 \mathrm{f}_{\mathrm{GS}}\left(\boldsymbol{x}^{\mathrm{GS}}\right) + w_3 \mathrm{f}_{\mathrm{HS}}\left(\boldsymbol{x}^{\mathrm{HS}}\right) \\
& \text{Equations (2-7)-(2-12),} \\
s.t.\ & \text{Equations (3-3)-(3-22),} \\
& \text{Equations (3-30)-(3-35)} \\
& \boldsymbol{x}^{\mathrm{PS}} \in \left[P_{i,t}^{\mathrm{CFP}}, P_{i,t}^{\mathrm{CHP}}, P_{i,t}^{\mathrm{EB}}, P_{i,t}^{\mathrm{P2G}}, P_{i,t}^{\mathrm{WC}}\right] \\
\text{where, } & \boldsymbol{x}^{\mathrm{GS}} \in \left[G_{j,t}^{\mathrm{SN}}, G_{j,t}^{\mathrm{CHP}}, G_{j,t}^{\mathrm{P2G}}, G_{j,t}^{\mathrm{GB}}, G_{j,t}^{\mathrm{GS}}\right] \\
& \boldsymbol{x}^{\mathrm{HS}} \in \left[H_{m,t}^{\mathrm{CHP}}, H_{m,t}^{\mathrm{EB}}, H_{m,t}^{\mathrm{GB}}, H_{m,t}^{\mathrm{HS}}\right]
\end{aligned} \tag{3-36}$$

where $w_1 = w_2 = w_3 = 1$. Hence, a single-objective nonlinear programming problem is formulated, which can be solved by the IPOPT solver under the GAMS platform.

3.3.2. Description of test system and data

To verify the effectiveness of the proposed optimization model, an illustrative case is simulated. Fig. 3.4 shows the structure of the test system, which consists of a 4-node power system, a 4-node gas system and an 8-node heating system.

The scheduling period T is set to 24 hours. The energy production and consumption data of the Danish DK1 area on January 1, 2017, is selected as a typical day, which is scaled to fit the test case. The data on the energy facilities and market prices involved in the model is collected from Energinet. dk and the Danish Energy Agency [181, 182]. The detailed parameters are listed in Tab. I of Appendix A. Fig. 3.5 shows the input parameters of the model, including hourly wind power profile, electric load profile, gas load profile and heat load profile. Several interesting phenomena can be observed from Fig. 3.5.

- In this typical day, the night and early morning are the peak periods of wind power and heating demand;
- The daytime is the peak period of gas demand, while the electricity peak load is in the evening;

- The demand profiles for gas and electricity are complementary to the demand profiles for wind power and heat.

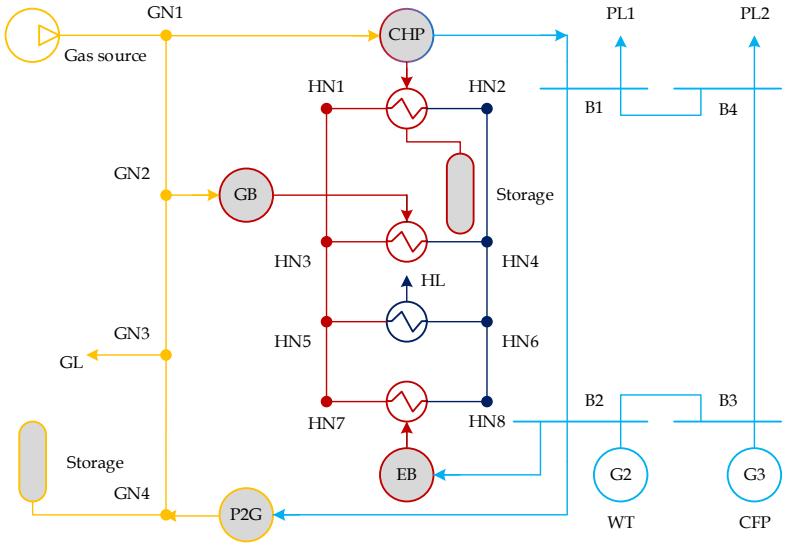

Fig. 3.4: Structure diagram of the test MES. Source: [C2].

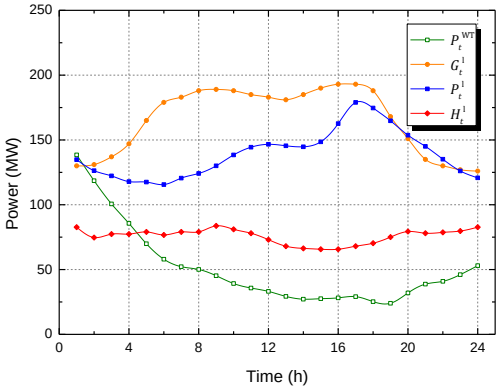

Fig. 3.5: Hourly wind power, electric load, gas load and heat load profiles. Source: [C2].

Fig. 3.6 shows the hourly prices of gas and electricity in the day-ahead market. The gas price is fixed at 17.407€/MWh on the day, while the electricity price varies between 11.1€/MWh and 30.93€/MWh. The changes in the electricity price is related to wind power production and electricity demand at that time.

Generally, the more the electricity demand, the higher the electricity price, and the more available wind power, the lower the electricity price.

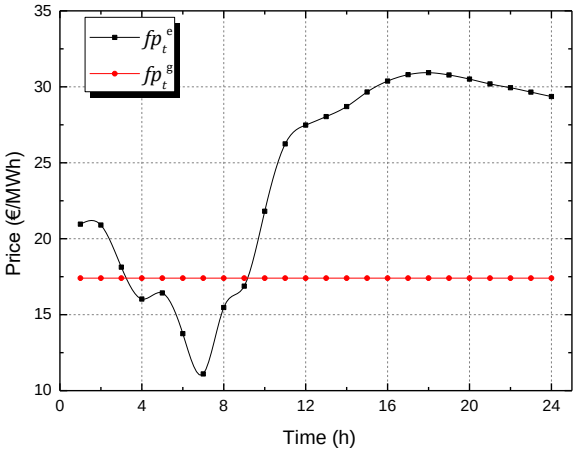

Fig. 3.6: Hourly prices of gas and electricity in the day-ahead market. Source: [C2].

3.3.3. Optimal generation and allocation of energy sources

In the scenario of LPF=0.2, Fig 3.7, Fig. 3.9 and Fig. 3.10 show the optimal operation of the power subsystem, heating subsystem and gas subsystem, respectively. P_t^{D} is the hourly actual electricity demand of the power subsystem, where $P_t^{\mathrm{D}} = P_t^{\mathrm{IDR}} + P_t^{\mathrm{P2G}} + P_t^{\mathrm{EB}}$; P_t^{GW} is the hourly grid-connected wind power, where $P_t^{\mathrm{GW}} = P_t^{\mathrm{WT}} - P_t^{\mathrm{WC}}$; G_t^{D} is the hourly actual gas demand of the gas subsystem, where $G_t^{\mathrm{D}} = G_t^{\mathrm{I}} + G_t^{\mathrm{CHP}} + G_t^{\mathrm{GB}} + G_t^{\mathrm{GS}}$; H_t^{D} is the hourly actual heat demand of the heating subsystem, where $H_t^{\mathrm{D}} = H_t^{\mathrm{I}} + H_t^{\mathrm{HS}}$.

Fig. 3.8 shows the adjustment of the DR service to the initial power load during the scheduling period. According to changes in electricity prices (in Fig. 3.6), the scheduling period can be divided into 5 time-slices for discussing and analyzing the simulation results:

- Periods 1h-4h: The electricity price rapidly decreases to the minimum price 11.1€/MWh;
- Period 5h: There is a small increase in the electricity price;
- Periods 6h-7h: The electricity price continues to drop;
- Periods 8h-18h: The electricity price rapidly increases to the maximum price 30.93€/MWh;
- Periods 19-24h: The electricity price gradually falls off.

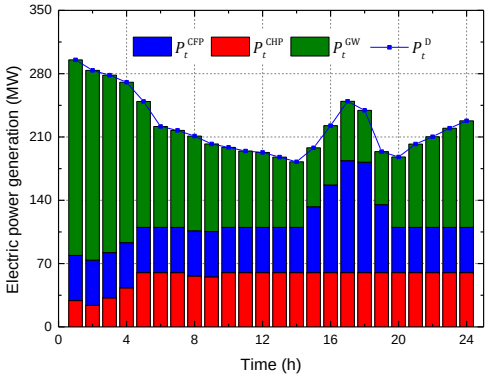

Fig. 3.7: Optimal generation and allocation of the power subsystem. Source: [C2].

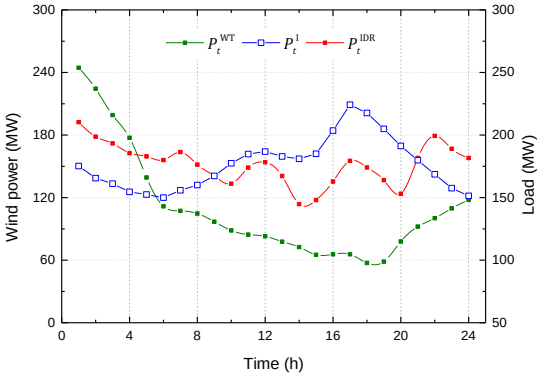

Fig. 3.8: Comparison of DR-adjusted electric load with its initial load and the wind power output. Source: [C2].

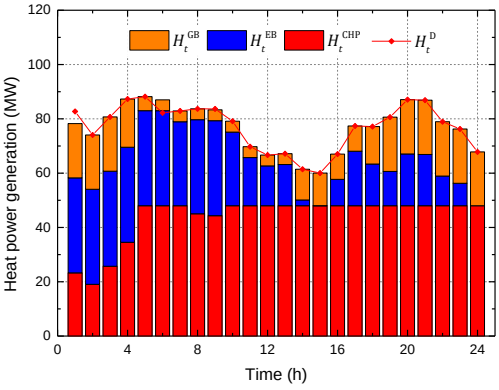

Fig. 3.9: Optimal generation and allocation of the heat subsystem. Source: [C2].

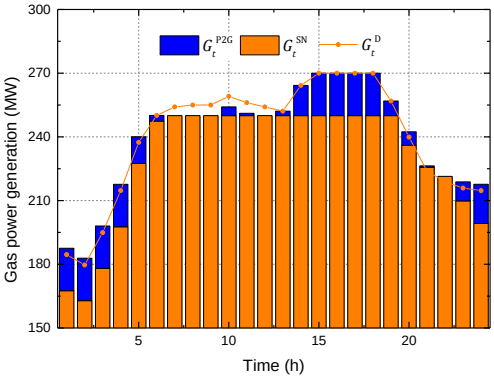

Fig. 3.10: Optimal generation and allocation of the gas subsystem. Source: [C2].

During periods 1h-4h, the MES is in the high-wind operating condition. Due to sufficient wind power and the low electricity price, the power subsystem operator encourages DR consumers to use electricity during these periods. On the other hand, the gas subsystem operator and the heating subsystem operator prefer to run P2G units and EBs to produce gas and heat, respectively.

During period 5h, the wind power of the MES rapidly decreases. This is also the first peak period of the heat and gas loads. Besides the operation of DR regulation, P2G units and EBs, another reason for the increase in the power demand is that the heat and gas storage units are actively storing the heat and gas, which are converted from the cheap electricity.

During periods 6h-7h, the available wind power of the MES can still support most of the power demand. At the same time, the heat load drops, and the gas subsystem operator uses gas storage units instead of P2G units to supply gas. Thus, the power demand is slightly reduced.

During periods 8h-18h, the MES is in the low-wind operating condition. The power and gas loads gradually increase. In particular, period 18h is the peak period of power, gas and heat loads, as well as the peak energy demand of the entire MES. Due to the low wind power and the increasing electricity price, the power subsystem operator encourages DR consumers to reduce electricity consumption during these periods. On the other hand, energy storage devices are used to release energy to supply gas and heat.

During periods 19-24h, the wind power of the MES gradually rises, while the gas and power loads drop. The power subsystem operator once again encourages DR consumers to use electricity during these periods. Due to

sufficient gas supply, the heating subsystem operator prefers to run GFCHP units and GBs to produce heat.

The above simulation results show the effectiveness of the proposed optimization model. Under the objective of maximum social welfare, the model allows optimizing and coordinating all controllable resources of the MES to satisfy multiple energy demands using market price signals. The following will explore the impact of DR participation levels on the MES.

3.3.4. Impacts of LPF on MESs

The scenario of LPF=0 is set as a comparison group. Fig. 3.11 shows the SOC results of the gas and heat storage units in two scenarios (LPF=0 and LPF=0.2) after running the optimization model. It can be seen that $\left|SOC_t^{\mathrm{GS}}\right|$ and $\left|SOC_t^{\mathrm{HS}}\right|$ (the amplitude of the gas and heat storage units) in the scenario of LPF=0.2 are smaller. In other words, the actual used capacity of the energy storage device becomes smaller in the scenario of LPF=0.2. For this reason, the subsystem operators can reduce their investments in storage capacity.

Fig. 3.12 shows the total social welfare (SW) and wind curtailment (WC) of the MES in the scenarios of different LPFs. Here, only the results in the scenarios of LPF≤0.4 are shown. Because in the DR adjustment, obtaining a completely flat electrical load is impractical. From Fig. 3.12, it can be seen that even though P2G devices and EBs are installed in the test system, there is still unusable wind power because of their capacity limitations. With the increase in LPF, the total social welfare improves and the wind curtailment decreases.

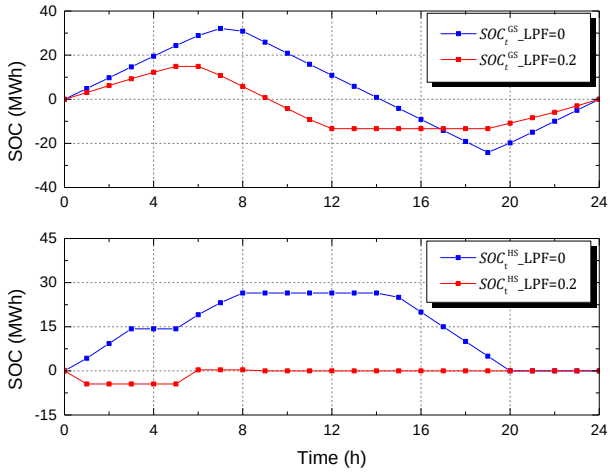

Fig. 3.11: SOCs of gas and heat storage units in the scenarios of LPF=0 and LPF=0.2. Source: [C2].

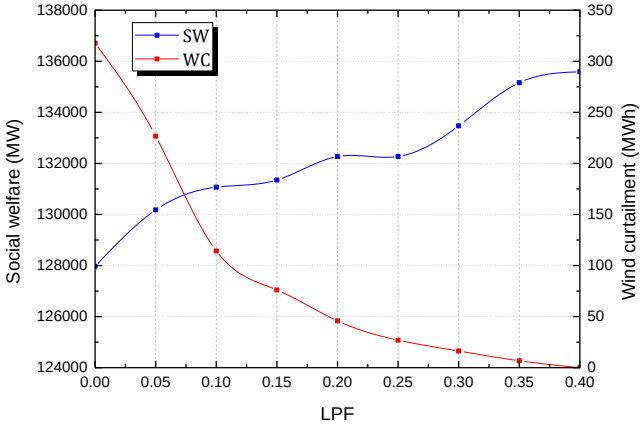

Fig. 3.12: Total social welfare and wind curtailment of the MES in the scenarios of different LPFs. Source: [C2].

3.4. Summary

In this chapter, the integration and coordination of FRs in MESs have been discussed. A multi-objective scheduling model has been proposed to intelligently use FRs and optimize system operation. This is achieved by collecting hourly energy prices in the day-ahead market as the signal for dispatching controllable resources. The proposed approach enables subsystem operators to maximize their own social welfare, while satisfying their individual network constraints. The MES studied in the case has been appropriately improved by referring to the energy supply options in Aalborg, Denmark. The optimization model is solved on the GAMS platform. The simulation results show that FRs are no longer confined to their individual energy subsystems, but are instead interconnected and coordinated through energy networks, which greatly improve the flexibility of the MES. Besides, as a typical demand-side FR, DR participation has positive effects in reducing storage investment, promoting social welfare and wind accommodation. The related publication is C2.

Chapter 4

Bi-level Programming Model for the MES with Flexible Demand

4.1. Background

In Chapter 3, the day-ahead price information is used as a dispatch signal to optimize the operation of the MES. In the proposed optimization problem, electricity and gas prices are a set of input parameters rather than variables. However, in the real-time short-term energy market, the energy prices are determined by the bid between energy supply and demand. More specifically, the system operator needs to submit energy supply and demand information to the market operator, make a plan of the next period for its controllable resources based on the received price, and then repeats this process. Thus, an optimal strategy to design energy pricing, allocate FRs and optimize energy generation is of great significance for improving the economic performance and the utilization of renewable energy.

For the business model of centralized dispatch and operation, the initial studies emphasized the FRs of controlling the energy production and transmission [5, 24, 70]. Recently, researchers have paid more attention to the flexible demand with controllable loads, distributed generators and energy storage [91, 156, 157]. Their core ideas are the integration of electricity and heat at the distribution level. The most typical applications include active distribution networks and smart building management [106, 139, 157, 164]. For instance, the COSES laboratory of the Technical University of Munich has established a small micro-grid in which the consumers are the buildings with a series of flexible facilities [183]. These consumers are aggregated and connected to the demand-side of the upper network to adjust energy flows and participate in market bidding. Several solutions to coordinate the market outcome and system operation have been proposed in [69, 157]. These solutions revolve around the electricity market and emphasize the integrated power distribution and district heating system, while rarely consider the gas system and its short-term market.

Therefore, this chapter builds an MES that integrates gas, electricity and district heating based on the components of the micro-grid proposed by the COSES laboratory. In this MES, consumers are described as smart buildings with PV generation, EV chargers, energy storage facilities and heat pumps. In the next, a bi-level optimization model is proposed in which the upper purpose is to maximize the social welfare of the MES and the lower aims at minimizing the energy purchase cost of consumers. To test the effectiveness of the proposed model, an illustrative case is simulated. By doing so, market outcomes and system operation under the optimal strategy are obtained. Furthermore, the positive impacts of smart buildings as flexible demand on the MES are discussed.

4.2. Bi-level Optimization Formulation and Methodology

Fig. 3.1 shows the structure of the MES with smart buildings as flexible demand. The entire system consists of energy generators, conversion units, storage units, integrated networks, and energy demand. The structure of the smart buildings consults the facility options of the combined smart energy system (COSES) proposed in [183].

The upper structure of the MES focuses on the energy transmission and distribution level. The energy generators include wind turbines (WT), CFP units and gas source nodes. The energy conversion facilities include GFCHP units, GBs and P2G units. The electricity produced by the wind farm, the CFP plant and the GFCHP plant is transmitted to the medium-voltage distribution network through the high-voltage transmission network, and then supplied to the local users. The heat produced by the GBs and the GFCHP plant is delivered to the local heat stations through the district heating (DH) network, and then directly supplied to the local users. The P2G plant is installed near the wind farm. By doing so, the surplus and cheap electricity is timely converted to the gas that can be injected into the gas network directly or after processing. In addition, the DH and gas networks also install their independent storage devices.

The lower structure of the MES focuses on the energy demand level. Each building is a consumer unit that integrates electricity and heat demands. These buildings are connected to the demand-side of the power distribution network and the DH network through the aggregators. Each of them combines solar panels, EV interfaces, power outlets (to drive appliances), and heat pumps. As a result, their energy consumption patterns are diversified. Here the aggregator acts as an intermediate agency between public utilities and end-users [184]. On the one hand, the aggregator needs to reasonably arrange and control the buildings' energy facilities to meet the daily electricity

and heat demands of users. On the other hand, it collects and submits bidding information and participates in the market on behalf of the demand side of the MES.

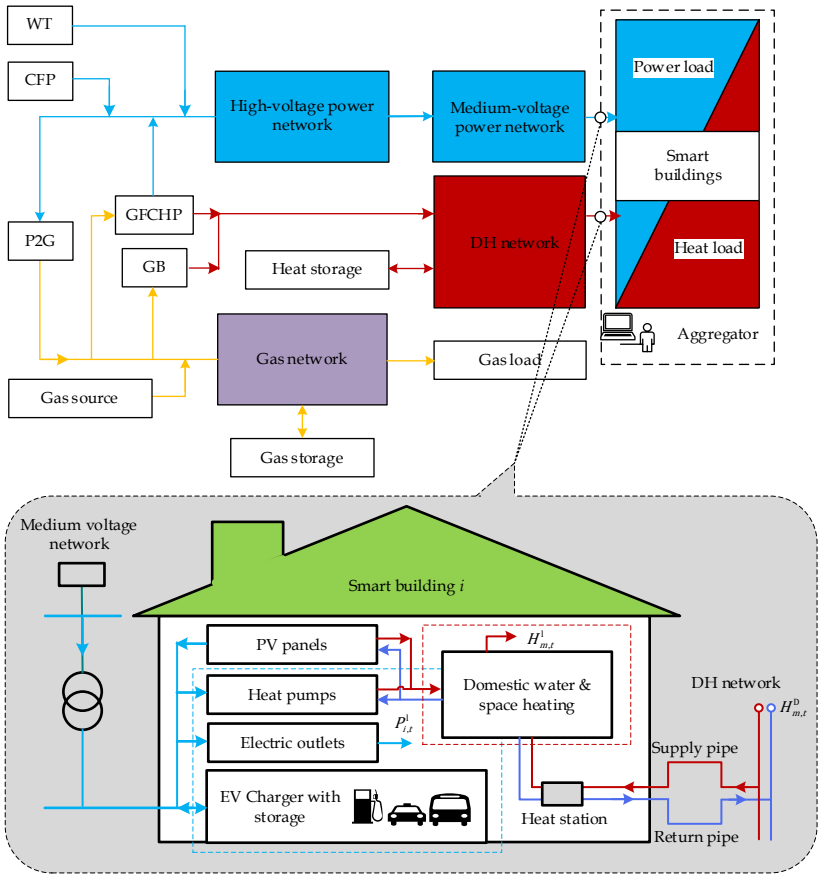

Fig. 4.1: Schematic graph of the MES with smart buildings as flexible demand. Source: [C1].

The formulation and methodology of the bi-level optimization model will be described in detail below.

4.2.1. Model formulation

Before formulating the model, there are several assumptions:

- In the proposed MES, there is an entity, namely independent system operator (ISO), who manages the integrated system including

electricity, gas and DH subsystems by running a centralized dispatch approach;

- The aggregator has an information service platform to ensure the interaction and communication with the upper-level system, as well as to convey information on market decisions and operating arrangements to the lower-level buildings;
- The operating cost is replaced with the corresponding fuel cost. For example, the operating cost of the CFP unit is equal to the marginal cost of its coal consumed;
- The marginal cost of wind and solar generation is set to 0, and there is no penalty for wind power curtailment.

As mentioned in Section 3.2, the DH system is a pure consumer of the power and gas systems. The electricity and gas prices can be used as economic incentives to adjust the consumption patterns of downstream buildings. In return, these smart buildings bring demand-side flexibility to the MES. Based on the clearing price and quantity released by the market operator, the aggregator proposes a plan for the minimum cost of purchasing energy for lower-level users and conveys the related information to the upper-level ISO. Then the ISO optimizes the production and allocation of resources in the MES by centralized scheduling. This process results in a bi-level collaborative optimization problem.

Upper-level optimization problem

In the upper-level optimization problem, the ISO aims to maximize the social welfare of the MES, which has been defined in Equation (3-23). The upper-level objective function consists of 4 components - the benefit created by the integrated electricity and heat consumption of the aggregators, the benefit created by the gas load, the fuel costs of the energy generators and the operating costs of energy storage facilities, which can be expressed as:

$$\text{Max } F=\sum_{t=1}^{T}\left[\begin{array}{l}\sum_{a=1}^{N^{\mathrm{AG}}}\left(B^{\mathrm{e}}P_{a,t}^{\mathrm{D}}+B^{\mathrm{h}}H_{a,t}^{\mathrm{D}}\right)+\sum_{j=1}^{N^{\mathrm{GL}}}B^{\mathrm{g}}G_{j,t}^{\mathrm{l}}\\ -\left(\sum_{i=1}^{N^{\mathrm{CFP}}}c_{i}^{\mathrm{CFP}}P_{i,t}^{\mathrm{CFP}}+\sum_{j=1}^{N^{\mathrm{SN}}}c_{j}^{\mathrm{SN}}G_{j,t}^{\mathrm{SN}}\right)\\ -\left(\sum_{j=1}^{N^{\mathrm{GS}}}c_{j}^{\mathrm{GS}}\left|G_{j,t}^{\mathrm{GS}}\right|+\sum_{i=1}^{N^{\mathrm{HS}}}c_{m}^{\mathrm{HS}}\left|H_{m,t}^{\mathrm{HS}}\right|\right)\end{array}\right] \tag{4-1}$$

where N is the number set of energy units or nodes. T sets time horizon as 24h. c and B represent the marginal cost and the marginal benefit,

respectively. $P_{a,t}^{\mathrm{D}}$ and $H_{a,t}^{\mathrm{D}}$ are the hourly electricity demand and the heat demand of the buildings integrated by aggregator a. $G_{j,t}^{\mathrm{l}}$ is the nodal gas load at time t. $P_{i,t}^{\mathrm{CFP}}$ and $G_{j,t}^{\mathrm{SN}}$ are the hourly electric power generated by CFP unit i and the hourly gas power generated by gas source j. $G_{j,t}^{\mathrm{GS}}$ and $H_{m,t}^{\mathrm{HS}}$ are the hourly gas power change of gas storage j and the hourly heat power change of heat storage m. Variable $P_{i,t}^{\mathrm{CFP}}$, $G_{j,t}^{\mathrm{SN}}$, $G_{j,t}^{\mathrm{GS}}$ and $H_{m,t}^{\mathrm{HS}}$ are subject to the operation constraints of the CFP unit in Equation (3-32), the gas source node in Equation (3-31), gas storage in Equation (3-18) and heat storage units in Equation (3-19), respectively.

In the MES, the ISO is subject to the constraints of network transmission and facility operation to ensure the balance between energy supply and demand over time. Thus, the energy balance of each energy subsystem is determined by:

$$\sum_{i=1}^{N^{\mathrm{CFP}}} P_{i,t}^{\mathrm{CFP}} + \sum_{i=1}^{N^{\mathrm{CHP}}} P_{i,t}^{\mathrm{CHP}} + \sum_{i=1}^{N^{\mathrm{WT}}} P_{i,t}^{\mathrm{GW}} - \sum_{i=1}^{N^{\mathrm{P2G}}} P_{i,t}^{\mathrm{P2G}} - \sum_{a=1}^{N^{\mathrm{AG}}} P_{a,t}^{\mathrm{D}} = 0 \tag{4-2}$$

$$\begin{aligned} \sum_{j=1}^{N^{\mathrm{SN}}} G_{j,t}^{\mathrm{SN}} + \sum_{i=j}^{N^{\mathrm{P2G}}} G_{j,t}^{\mathrm{P2G}} - \sum_{j=1}^{N^{\mathrm{GS}}} G_{j,t}^{\mathrm{GS}} - \sum_{j=1}^{N^{\mathrm{LP}}} \left(G_{j,h}^{\mathrm{in}} - G_{j,h}^{\mathrm{with}} \right) \\ - \sum_{j=1}^{N^{\mathrm{GB}}} G_{j,t}^{\mathrm{GB}} - \sum_{j=1}^{N^{\mathrm{CHP}}} G_{j,t}^{\mathrm{CHP}} - \sum_{j=1}^{N^{\mathrm{GL}}} G_{j,t}^{\mathrm{l}} = 0 \end{aligned} \tag{4-3}$$

$$\sum_{m=1}^{N^{\mathrm{GB}}} H_{m,t}^{\mathrm{GB}} + \sum_{m=1}^{N^{\mathrm{CHP}}} H_{m,t}^{\mathrm{CHP}} - \sum_{m=1}^{N^{\mathrm{HS}}} H_{m,t}^{\mathrm{HS}} - \sum_{a=1}^{N^{\mathrm{AG}}} H_{a,t}^{\mathrm{D}} = 0 \tag{4-4}$$

The transmission constraints of energy networks are expressed in Equations (3-33)-(3-35). The operating constraints of the energy conversion facilities including the P2G unit, the GB unit and the GFCHP unit are given in Equation (3-20), Equation (3-21) and Equations (3-16)-(3-17), respectively.

Lower-level optimization problem

In the lower-level optimization problem, the aggregator aims to minimize the energy purchase cost of the downstream buildings. The lower-level objective function can be expressed as:

$$\begin{aligned}\left(P_{a,t}^{\mathrm{D}}, H_{a,t}^{\mathrm{D}}\right) \in \arg\ \min\ \mathrm{f} &= \begin{bmatrix} fp_t^{\mathrm{e}} \\ fp_t^{\mathrm{g}} \end{bmatrix} \cdot \sum_{a=1}^{N^{\mathrm{AG}}} \left(P_{a,t}^{\mathrm{D}}, H_{a,t}^{\mathrm{D}}\right) \\ &= fp_t^{\mathrm{g}} \sum_{j=1}^{N^{\mathrm{CHP} \cup \mathrm{GB}}} \left(G_{j,t}^{\mathrm{CHP}} + G_{j,t}^{\mathrm{GB}}\right) - fp_t^{\mathrm{e}} \sum_{i=1}^{N^{\mathrm{P2G}}} P_{i,t}^{\mathrm{P2G}}\end{aligned} \tag{4-5}$$

where fp_t^{e} and fp_t^{g} still represent the hourly electricity and gas prices in the real-time market. From the downstream smart buildings, the aggregator is an energy provider. For aggregator a, the energy balance in supply and demand needs to be maintained over time, as shown below.

$$\begin{cases} P_{a,t}^{\mathrm{D}} = \sum_{b=1}^{N^{\mathrm{B}}} \left(P_{b,t}^{\mathrm{l}} + P_{b,t}^{\mathrm{HP}} + P_{b,t}^{\mathrm{EV}} - P_{b,t}^{\mathrm{PV}}\right) \\ H_{a,t}^{\mathrm{D}} = \sum_{b=1}^{N^{\mathrm{B}}} \left(H_{b,t}^{\mathrm{loss}} + H_{b,t}^{\mathrm{l}} - H_{b,t}^{\mathrm{HP}} - H_{b,t}^{\mathrm{PV}}\right) \end{cases} \tag{4-6}$$

For smart building b at time t, its power demand includes 4 components - the basic power load of the building ($P_{b,t}^{\mathrm{l}}$), the electric power consumed by the heat pump ($P_{b,t}^{\mathrm{HP}}$), the charging/discharging change of the EV ($P_{b,t}^{\mathrm{EV}}$), and power generated by the solar panels ($P_{b,t}^{\mathrm{PV}}$); Its heat demand consists of 4 components as well - the heat loss from the heat station to the building ($H_{b,t}^{\mathrm{loss}}$), the basic heat load of the building ($H_{b,t}^{\mathrm{l}}$), heat power generated by the heat pump ($H_{b,t}^{\mathrm{HP}}$) and the PV facilities ($H_{b,t}^{\mathrm{PV}}$). Variable $H_{b,t}^{\mathrm{loss}}$ can be determined by:

$$H_{b,t}^{\mathrm{loss}} = c_w m_{mn} \left[\left(T_{mn,t}^{\mathrm{s,in}} - T_{mn,t}^{\mathrm{r,out}}\right) - \left(T_{mn,t}^{\mathrm{s,out}} - T_{mn,t}^{\mathrm{r,in}}\right)\right] \tag{4-7}$$

where $T_{mn,t}^{\mathrm{s,in}}$ and $T_{mn,t}^{\mathrm{s,out}}$ are the inlet temperature and outlet temperature of the water supply pipe $m-n$ connecting the heat station to the building. $T_{mn,t}^{\mathrm{r,in}}$ and $T_{mn,t}^{\mathrm{r,out}}$ are the inlet temperature and outlet temperature of the water return pipe $m-n$ connecting the heat station to the building. If the DH network adopts the constant flow control strategy (CFCT or CFVT), the temperature variables in equation (4-7) can be calculated by the function method in [25]. Fig 4.2 shows the physical relation of the four temperature variables in Equation (4-7).

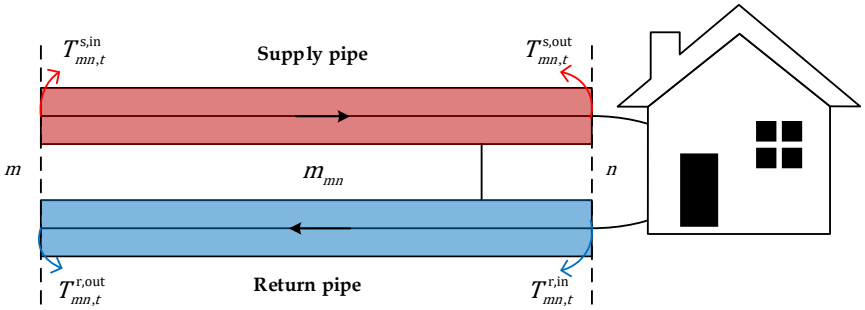

Fig. 4.2: Physical locations of the temperature markers in the pipe $m-n$.

In a smart building, the operating constraints of the heat pump, PV, and the EV charging facility with electricity storage can be expressed as:

$$\begin{cases} H_{b,t}^{\mathrm{HP}} = COP_b^{\mathrm{HP}} P_{b,t}^{\mathrm{HP}} \\ H_{b,t}^{\mathrm{HP,min}} \le H_{b,t}^{\mathrm{HP}} \le H_{b,t}^{\mathrm{HP,max}} \end{cases} \tag{4-8}$$

$$\begin{cases} H_{b,t}^{\mathrm{PV}} = \eta_b^{\mathrm{PV}} P_{b,t}^{\mathrm{PV}} \\ 0 \le P_{b,t}^{\mathrm{PV}} \le P_{b,t}^{\mathrm{PV,max}} \end{cases} \tag{4-9}$$

$$\begin{cases} P_{b,t}^{\mathrm{EV,min}} \le \left| P_{b,t}^{\mathrm{EV}} \right| \le P_{b,t}^{\mathrm{EV,max}} \\ SOC_{b,t+1}^{\mathrm{EV}} = SOC_{b,t}^{\mathrm{EV}} + P_{b,t}^{\mathrm{EV}} \Delta t \\ S_{b,t}^{\mathrm{EV,min}} \le SOC_{b,t}^{\mathrm{EV}} \le S_{b,t}^{\mathrm{EV,max}} \\ SOC_{b,0}^{\mathrm{EV}} = SOC_{b,T}^{\mathrm{EV}} \end{cases} \tag{4-10}$$

where COP_b^{HP} and η_b^{PV} are conversion efficiencies of the heat pump and PV panels. $H_{b,t}^{\mathrm{HP}}$ and $P_{b,t}^{\mathrm{HP}}$ are the heat power generated and electric power consumed of the heat pump, respectively. $H_{b,t}^{\mathrm{HP,min}}$ and $H_{b,t}^{\mathrm{HP,max}}$ are the bounds of the heat output of the heat pump. $H_{b,t}^{\mathrm{PV}}$ and $P_{b,t}^{\mathrm{PV}}$ represent the heat power and electric power generated by the solar panels, respectively. $P_{b,t}^{\mathrm{PV,max}}$ is the maximum output power of the solar panels. $P_{b,t}^{\mathrm{EV}}$ is the changing/discharging power of the EVs. $P_{b,t}^{\mathrm{EV}} > 0$ means that the EV is charging at this time, while $P_{b,t}^{\mathrm{EV}} < 0$ represents that the stored electricity is used. $SOC_{b,t}^{\mathrm{EV}}$ is the state of charge for the EVs. $SOC_{b,T}^{\mathrm{EV}}$ and $SOC_{b,0}^{\mathrm{EV}}$ are the initial and final states of charge for the EVs. $P_{b,t}^{\mathrm{EV,min}}$ and $P_{b,t}^{\mathrm{EV,max}}$ represent the allowable minimum and maximum charging/discharging power of the EVs, respectively.

In order to standardize the model form, Equation (4-1) is negated. The upper function is transformed to minimize the negative social welfare of the MES. Therefore, the proposed multi-objective optimization model can be summarized as:

$$\begin{aligned} &\min\ \mathrm{F}(\boldsymbol{x},\boldsymbol{y}) \\ &\quad \text{Equations (4-2)-(4-4),} \\ &s.t.\ \text{Equations (3-20), (3-21),} \\ &\quad \text{Equations (3-33)-(3-35)} \\ &\text{where } \boldsymbol{y}=\left[P_{a,t}^{\mathrm{D}},H_{a,t}^{\mathrm{D}}\right]\in \min\ \mathrm{f}(\boldsymbol{x},\boldsymbol{z}) \\ &\qquad\qquad s.t.\ \text{Equations (4-6)-(4-10)} \end{aligned} \tag{4-11}$$

4.2.2. Methodology

The solution to the bi-level optimization model has been proposed in [41, 185]. In general, the KKT conditions of the lower model are used to reform the bi-level optimization problem into an equivalent single-level problem of the mathematical programming with equilibrium constraints (MPEC). Then, the strong duality theory, binary expansion approach, big-M method, etc. are used to further transform it into a linear model [46, 50].

In this optimization model, the lower-level model is linear and convex. As a result, it can be rewritten with the KKT conditions from Equation (4-12) to Equation (4-13):

$$\begin{aligned} &\min\ \mathrm{F}(\boldsymbol{x},\boldsymbol{y}) \\ &s.t.\ \begin{matrix} h_i(\boldsymbol{x},\boldsymbol{y})=0,\ i=1,2...I \\ g_j(\boldsymbol{x},\boldsymbol{y})\le 0,\ j=1,2...J \end{matrix} \\ &\text{where } \boldsymbol{y}\in \min\ \mathrm{f}(\boldsymbol{x},\boldsymbol{z}) \\ &\qquad s.t.\ \begin{matrix} h_m(\boldsymbol{x},\boldsymbol{z})=0,\ m=1,2...M \\ g_n(\boldsymbol{x},\boldsymbol{z})\le 0,\ n=1,2...N \end{matrix} \end{aligned} \tag{4-12}$$

$$\min \ \mathrm{F}(\boldsymbol{x},\boldsymbol{y})$$

$$s.t. \quad \begin{aligned} h_i(\boldsymbol{x},\boldsymbol{y}) &= 0, i = 1,2...I \\ g_j(\boldsymbol{x},\boldsymbol{y}) &\le 0, j = 1,2...J \end{aligned}$$

Define Lagrangian Function: (4-13)

$$\mathrm{L}(\boldsymbol{x},\boldsymbol{z},\boldsymbol{\lambda},\boldsymbol{\mu}) = \mathrm{f}(\boldsymbol{x},\boldsymbol{z}) + \sum_{m=1}^{M} \lambda_m h_m(\boldsymbol{x},\boldsymbol{z}) + \sum_{n=1}^{N} \mu_n g_n(\boldsymbol{x},\boldsymbol{z})$$

$$\nabla_{(\boldsymbol{x},\boldsymbol{z})} \mathrm{L}(\boldsymbol{x},\boldsymbol{z},\boldsymbol{\lambda},\boldsymbol{\mu}) = 0$$

$$K.K.T. \quad \begin{aligned} \mu_n g_n(\boldsymbol{x},\boldsymbol{z}) &= 0 \\ \mu_n &\ge 0 \qquad m = 1,2...M \\ h_m(\boldsymbol{x},\boldsymbol{z}) &= 0 \qquad , n = 1,2...N \\ g_n(\boldsymbol{x},\boldsymbol{z}) &\le 0 \end{aligned}$$

where λ_m and μ_n are called 'Lagrange multipliers'. They are introduced as the new sets of variables, leading to the multiplication of two decision variables in the model, such as $\lambda_m h(\boldsymbol{x},\boldsymbol{z})$ and $\mu_n h(\boldsymbol{x},\boldsymbol{z})$. This is why the rewritten MEPC model is non-linear.

Next, the NLPEC solver of the GAMS simulation platform is used to solve the proposed optimization model. More specifically, the NLPEC solver can solve the rewritten MPEC model by reformulating the complementarity constraints, where the model is further reconstructed into a general non-linear programming (NLP) model and solved by the existing NLP solvers. The flowchart of the optimization procedures is shown in Fig. 4.3.

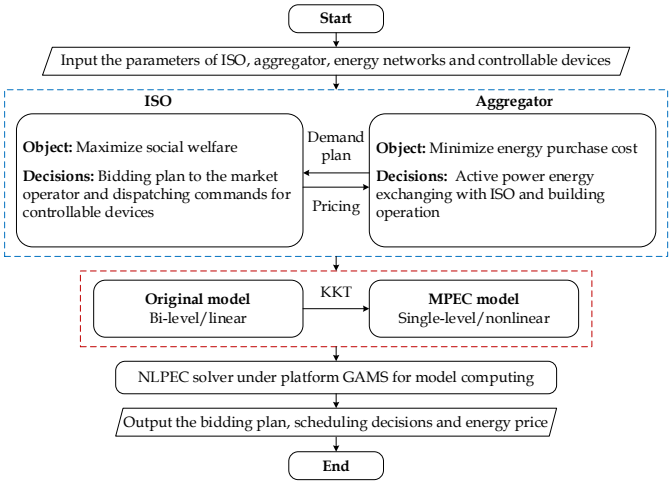

Fig. 4.3: Flowchart of the optimization procedures. Source: [C1].

4.3. Optimal Strategy of the MES

To verify the effectiveness of the proposed optimization model, an illustrative case is simulated. Fig. 4.4 shows the topology diagram of the test system, which is composed of a 24-bus power system, a 4-node gas system and a 20-node DH system. The integrated 24-bus power system is an improvement of the IEEE RTS 24-bus system, as shown in Fig. 4.5.

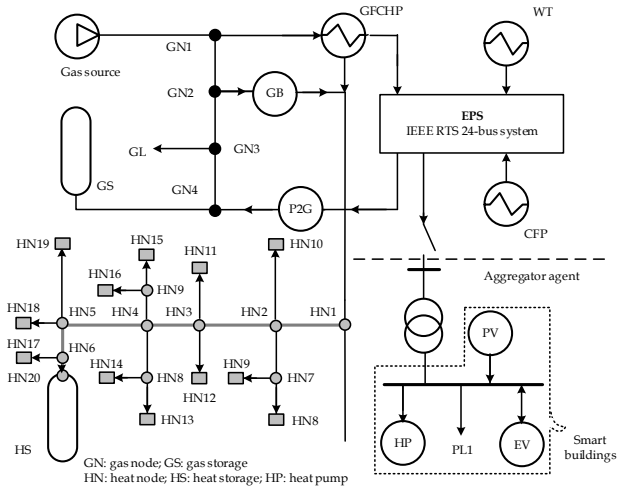

Fig. 4.4: Topology diagram of the test system. Source: [C1].

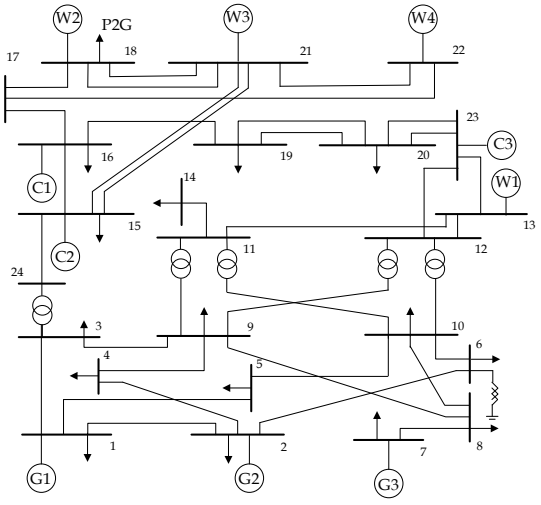

Fig. 4.5: Improved IEEE RTS 24-bus system. Source: [C1].

In the gas subsystem, GN1 and GN3 are the gas source node and the load node, respectively. The GFCHP and GB devices are connected to GN1 and GN2, respectively, corresponding to the heat source node HN1 of the DH subsystem. The gas storage and P2G units are connected to GN4, in which the P2G unit is also connected to bus 18 of the power subsystem. In the DH subsystem, there are 12 heat stations (shown as gray squares) and 38 pipelines (including supply and return water pipes). From the supply side, the heat sources include GBs and GFCHP units. From the load side, the heat pumps and solar panels installed in the building can also supply heat. Besides, the heat storage unit is installed at HN20. In the power subsystem, G1-G3, C1-C3 and W1-W4 represent the GFCHP units, CFP units and wind turbines, respectively. Considering the advantages of installation location, the P2G unit is installed near wind turbine W2.

The scheduling period T is set to 24 hours. The Danish February 1, 2021, is selected as a typical day. The historical data of the Danish DK1 area is scaled to fit the test case [186]. The detailed parameters are listed in Tab. II of Appendix A. Fig. 4.6 shows the input parameters of the model, including the hourly wind power, hourly solar power, electric load, gas load and heat load profiles.

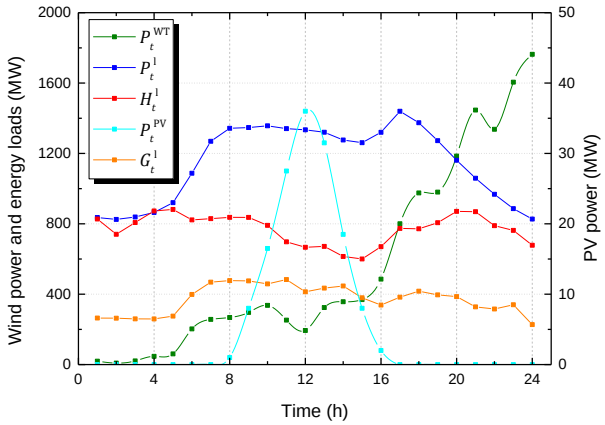

Fig. 4.6: Profiles of the input parameters for the model. Source: [C1].

4.3.1. Optimal generation and market outcomes

Fig. 4.7, Fig. 4.8 and Fig. 4.9 respectively show the simulation results of the optimal energy generation of the MES. Fig. 4.10 shows energy pricing in the market at the maximum social welfare of the MES.

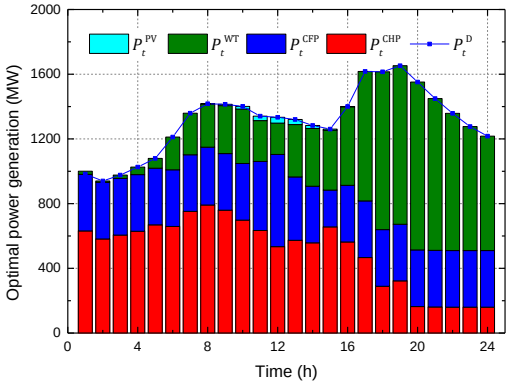

Fig. 4.7: Optimal generation of the power subsystem. Source: [C1].

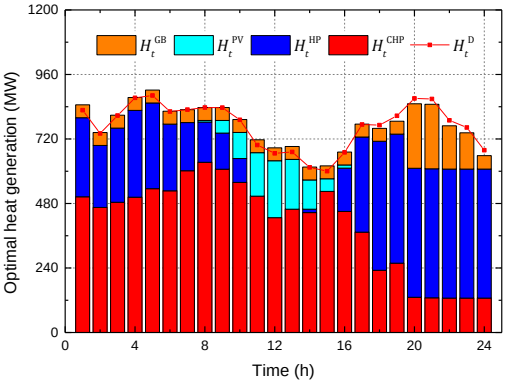

Fig. 4.8: Optimal generation of the heat subsystem. Source: [C1].

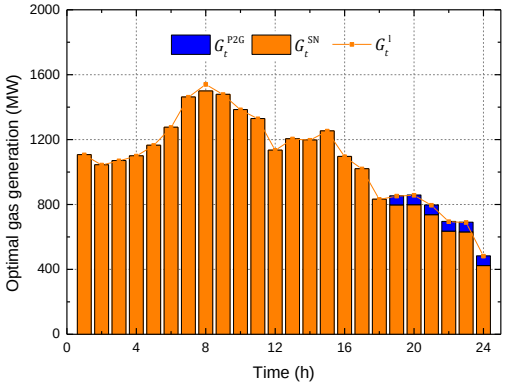

Fig. 4.9: Optimal generation of the gas subsystem. Source: [C1].

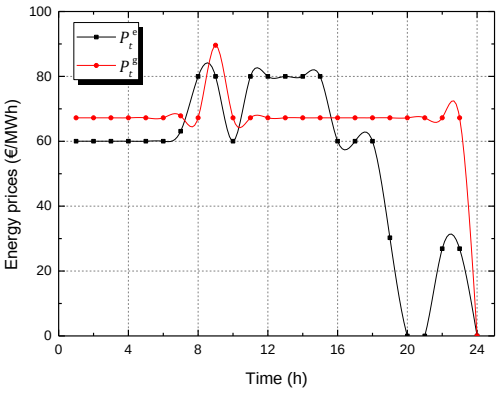

Fig. 4.10: Hourly energy prices in the market. Source: [C1].

It should be noted that CFP and GFCHP units have minimum output constraints during the short-term scheduling to prevent the high cost of unit startup/shutdown [184]. According to the profiles of energy loads and renewable outputs in Fig. 4.6, the scheduling period can be divided into 6 time-slices for discussing and analyzing the simulation results.

During periods 1h-7h, the MES is in the scenario of low wind, no sunshine, non-peaks of gas and electricity demands. As there is not enough wind power to run P2G units, the gas demand is met entirely by the gas source. Although it is a valley of electricity demand, there is a peak of heat demand during these periods. The CHP units produce additional electricity while filling heat demand. This is the reason why the HPs can still actively participate in heating when wind power is insufficient. During these periods, electricity and gas prices stabilize at 60.03 €/MWh and 67.23 €/MWh, respectively.

During periods 8h-9h, the MES is in the scenario of low wind, a little sunshine, peaks of electricity, heat and gas demands. Since the output of wind power is low, the gas source continues to meet the gas demand. The emergence of sunshine makes the PV units begin to produce electricity and heat. As a result, the heat and electricity outputs of CHP units are reduced, as well as the heat production of the pumps. The CFP units have to increase electricity production. Coupled with the impact of peaks of energy demands, the electricity price rises to the marginal cost of CFP unit 80 €/MWh, and the gas price increase to a peak of 89.6 €/MWh.

During periods 10h-15h, the MES is in the scenario of low wind, high solar irradiance, non-peaks of electricity, heat and gas demands. During period 10h, electricity and gas prices fall back to the initial prices due to the reduction of energy demands. However, the heat demand gradually decreased to a

valley after a period of 10h. The rapid growth of the heat output of PV units further restricts the output of the CHP units. As a result, the CFP units increase electricity production and the electricity price rise again to the marginal cost of CFP unit 80 €/MWh.

During periods 16h-21h, the MES is in the scenario of high wind, no sunshine, peaks of electricity and heat demands. Wind power is used extensively for electricity supply as well as heat supply via heat pumps. The electricity price drops rapidly. After a period of 18h, there is enough wind power that can be used to run P2G units. The gas demand can be satisfied by P2G units and the gas source node.

During periods 22h-24h, the MES is in the scenario of high wind, no sunshine, non-peaks of electricity, gas and heat demands. The DH subsystem prefers to operate HPs to supply heat. However, during period 22h, there is a drop in the wind power output, which corresponds to a slight increase in the electricity price. After a period of 23h, with the decrease in energy demands and the rapid increase in the wind power output, the electricity and gas prices both eventually drop to zero.

4.3.2. Optimal operation of energy storage facilities

Fig. 4.11 shows the optimal operation of energy storage facilities in the MES, including gas storage, heat storage and EV charging with storage facilities.

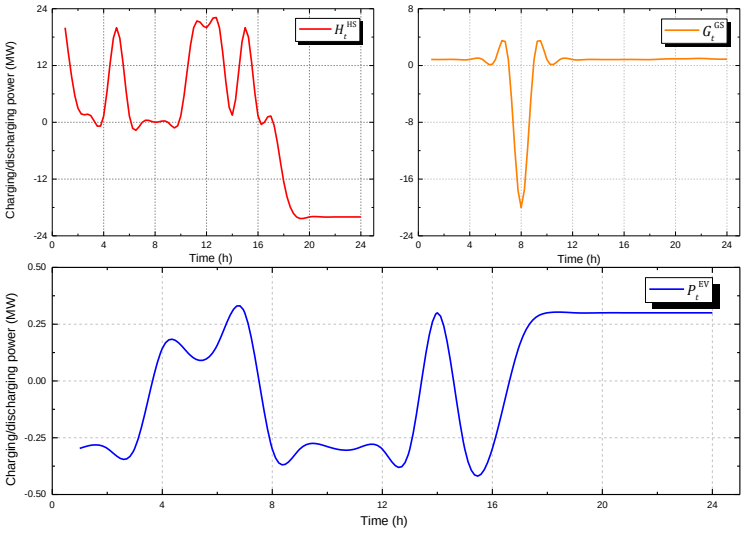

Fig. 4.11: Optimal operation of heat storage, gas storage, and EV charging facilities. Source: [C1].

During the dispatch period, gas and heat storage devices can store cheap energy, thereby assist to supply energy when needed. Analogously, the EV charging facility that combines PV and energy storage can store the excess electricity in batteries for emergencies. From Fig. 4.11, the EVs on the demand side are charged in the periods of 4h-7h, 14h and 17-24h. It should be noted that in shorter charging periods like 4h-7h and14h, EVs are encouraged to use fast charging or battery replacement; In longer charging periods like 17-24h, EVs can use the slow charging pattern. This might match people's daily life and expected actions.

4.4. Impacts of Smart Buildings on MESs

Scenario 1 without smart buildings is set as a comparison group. The control case without smart buildings is achieved by removing heat pumps and EV charging facilities. More specifically, the integrated power and heat demand of each building is decoupled and the storage ability is removed as well.

Tab. 4.1 shows evaluation results in two scenarios (without smart buildings and with smart buildings). It can be seen that, after the building becomes 'smart', the total social welfare of the MES increases and the energy purchase cost of the aggregator decreases. In terms of wind power accommodation, the wind curtailment rate in scenario 2 (22.36%) is much lower than that in scenario 1 (61.70%). In terms of the used capacity of energy storage facilities, the numerical results of gas storage and heat storage in scenario 2 are both lower than those in scenario 1. In summary, smart buildings with HPs and EVs charging provide great flexibility for the demand side of the MES, thereby improving social welfare, increasing wind power accommodation and reducing the investment in storage capacity.

Scenario	**1**	**2**
Social welfare	879,410 €	1,434,500 €
Energy purchase cost	2,061,253 €	1,146,819 €
Wind curtailment rate	61.70%	22.36%
Used capacity of gas storage	23.92MWh	14.10MWh
Used capacity of heat storage	150.31MWh	132.56MWh

Tab. 4.1: Evaluation results in two scenarios. Source: [C1].

4.5. Summary

This chapter proposes an optimal strategy for the MES with flexible demand. This strategy aims to set reasonable market prices and optimize the generation and distribution of controllable resources by centralized scheduling. A bi-level collaborative optimization model and its solution have been developed. In the model, the smart buildings are integrated and aggregated as a flexible demand side of the MES. The MES studied in the case consults the components of the combined energy system proposed by the COSES laboratory, and based on this, the gas system is integrated. The optimization model is solved on the GAMS platform. Numerical studies have confirmed the built-in flexibility of smart buildings. The related publication is C1.

Chapter 5

Nash Equilibrium Market Model For the MES with Multiple FRs

5.1. Background

In Chapter 4, all coupled energy subsystems are controlled and operated by a central entity - ISO in the proposed optimization problem. However, in the existing market mechanism, the power, gas and DH systems have independent operators with limited communication. More specifically, their individual operators pursue their own benefits in the market, in which there is limited cooperation between them. Therefore, it is necessary to propose optimal strategies for collaborative bidding and resource management among multiple market participants.

Game theory provides a theoretical framework for analyzing this interaction among competing market players [187]. Several mathematical programs have been developed to simulate the behaviors of such multi-market participants, such as the mathematical programs with equilibrium constraints (MPEC) and the equilibrium problem with equilibrium constraints (EPEC) [185,188]. As mentioned in Chapter 4, the MPEC is used to describe the single-leader-multi-follower game [185], where the follower's optimal strategy is proposed based on the leader's strategy. The EPEC is used to describe the multi-leader-follower game, in which the equilibrium solution can be obtained by jointly solving the KKT conditions of the multiple MPEC problems [189,190]. However, these equilibrium models are mainly applied to the power system and its market.

Inspired by this, this chapter focuses on the optimal coordination of the MES with multiple FRs under a multi-leader business model, involving generation scheduling, resource allocation, and market pricing. First, a Nash equilibrium model is developed to reflect the decisions of the power, gas, and DH subsystem operators. The energy subsystems play a game for their own benefits until making everyone satisfied. Secondly, the proposed model is simulated under different wind power levels, in which the corresponding optimal strategy is proposed. Then, the centralized scheduling model is

formulated to compare with the proposed equilibrium model. Besides, the impact of different FRs on the MES is also discussed.

5.2. Nash Equilibrium Formulation and Methodology

Fig. 5.1 shows the structure of the MES with multiple FRs. This structure follows the integration of MESs in Section 3, as shown in Fig. 3.1 [179,168]. The constructed MES includes a power system, a gas system and a district heating system. The gas subsystem is composed of the gas source, P2G units, energy storage facilities, the gas network and gas demand. The power subsystem is composed of CFP units, the wind farm, the power network and power demand with DR management. The DH system consists of GFCHP units, GBs, EBs/HPs, heat storage facilities and heat demand. In this MES, there are still energy transactions for electricity and gas (marked as the lines with the moneybag symbol). Electricity trading takes place between

- the power and DH subsystems: On the one hand, the DH subsystem sells electricity to the power subsystem through the GFCHP units; On the other hand, the DH subsystem purchases electricity from the power subsystem through EBs/HPs.
- the electricity and gas subsystem: The gas system purchases electricity from the power subsystem through the P2G units.

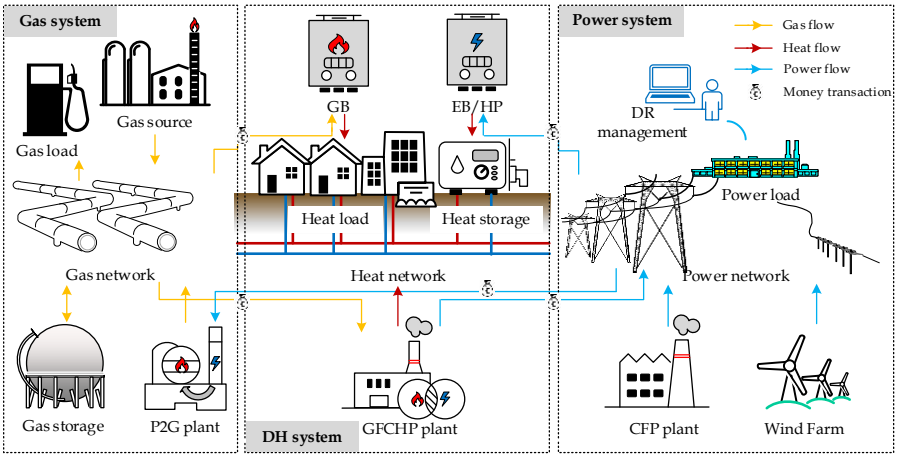

Fig. 5.1: Schematic graph of the MES with multiple FRs. Source: [J1].

The gas transaction mainly occurs between the gas subsystem and the DH system. The DH system purchases gas from the gas subsystem through GFCHP units and GBs.

It needs to be pointed out again that the gas and power subsystem are prosumers, while the DH system is a pure consumer. In this doctoral dissertation, the heat demand is treated as a byproduct of the gas and power subsystems satisfying their own needs. This setting is consistent with the non-profit Danish heat market.

The formulation and solution of the proposed equilibrium optimization model will be described in detail below.

5.2.1. Model formulation

Before formulating the model, there are several assumptions:

- In the proposed MES, each energy subsystem has an individual operator to control its internal resources and manage its market transactions;
- The operating cost is replaced with the corresponding fuel cost.
- The marginal cost of wind and solar generation is set to 0, and there is no penalty for wind power curtailment.

As we mentioned above, centralized scheduling is a cooperative process in which the ISO collaborates with all energy subsystems to pursue a unified goal. This requires perfect and unreserved communication between all energy subsystems. However, in the actual market environment, the subsystem operators can only accept limited coordination due to the confidentiality of their own data information and marketing strategies. Therefore, centralized optimization strategies may not be appropriate for describing existing market procedures.

Different from centralized scheduling, Nash equilibrium can describe this non-cooperative game [185, 190, 191]. The Nash equilibrium model proposed in this thesis provides an opportunity to retain independence for each energy subsystem. In this model, each subsystem operator considers its own operating constraints while pursuing its own benefit in the limited communication with other subsystems. Thus, the optimization of the three subsystems is to be formulated separately, in which each objective function is expressed as the minimization of the negative social welfare.

Power subsystem optimization

In the optimization problem of the power subsystem, the objective function and decision variables can be expressed as:

$$\min \ \mathrm{f}_{\mathrm{PS}}\left(\boldsymbol{x}^{\mathrm{PS}}, \boldsymbol{x}^{\mathrm{PS}'}, \boldsymbol{fp}\right)=\sum_{t=1}^{T}\left(\begin{array}{l}\sum_{i=1}^{N^{\mathrm{CFP}}} c_i^{\mathrm{CFP}} P_{i,t}^{\mathrm{CFP}}+\sum_{i=1}^{N^{\mathrm{CHP}}} fp_t^{\mathrm{e}} P_{i,t}^{\mathrm{CHP}} \\ -\sum_{i=1}^{N^{\mathrm{EB/HP}}} fp_t^{\mathrm{e}} P_{i,t}^{\mathrm{EB/HP}}-\sum_{i=1}^{N^{\mathrm{P2G}}} fp_t^{\mathrm{e}} P_{i,t}^{\mathrm{P2G}}-\sum_{i=1}^{N^{\mathrm{PL}}} B^{\mathrm{PL}} P_{i,t}^{\mathrm{lDR}}\end{array}\right) \tag{5-1}$$

where $\boldsymbol{x}^{\mathrm{PS}} \in \left[P_{i,t}^{\mathrm{CFP}}, P_{i,t}^{\mathrm{GW}}, P_{i,t}^{\mathrm{lDR}}, \theta_{i,t}\right]$, $\boldsymbol{x}^{\mathrm{PS}'} \in \left[P_{i,t}^{\mathrm{CHP}}, P_{i,t}^{\mathrm{EB/HP}}, P_{i,t}^{\mathrm{P2G}}\right]$ and $\boldsymbol{fp} \in \left[fp_t^{\mathrm{e}}, fp_t^{\mathrm{g}}\right]$. It is worth mentioning that the essential difference between Equation (5-1) and Equation (3-24) is that $\boldsymbol{fp}$ here is the decision variables to be solved, which represent the real-time market prices rather than that in Section 3 represent the day-ahead market prices which is the given parameters of the model. The same applies to Equations (5-3) and (3-25), and Equations (5-5) and (3-26).

In the power subsystem, the overall balance between electricity supply and demand can be expressed as:

$$\begin{aligned}&\sum_{i=1}^{N^{\mathrm{CFP}}} P_{i,t}^{\mathrm{CFP}}+\sum_{i=1}^{N^{\mathrm{CHP}}} P_{i,t}^{\mathrm{CHP}}+\sum_{i=1}^{N^{\mathrm{WT}}}\left(P_{i,t}^{\mathrm{WT}}-P_{i,t}^{\mathrm{WC}}\right) \\ &\quad-\sum_{i=1}^{N^{\mathrm{EB/HP}}} P_{i,t}^{\mathrm{EB/HP}}-\sum_{i=1}^{N^{\mathrm{P2G}}} P_{i,t}^{\mathrm{P2G}}-\sum_{i=1}^{N^{\mathrm{PL}}} P_{i,t}^{\mathrm{lDR}}=0\end{aligned} \tag{5-2}$$

The power flow and transmission constraints of the power subsystem are shown in Equations (3-3) and (3-33), respectively.

The operating constraints of the CFP unit, wind turbines and the DR adjustment are expressed as Equations (3-32), (3-30) and (2-7)-(2-12), respectively.

Gas subsystem optimization

In the optimization problem of the gas subsystem, the objective function and decision variables can be expressed as:

$$\min \ \mathrm{f}_{\mathrm{GS}}\left(\boldsymbol{x}^{\mathrm{GS}}, \boldsymbol{x}^{\mathrm{GS}'}, \boldsymbol{fp}\right)=\sum_{t=1}^{T}\left(\begin{array}{l}\sum_{j=1}^{N^{\mathrm{SN}}} c_j^{\mathrm{SN}} G_{j,t}^{\mathrm{SN}}+\sum_{i=1}^{N^{\mathrm{P2G}}} fp_t^{\mathrm{e}} P_{i,t}^{\mathrm{P2G}}+\sum_{j=1}^{N^{\mathrm{GS}}} c_j^{\mathrm{GS}}\left|G_{j,t}^{\mathrm{GS}}\right| \\ -\sum_{j=1}^{N^{\mathrm{GB}}} fp_t^{\mathrm{g}} G_{j,t}^{\mathrm{GB}}-\sum_{j=1}^{N^{\mathrm{CHP}}} fp_t^{\mathrm{g}} G_{j,t}^{\mathrm{CHP}}-\sum_{j=1}^{N^{\mathrm{GL}}} B^{\mathrm{GL}} G_{j,t}^{\mathrm{l}}\end{array}\right) \tag{5-3}$$

where $\boldsymbol{x}^{\mathrm{GS}} \in \left[G_{j,t}^{\mathrm{SN}}, G_{j,t}^{\mathrm{P2G}}, G_{j,t}^{\mathrm{GS}}, G_{j,t}^{\mathrm{LP}}, p_{j,t}\right]$, $\boldsymbol{x}^{\mathrm{GS}'} \in \left[G_{j,t}^{\mathrm{CHP}}, G_{j,t}^{\mathrm{GB}}\right]$ and $\boldsymbol{fp} \in \left[fp_t^{\mathrm{e}}, fp_t^{\mathrm{g}}\right]$.

In the gas subsystem, the energy balance between gas supply and demand can be expressed as:

$$\begin{aligned}\sum_{j=1}^{N^{\mathrm{SN}}} G_{j,t}^{\mathrm{SN}} + \sum_{i=j}^{N^{\mathrm{P2G}}} G_{j,t}^{\mathrm{P2G}} - \sum_{j=1}^{N^{\mathrm{GS}}} G_{j,t}^{\mathrm{GS}} - \sum_{j=1}^{N^{\mathrm{LP}}} \left(G_{j,h}^{\mathrm{in}} - G_{j,h}^{\mathrm{with}} \right) \\ - \sum_{j=1}^{N^{\mathrm{GB}}} G_{j,t}^{\mathrm{GB}} - \sum_{j=1}^{N^{\mathrm{CHP}}} G_{j,t}^{\mathrm{CHP}} - \sum_{j=1}^{N^{\mathrm{GL}}} G_{j,t}^{\mathrm{l}} = 0\end{aligned} \tag{5-4}$$

The gas flow and transmission constraints of the gas subsystem are shown in Equations (3-5)-(3-10) and (3-34), respectively.

The operating constraints of the gas source, P2G units and the gas storage facility are expressed as Equations (3-31), (3-20) and (3-18), respectively.

Heat subsystem optimization

In the optimization problem of the DH subsystem, the objective function and decision variables can be expressed as:

$$\min \ \mathrm{f}_{\mathrm{HS}}\left(\boldsymbol{x}^{\mathrm{HS}}, \boldsymbol{fp} \right) = \sum_{t=1}^{T} \left(\begin{array}{l} \sum_{i=1}^{N^{\mathrm{EB/HP}}} fp_t^{\mathrm{e}} P_{i,t}^{\mathrm{EB/HP}} + \sum_{j=1}^{N^{\mathrm{GB}}} fp_t^{\mathrm{g}} G_{j,t}^{\mathrm{GB}} + \sum_{j=1}^{N^{\mathrm{CHP}}} fp_t^{\mathrm{g}} G_{j,t}^{\mathrm{CHP}} \\ + \sum_{m=1}^{N^{\mathrm{HS}}} c_m^{\mathrm{HS}} \left| H_{m,t}^{\mathrm{HS}} \right| - \sum_{i=1}^{N^{\mathrm{CHP}}} fp_t^{\mathrm{e}} P_{i,t}^{\mathrm{CHP}} - \sum_{m=1}^{N^{\mathrm{HL}}} B^{\mathrm{HL}} H_{m,t}^{\mathrm{l}} \end{array} \right) \tag{5-5}$$

where $\boldsymbol{x}^{\mathrm{HS}} \in \left[H_{m,t}^{\mathrm{EB/HP}}, H_{m,t}^{\mathrm{GB}}, H_{m,t}^{\mathrm{CHP}}, H_{m,t}^{\mathrm{HS}}, T_{m,t} \right]$ and $\boldsymbol{fp} \in \left[fp_t^{\mathrm{e}}, fp_t^{\mathrm{g}} \right]$.

In the DH subsystem, the energy balance between heat supply and demand can be expressed as:

$$\sum_{m=1}^{N^{\mathrm{GB}}} H_{m,t}^{\mathrm{GB}} + \sum_{m=1}^{N^{\mathrm{EB/HP}}} H_{m,t}^{\mathrm{EB/HP}} + \sum_{m=1}^{N^{\mathrm{CHP}}} H_{m,t}^{\mathrm{CHP}} - \sum_{m=1}^{N^{\mathrm{HS}}} H_{m,t}^{\mathrm{HS}} - \sum_{m=1}^{N^{\mathrm{HL}}} H_{m,t}^{\mathrm{l}} = 0 \tag{5-6}$$

The heat flow and transmission constraints of the DH subsystem are shown in Equations (3-11)-(3-15) and (3-35), respectively.

The operating constraints of the GBs, EBs/HPs, the GFCHP unit and the heat storage facility are expressed as Equations (3-21), (3-22), (3-16)-(3-17) and (3-19), respectively. It should be noted that the operating constraint expressions of the EB and the HP are very similar, and the only difference in this

optimization problem is the value of COP. In general, COP_i^{HP} is 2-4 times larger than COP_i^{EB}.

Therefore, the Nash equilibrium market model can be summarized as:

$$
\begin{aligned}
&\text{Find}\left(\boldsymbol{x}^{\mathrm{PS}}, \boldsymbol{x}^{\mathrm{GS}}, \boldsymbol{x}^{\mathrm{HS}}, \boldsymbol{fp}\right) \text{satisfying, } \boldsymbol{fp} \in \left[\boldsymbol{fp}_t^{\mathrm{e}}, \boldsymbol{fp}_t^{\mathrm{g}}\right] \\
&\min\ \mathrm{f}_{\mathrm{PS}}\left(\boldsymbol{x}^{\mathrm{PS}}, \boldsymbol{x}^{\mathrm{PS}'}\right), \begin{cases} \boldsymbol{x}^{\mathrm{PS}} \in \left[P_{i,t}^{\mathrm{CFP}}, P_{i,t}^{\mathrm{GW}}, P_{i,t}^{\mathrm{IDR}}, \theta_{i,t}\right] \\ \boldsymbol{x}^{\mathrm{PS}'} \in \left[P_{i,t}^{\mathrm{CHP}}, P_{i,t}^{\mathrm{EB/HP}}, P_{i,t}^{\mathrm{P2G}}\right] \end{cases} \\
&s.t. \begin{cases} \text{Link constraints } (3-16), (3-17), (3-20), (3-22) \\ \text{Internal constraints } \begin{matrix} (3-3), (3-33), (3-31), (3-32), \\ (2-7)-(2-12), (5-2) \end{matrix} \end{cases} \\
&\min\ \mathrm{f}_{\mathrm{GS}}\left(\boldsymbol{x}^{\mathrm{GS}}, \boldsymbol{x}^{\mathrm{GS}'}\right), \begin{cases} \boldsymbol{x}^{\mathrm{GS}} \in \left[G_{j,t}^{\mathrm{SN}}, P_{i,t}^{\mathrm{P2G}}, G_{j,t}^{\mathrm{GS}}, G_{j,t}^{\mathrm{LP}}, p_{j,t}\right] \\ \boldsymbol{x}^{\mathrm{GS}'} \in \left[G_{j,t}^{\mathrm{CHP}}, G_{j,t}^{\mathrm{GB}}\right] \end{cases} \\
&s.t. \begin{cases} \text{Link constraints } (3-20), (3-21), (3-16), (3-17) \\ \text{Internal constraints } (3-5)-(3-10), (3-34), (5-4) \end{cases} \\
&\min\ \mathrm{f}_{\mathrm{HS}}\left(\boldsymbol{x}^{\mathrm{HS}}\right), \boldsymbol{x}^{\mathrm{HS}} \in \left[H_{m,t}^{\mathrm{EB/HP}}, H_{m,t}^{\mathrm{GB}}, H_{m,t}^{\mathrm{CHP}}, H_{m,t}^{\mathrm{HS}}, T_{m,t}\right] \\
&s.t. \begin{cases} \text{Link constraints } (3-21), (3-22), (3-16), (3-17) \\ \text{Internal constraints } (3-11)-(3-15), (3-35), (5-6) \end{cases}
\end{aligned}
\tag{5-7}
$$

where $\boldsymbol{x}^{\mathrm{PS}}$, $\boldsymbol{x}^{\mathrm{GS}}$ and $\boldsymbol{x}^{\mathrm{HS}}$ represent the internal decision variables in the optimization of power, gas, and DH subsystems, respectively. $\boldsymbol{x}^{\mathrm{PS}'}$ and $\boldsymbol{x}^{\mathrm{GS}'}$ describe the variables that are in the model of the corresponding subsystem but controlled by other subsystems through the link constraints. The link constraints are those operating constraints of the related energy conversion facilities (such as CHP, EBs/HPs, P2G and GBs). In the proposed equilibrium model, the optimization of each energy subsystem should be both subject to its own internal constraints and link constraints when pursuing its objective. $\boldsymbol{fp}$ represents the market price variables, which depends on the decisions of all subsystem operators.

5.2.2. Methodology

Overall, an individual operator can receive no incremental benefit from changing actions, assuming other operators remain constant in their strategies [189, 190]. In other words, each subsystem operator's strategy is optimal when considering the decisions of other subsystem operators. Because every subsystem operator gets the market outcome they desire. As shown in

Equation (5-7), the equilibrium problem needs to optimize the objectives with constraints of all subsystems simultaneously [189]. To this end, the proposed equilibrium model can be written in a standard form as shown in Fig.5.2.

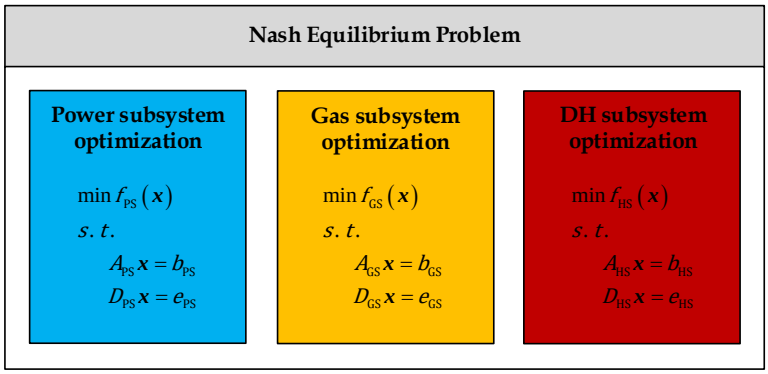

Fig. 5.2: Equilibrium problem: Joint solution of subsystem optimization problems. Source: [J2].

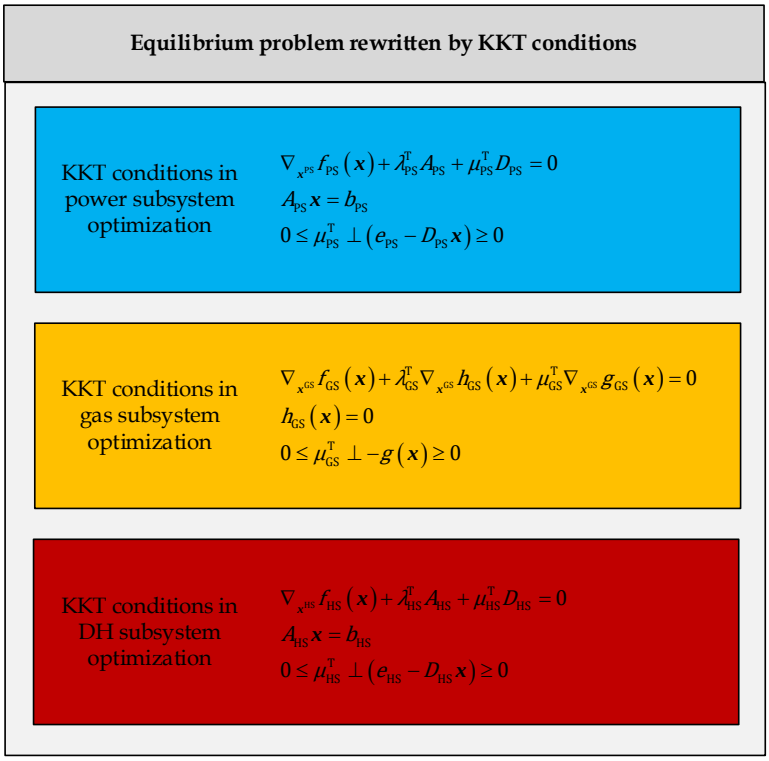

Fig. 5.3: Reformulated equilibrium problem using KKT conditions. Source: [J2].

In the optimization problem of the gas subsystem, the constraint equation (3-5) is nonlinear. This equation can be linearized using the method proposed in [32]. After that, all subsystem optimization problems are linear and convex. The proposed equilibrium model can be reformulated using KKT conditions as shown in Fig. 5.3 and it is solved using the PATH solver on the GAMS platform.

5.3. Optimal Strategy of the MES

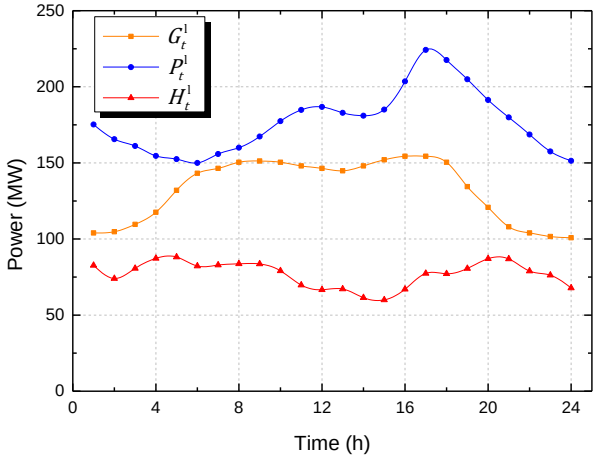

Fig. 5.4: Hourly electric load, gas load and heat load profiles. Source: [J1].

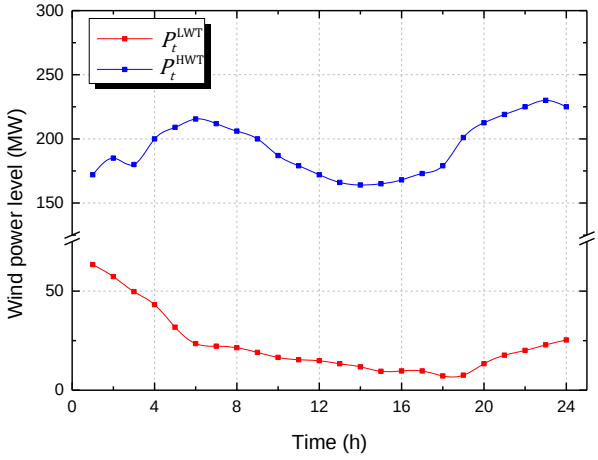

Fig. 5.5: High- and low- wind power levels. Source: [J1].

The test system used in this chapter follows the MES in Section 3.3.2, as shown in Fig. 3.4. The scheduling period T is set to 24 hours. The historical data of the Danish DK1 area is scaled to fit the test case [186]. Fig. 5.4 shows the hourly electric load, gas load and heat load profiles. Fig. 5.5 shows the typical profiles of wind power output in two scenarios of high- and low- wind levels, in which the high-wind output is within the range of [160MW, 230MW] and low-wind output is within the range of [7.2MW, 63.4MW]. The detailed parameters are listed in Tab. III of Appendix A.

5.3.1. Optimal scheduling and pricing in the low-wind scenario

LPF is set to 0.2. Fig. 5.6, Fig. 5.7, Fig. 5.8 and Fig. 5.9 show the optimal schedules of energy facilities in the low-wind scenario. Fig. 5.10 shows energy pricing in the market at the optimal strategy of the MES. Here, the large units such as the CFP and CHP units still adopt the control scheme of maintaining minimum output instead of shutting down during the 24h dispatch period [184]. Based on the profiles of energy loads and low-wind power in Fig. 5.4 and Fig 5.5, the scheduling period can be divided into 5 time-slices for discussing and analyzing the simulation results.

During periods 1h-3h, the gas valley load and the wind power support make the gas and electricity prices (10.028 €/MWh and 6.964 €/MWh, respectively) both cheap in the market. The gas storage facility starts to store the surplus cheap gas.

During periods 4h-5h, the heat peak load, rapid increase in gas load and decrease in wind power make the gas and electricity prices rise to 17.406 €/MWh (equal to the marginal cost of gas source) and 12.088 €/MWh, respectively. The heat storage facility releases heat to participate in heating.

During periods 6h-17h, the wind power drops to a very low level. On the one hand, the gas price remains stable since the gas source node meets all gas demand. On the other hand, the electricity price varies according to the changes in heat and electricity demands.

Until period 17h, the MES is in the condition of electricity and gas peak loads, the increase in the heat load and the wind power valley. Although all FRs are working to alleviate energy peak demand, the shortage of energy supply still leads to the extremely expensive prices of electricity and gas (144.916 €/MWh and 208.679 €/MWh, respectively).

During periods 18h-24h, the wind power picks up slightly. With the reduction of gas and electricity loads. The electricity price drops rapidly to 12.087 €/MWh.

In a low-wind scenario, the behaviors of the MES under the optimal strategy given by the proposed model can be summarized as:

- The gas source node has to meet all gas demand..
- The DH subsystem operator prefers to operate CHP units to supply heat.
- DR management strives to smooth the electrical load by shifting electricity consumption.
- Energy storage facilities are used in a flexible way to store cheap energy and release energy as required.

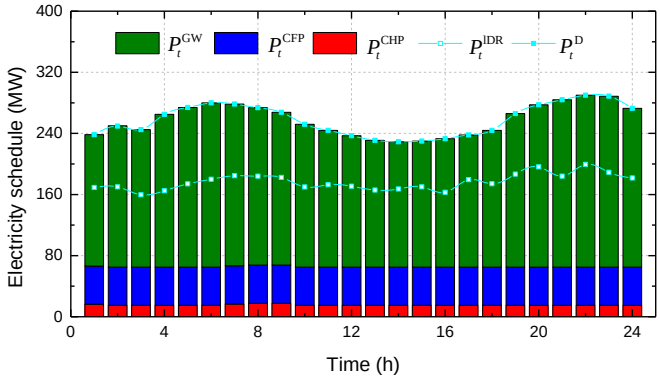

Fig. 5.6: Optimal electricity schedule in low-wind scenario. Source: [J1].

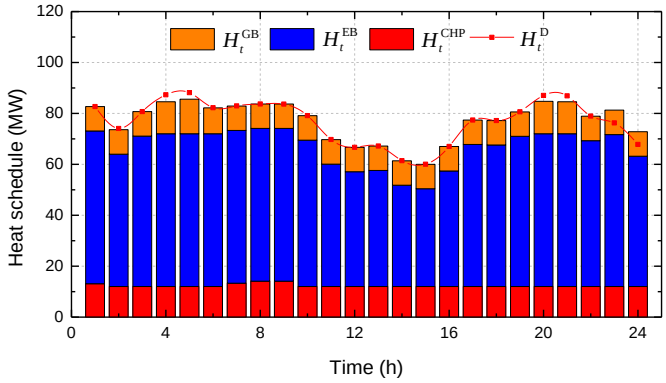

Fig. 5.7: Optimal heat schedule in low-wind scenario. Source: [J1].

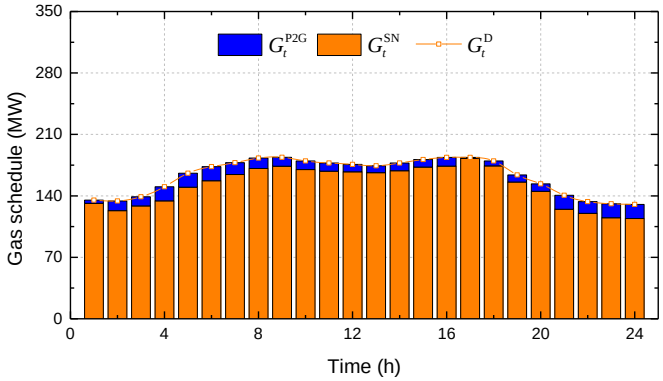

Fig. 5.8: Optimal gas schedule in low-wind scenario. Source: [J1].

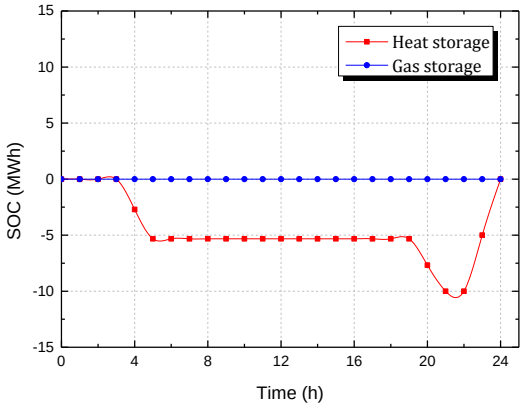

Fig. 5.9: SOC of energy storage facilities in low-wind scenario. Source: [J1].

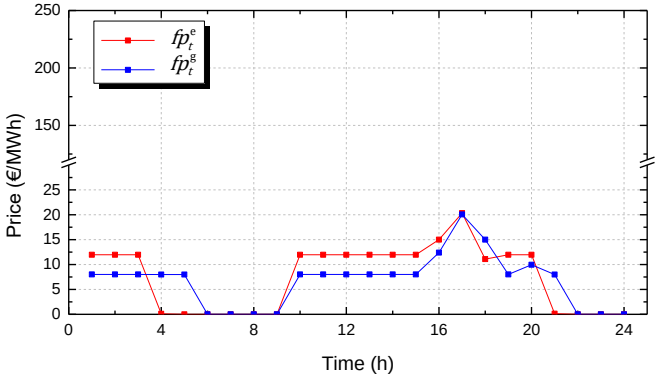

Fig. 5.10: Hourly energy prices in low-wind scenario. Source: [J1].

5.3.2. Optimal scheduling and pricing in the high-wind scenario

LPF is set to 0.2. Fig. 5.11, Fig. 5.12, Fig. 5.13 and Fig. 5.14 show the optimal schedules of energy facilities in the high-wind scenario. Fig. 5.15 shows the corresponding energy pricing in the market at the optimal strategy of the MES. The scheduling period is divided into 4 time-slices for discussing and analyzing the simulation results.

During periods 1h-6h, the rapid growth of wind power makes the price of electricity and gas drop from the initial 6.963 €/MWh and 10.026 €/MWh to zero. The reason why the electricity price fall earlier than the gas price is that the electric load decreases while the gas load increases during the periods.

During periods 7h-9h, the wind power gradually decreases. Although the electrical load and gas load are not low, wind power can still cover most of the energy demand since the reduced heat load indirectly alleviates the heating pressure of EBs. Therefore, the electricity and gas prices both keep at zero.

During periods 10h-17h, wind power continues to drop to a valley. Coupled with rapid increases in electrical and gas loads, the electricity and gas prices both rise to the initial values. Until period 17h, there is a wind power valley and the peak loads of gas and electricity. As a result, the electricity and gas prices rise again to their peaks of 15.332 €/MWh and 22.078 €/MWh, respectively.

During periods 18h-24h, wind power starts to increase rapidly, while the electrical and gas loads decrease rapidly. Thus, the electricity and gas prices both start to fall until they become zero.

In a high-wind scenario, the behaviors of the MES under the optimal strategy given by the proposed model can be summarized as:

- P2G units and the gas source work together to satisfy gas demand.
- The DH subsystem operator prefers to operate EBs to supply heat.
- DR management is still working to smooth the power load profile.
- Only the heat storage facility is operated. This is because, in the condition of sufficient wind power, power subsystem can run P2G units at any time to produce gas so that the gas subsystem no longer relies on the gas storage device, thereby saving its operating cost.

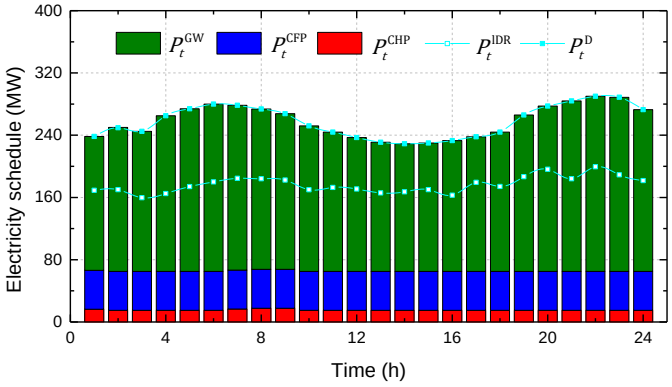

Fig. 5.11: Optimal electricity schedule in high-wind scenario. Source: [J1].

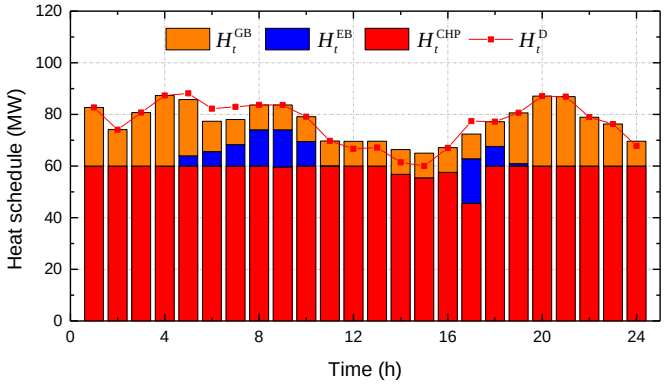

Fig. 5.12: Optimal heat schedule in high-wind scenario. Source: [J1].

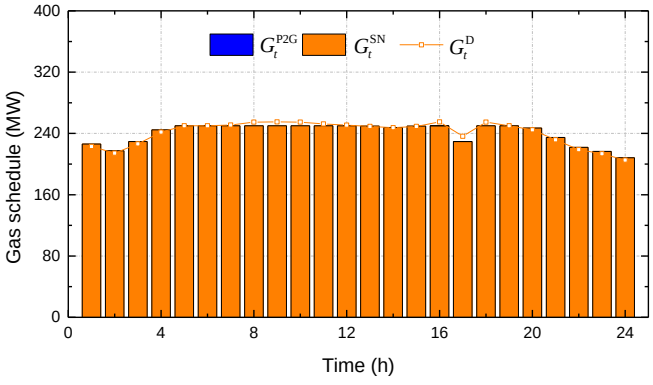

Fig. 5.13: Optimal gas schedule in high-wind scenario. Source: [J1].

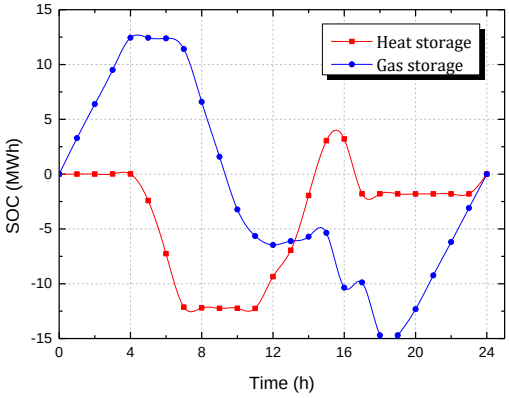

Fig. 5.14: SOC of energy storage facilities in high-wind scenario. Source: [J1].

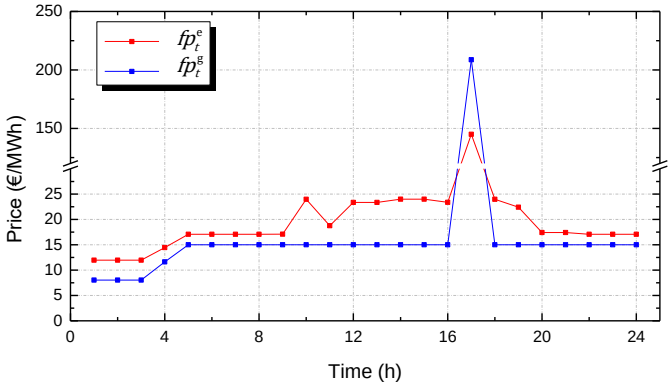

Fig. 5.15: Houly energy prices in high-wind scenario. Source: [J1].

5.4. Equilibrium and Centralized Optimization

In order to observe the results of balancing and centralized optimization, the centralized scheduling operated by an ISO is set as a control model. In the centralized optimization model, the ISO integrates and controls all the energy subsystems in maximizing total societal welfare. The objective function can be expressed as:

$$\text{Max } F=\sum_{t=1}^{T}\left[\begin{array}{l}\left(\sum_{i=1}^{N^{\mathrm{PL}}}B^{\mathrm{PL}}P_{i,t}^{\mathrm{IDR}}+\sum_{j=1}^{N^{\mathrm{GL}}}B^{\mathrm{GL}}G_{j,t}^{\mathrm{l}}+\sum_{m=1}^{N^{\mathrm{HL}}}B^{\mathrm{HL}}H_{m,t}^{\mathrm{l}}\right)\\ -\left(\sum_{i=1}^{N^{\mathrm{CFP}}}c_i^{\mathrm{CFP}}P_{i,t}^{\mathrm{CFP}}+\sum_{j=1}^{N^{\mathrm{SN}}}c_j^{\mathrm{SN}}G_{j,t}^{\mathrm{SN}}+\sum_{j=1}^{N^{\mathrm{GS}}}c_j^{\mathrm{GS}}\left|G_{j,t}^{\mathrm{GS}}\right|+\sum_{m=1}^{N^{\mathrm{HS}}}c_m^{\mathrm{HS}}\left|H_{m,t}^{\mathrm{HS}}\right|\right)\end{array}\right] \quad (5\text{-}7)$$

Equation (5-7) has seven components: the benefits including power, gas and heat consumption, and the operating costs including CFP units, gas injection from the gas source, gas and heat storage facilities. It is noted that the objective function does not involve the operating costs of energy conversion devices such as CHP units, P2G units, GBs and EBs. The reason is that their operating costs are part of the energy supply cost of the corresponding subsystem. For example, the fuel of the CHP unit is natural gas, and its cost is already included in the gas supply cost of the gas subsystem without separate calculation.

The objective function is subject to operating constraints of all energy subsystems, including:

- The constraints of the power subsystem as shown in Equations (2-7)-(2-12), (3-3), (3-30), (3-32), (3-33);
- The constraints of the gas subsystem as shown in Equations (2-7)-(3-5)-(3-10), (3-20), (3-34);
- The constraints of the DH subsystem as shown in Equations (3-11)-(3-17), (3-21), (3-22) and (3-35).

It is assumed that in the centralized optimization model, each energy subsystem shares information with the other without reservation. Tab. 5.1 shows the simulation results of the centralized optimization and the equilibrium optimization. The results show that if there is perfect communication between energy subsystems, the Nash equilibrium is the global optimal solution. The total social welfare and the total cost of the two optimization models are the same. However, from a market perspective, the core ideas of the two optimization models are essentially different. On the one hand, the existing market mechanism has both perfect competition and monopoly. The energy subsystem operators cannot perfectly exchange information (network parameters, real-time prices, etc.) because of the confidentiality contract. Therefore, it is unrealistic that the ISO coordinates and dispatches all energy subsystems in a short term. On the other hand, equilibrium optimization allows each subsystem operator to construct its own internal optimization for system operation, and then to solve the formed game problem. Although the resulting equilibrium solution may not be the global optimal solution, the equilibrium optimization provides an opportunity to make everyone obtain his or her satisfactory benefit while protecting the necessary information.

Model	Profit_GS	Profit_PS	Profit_DHS	Total SW	Total cost
CO	-	-	-	122270 €	92509 €
EO	17570 €	71810 €	32893 €	122270 €	92509 €

CO: Centralized optimization; EO: Equilibrium optimization
SW: Social welfare; GS: Gas subsystem; PS: Power subsystem; DHS: DH subsystem

Tab. 5.1: Numerical results of equilibrium and centralized optimization.

5.5. Impacts of Multiple FRs on the MES

To investigate the impact of different FRs on the MES, five cases with different combinations of FRs are set as control groups. Tab. 5.2 show the simulation results of the test MES. It can be seen that the more FRs used, the higher the total social welfare of the MES, and the lower the wind power curtailment. On the one hand, energy production and consumption are no longer confined to a single energy system thanks to the conversion FRs. For example, through P2G units and EBs, the gas subsystem and the DH subsystem play roles as reserves of the power subsystem to accommodate more renewable energy. On the other hand, the demand FRs adjust the energy load through DR management to improve the mismatch between supply and demand.

Case	Used FRs	Total SW (€)	WPC (MWh)
1	GB, CHP	89962	2444.4
2	GB, CHP, P2G	96083	1523.1
3	GB, CHP, EB	98041	752.9
4	GB, CHP, EB, P2G	120480	217.7
5	GB, CHP, EB, P2G, GS, HS	120530	205.0
6	GB, CHP, EB, P2G, GS, HS, DR (LPF=0.2)	122270	23.92

SW: Social welfare; WPC: Wind power curtailment

Tab. 5.2: Numerical results of different cases with used FRs. Source: [J1]

In addition, Fig. 5.16 and Fig. 5.17 give the used heat storage capacity, total social welfare (SW) and wind power curtailment (WPC) of the MES in the high-wind scenarios with different LPFs. It should be noted that only the simulation results of LPF$\leqslant$0.35 are shown. The results further validate the conclusion drawn in Section 3.3. The more electrical loads participate in DR adjustment, the greater the positive impact on MES operation. This is mainly

reflected in reducing the capacity investment of energy storage facilities, improving social welfare and decreasing wind power curtailment.

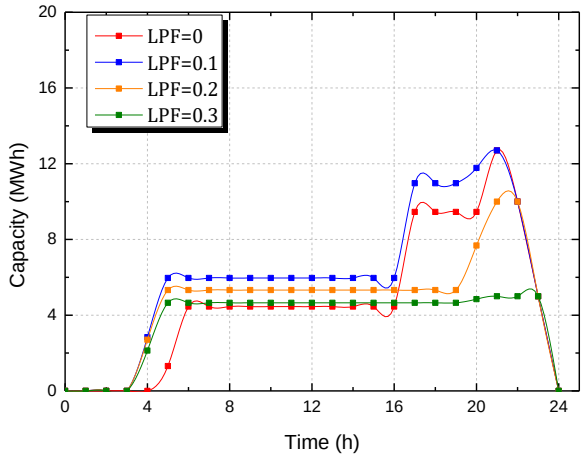

Fig. 5.16: Impacts of different LPFs on used heat storage capacity. Source: [J1].

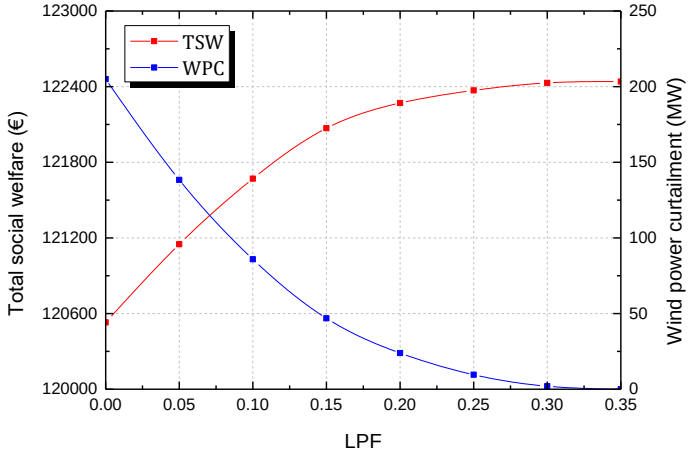

Fig. 5.17: Impacts of different LPFs on social welfare and wind power curtailment. Source: [J1].

5.6. Summary

This chapter proposes an optimal strategy for the MES with multiple FRs. Considering the actual market mechanism, the electricity, gas and DH systems prefer independent operation or limited communication and cooperation. To this end, a Nash equilibrium model has been developed to describe energy exchange and transaction among the integrated subsystems

in the MES. Each energy subsystem can pursue its own benefit under the proposed model. The proposed equilibrium model and the corresponding centralized scheduling model are compared and analyzed. The simulation results show that: 1) The optimal strategies can be obtained by running the proposed model based on different wind power levels; 2) The more FRs involved in the operation, the more flexibility of the MES, which is reflected in the improvements of social welfare and wind power accommodation; 3) As a FR, DR can effectively improve the abnormal electricity price in peak period, correct energy supply imbalances and optimize electricity consumption patterns. The related publications are J1 and J2.

Chapter 6

Conclusions

This chapter sums up the main work in this Ph.D. project. The research content and conclusions of each chapter are summarized, respectively. Furthermore, the future research perspectives related to the management of FRs are discussed, involving the precise modeling of MESs, the practical applications of FRs and the ancillary market design.

6.1. Summary

Based on the high penetration of renewable energy, this Ph.D. project aims at the optimal management of FRs in the short-term market to achieve a flexible, efficient and economical MES. From two perspectives of the integration and optimization of FRs, several challenging issues have been discussed, and their solutions have been proposed. To address those issues, the research work is carried out one by one with the following topics:

- Identify the FRs available in MESs and describe their mathematical models;
- Integrate and coordinate FRs across MESs;
- Consider the market environment, propose optimal strategies based on different business models.

In Chapter 2, FRs in different energy systems have been uniformly classified in the four aspects of supply, storage, conversion and demand. Their working principles, practical applications and common modeling expressions have been described. Based on this, it is determined that this Ph.D. research mainly focuses on the FRs on the energy storage, conversion and demand side.

The first challenge is to integrate and coordinate multiple FRs across MESs. This integration is achieved through the interconnection of the energy subsystems. For this reason, in Chapter 3, a multi-objective scheduling model has been developed to coordinate FRs and optimize system operation. In this model, the steady energy flows of electricity, gas and heat, and the operating constraints of FRs are described. The proposed optimization model can give the optimal coordination of FRs by collecting day-ahead energy prices as a

scheduling signal. The simulation results of the case show that FRs have been no longer limited to their own energy subsystems. Their integration and coordination have brought great flexibility to the entire MES. In addition, the positive impact of load shifting on the operation of the MES has been discussed.

The second challenge is to propose optimal strategies based on different business models. These strategies involve the management of FRs, the optimization of energy production and distribution, and energy pricing. Unlike Chapter 2, in which the day-ahead market energy price is used as a reference signal, the real-time market price and the supply and demand of the MES interact with each other.

In Chapter 4, an optimal strategy for the MES with flexible demand has been proposed, where the energy subsystems are centralized dispatched by the ISO. This strategy aims at minimizing the energy purchase cost of downstream demand under the leadership of centralized scheduling. To this end, a bi-level collaborative optimization model has been developed. In this model, smart buildings are used as flexible consumption units, and they are aggregated on the demand side of the MES. The case study refers to the micro-grid structure of the COSES laboratory, and integrates the gas network on a basis. The optimization model has been solved on the GAMS platform. The simulation results show that the proposed model can optimize the generation and distribution of internal controllable resources and set corresponding market energy prices. Besides, the built-in flexibility of smart buildings has been verified.

Taking into account the actual market mechanism, electricity, gas, and DH systems prefer to operate independently or have limited cooperation. In Chapter 5, an optimal strategy for the MES with multiple FRs has been proposed, where energy subsystems are scheduled by their individual system operators. This strategy aims at a non-cooperative game in which each energy subsystem pursues its own benefit until an equilibrium that satisfies everyone. To this end, a Nash equilibrium model has been developed. Similarly, this model allows optimizing the operation of the MES and setting real-time energy prices. Numerical results show that the proposed model can give the corresponding optimal strategies of the MES according to different wind power scenarios. On the other hand, FRs have a positive impact on the operation of the MES, including improving social welfare, wind power curtailment and abnormal electricity prices. Furthermore, the proposed equilibrium model has been compared with the centralized scheduling model.

In summary, the contributions of this Ph. D. thesis are highlighted as:

- The available FRs in the MES has been fully investigated. The research focuses on the identification and utilization of FRs for storage, conversion and DR involving their working principles, mathematical models and application examples.
- Using the day-ahead price signals, a multi-objective optimization model has been proposed to address the issue of integrating and coordinating multiple FRs in the MES.
- Using smart buildings as flexible demand, a bi-level optimization model has been developed to achieve optimal resource management and market pricing.
- A Nash equilibrium market model has been developed to simulate the game process of energy subsystems with limited communication, and the coorsponding optimal strategy has been proposed for the MES with multiple FRs.

6.2. Future Research Perspectives

According to the state of art introduced in Section 1.3, current research mainly focuses on the integrated system with one or two carriers such as the electricity-gas system or the electricity-heat system. Although this Ph.D. thesis has discussed the MES including electricity, gas and heat systems, there is still a lack of similar and representative studies in the current literature. It is undeniable that the integrated energy system comprising electricity, gas, heating/cooling, and even transportation has many advantages such as energy independence, economic competitiveness, job creation, and smarter use of resources. Therefore, they and their related services should be an important topic in future research.

6.2.1. Precise modeling of MESs

Precise modeling has been an issue worthy of in-depth exploration. Generally, the more energy subsystems a MES has, the more complex coupling characteristics and the higher nonlinearity it has. This brings challenges to the accuracy of the joint model and increases the calculation difficulty of the model. Besides, multiple uncertainties like grid-connected renewable energy or natural disasters put forward higher requirements for collaborative operation. For example, the dynamic power model proposed in [192] uses methods such as decentralized decision-making and multi-layer robust optimization to improve the model accuracy, reduce the calculation complexity and respond to the uncertainties. Studies similar to this might be a starting point for future research.

6.2.2. Proper combination and application of FRs

In terms of the application of FRs, a large number of studies have proposed solutions for demand-side management (DSM) and conversion technology, while few studies have given detailed solutions for storage feasibility. In some conditions, the storage technology of electricity, heat or gas is not economical because of its high cost. Thus, it is unrealistic to rely on energy storage devices regardless of the situation. Analogously, not all consumers are willing to participate in DSM. Because they care more about comfort than getting a payment or discount on energy consumption. Conversion equipment seems to be a perfect solution to that problem. However, the premise for consumers to use them depends on the immediate price of the alternative energy and the installation cost of the equipment. Only a proper combination and application of those FRs allows unlocking the flexible potential of the MES. For instance, an energy hub is a promising option for integrated management of FRs [18, 82, 156].

6.2.3. Sound and Standard Market Mechanism

Another important research perspective is designing a market mechanism that is implementable to deal with the actual situation of future markets. Although this Ph.D. thesis has considered confidentiality constraints for different energy subsystems, the proposed model still has several limiting assumptions. In the future, a sound and standard market mechanism should include: 1) Design of regulation, which has fairness and cost-reflectiveness, make proper tariffs to incentive system-friendly behaviors; 2) Design of market prices, which encourages the innovation demanded to advance the clean energy transition and FR application. Thus, new economic thinking is needed to help reform energy taxation, energy rate design, and demand-side policies.

References

[1] K. Hansen, C. Breyer, and H. Lund, "Status and perspectives on 100% renewable energy systems," Energy, vol. 175, pp. 471–480, May. 2019.

[2] Preliminary Energy Statistics for Denmark for the year 2020, Danish Energy Agency, 2020. [online]. Available: https://ens.dk/en/our-services/statistics-data-key-figures-and-energy-maps/annual-and-monthly-statistics

[3] Basisfremskrivning, Energistyrelsen, 2020. [online]. Available: https://ens.dk/sites/ens.dk/files/Basisfremskrivning/deco_2020_27082020.pdf

[4] F. Bouffard and M. Ortega-Vazquez, "The value of operational flexibility in power systems with significant wind power generation," in Proc. 2011 IEEE Power and Energy Society General Meeting, Detroit, MI, USA, pp. 1–5, Jul. 2011.

[5] Y. Dvorkin, D. S. Kirschen and M. A. Ortega-Vazquez, "Assessing flexibility requirements in power systems," IET Generation, Transmission & Distribution, vol. 8, no. 11, pp. 1820-1830, 2014.

[6] J. Ma, V. Silva, R. Belhomme, D. S. Kirschen and L. F. Ochoa, "Evaluating and planning flexibility in sustainable power systems," in Proc. 2013 IEEE Power & Energy Society General Meeting, Vancouver, BC, Canada, pp. 1–11, 2013.

[7] M. Milligan, "Sources of grid reliability services," The Electricity Journal, vol. 31, no. 9, pp. 1–7, Oct. 2018.

[8] A. S. Ahmadyar, S. Riaz, G. Verbič, A. Chapman and D. J. Hill, "A framework for assessing renewable integration limits with respect to frequency performance," IEEE Transactions on Power Systems, vol. 33, no. 4, pp. 4444-4453, Jul. 2018.

[9] E. Muljadi, V. Gevorgian and A. Hoke, "Short-term forecasting of inertial response from a wind power plant," in Proc. 2016 IEEE Energy Conversion Congress and Exposition (ECCE), Milwaukee, WI, USA, pp. 1–5, 2016.

[10] V. Y. Singarao and V. S. Rao, "Frequency responsive services by wind generation resources in United States," Renewable and Sustainable Energy Reviews, vol. 55, pp.1097-1108, 2016.

[11] H. Xin, Y. Liu, Z. Wang, D. Gan and T. Yang, "A new frequency regulation strategy for photovoltaic systems without energy storage,"

IEEE Transactions on Sustainable Energy, vol. 4, no. 4, pp. 985-993, Oct. 2013.

[12] K. Kawabe, Y. Ota, A. Yokoyama and K. Tanaka, "Novel dynamic voltage support capability of photovoltaic systems for improvement of short-term voltage stability in power systems," IEEE Transactions on Power Systems, vol. 32, no. 3, pp. 1796-1804, May 2017.

[13] M. Doostizadeh, M. Khanabadi and M. Ettehadi, "Reactive power provision from distributed energy resources in market environment," in Proc. Electrical Engineering (ICEE), Mashhad, Iran, pp. 1362-1367, 2018.

[14] K. De Vos and J. Driesen, "Active participation of wind power in operating reserves," IET Renewable Power Generation, vol. 9, no. 6, pp. 566–575, Aug. 2015.

[15] D. Nock, V. Krishnan and J. D. McCalley, "Dispatching intermittent wind resources for ancillary services via wind control and its impact on power system economics," Renewable Energy, vol. 71, pp. 396–400, Nov. 2014.

[16] S. Clegg and P. Mancarella, "Integrated modeling and assessment of the operational impact of power-to-gas (p2g) on electrical and gas transmission networks," IEEE Transactions on Sustainable Energy, vol. 6, no. 4, pp. 1234-1244, Oct. 2015.

[17] C. Wang et al., "Impact of power-to-gas cost characteristics on power-gas-heating integrated system scheduling," IEEE Access, vol. 7, pp. 17654-17662, 2019

[18] R. Habibifar, M. Khoshjahan, V. S. Saravi and M. Kalantar, "Robust energy management of residential energy hubs integrated with power-to-x technology," in Proc. 2021 IEEE Texas Power and Energy Conference (TPEC), College Station, TX, USA, pp. 1-6, Feb. 2021.

[19] J. Li, J. Lin, Y. Song, X. Xing and C. Fu, "Operation optimization of power to hydrogen and heat (p2hh) in adn coordinated with the district heating network," IEEE Transactions on Sustainable Energy, vol. 10, no. 4, pp. 1672-1683, Oct. 2019.

[20] J. Wang et al., "Economic benefits of integrating solar-powered heat pumps into a CHP system," IEEE Transactions on Sustainable Energy, vol. 9, no. 4, pp. 1702-1712, Oct. 2018.

[21] J. Kozadajevs and D. Boreiko, "District heating system flexibility studies using thermal inertia of buildings," in Proc. 2020 IEEE 61th International Scientific Conference on Power and Electrical

Engineering of Riga Technical University (RTUCON), Riga, Latvia, pp. 1-5, Nov. 2020.

[22] Y. Shi, Y. Chen, H. Bai, S. Xu and C. Guo, "Enhancing the flexibility of integrated heat and electricity system with multi-stage robust programming considering thermal inertia of buildings," in Proc. 2020 IEEE/IAS Industrial and Commercial Power System Asia (I&CPS Asia), Weihai, China, pp. 1256-1261, Jul. 2020.

[23] X. Wu, Z. Chen and J. Fang, "Unit commitment of integrated electricity and heat system with bi-directional variable mass flow," in Proc. 2020 IEEE Power & Energy Society General Meeting (PESGM), Montreal, QC, Canada, pp. 1-5, Aug. 2020.

[24] Z. Li, W. Wu, J. Wang, B. Zhang and T. Zheng, "Transmission-constrained unit commitment considering combined electricity and district heating networks," IEEE Transactions on Sustainable Energy, vol. 7, no. 2, pp. 480-492, Apr. 2016.

[25] P. Jie et al., "Modeling the dynamic characteristics of a district heating network," Energy, vol. 39, no. 1, pp. 126–134, Mar. 2021.

[26] Z. Li, W. Wu, M. Shahidehpour, J. Wang and B. Zhang, "Combined heat and power dispatch considering pipeline energy storage of district heating network," IEEE Transactions on Sustainable Energy, vol. 7, no. 1, pp. 12-22, Jan. 2016.

[27] G. Mutani, V. Todeschi and M Pastorelli, "Thermal-electrical analogy for dynamic urban-scale energy modeling," International Journal of Heat and Technology, vol. 38, no. 3, pp. 571-82, Sept. 2020.

[28] R. Bani and W. Schütz, "Prediction of Long Periods Heating Demand at Small Time Intervals for a Single Story Building using a Black Box Method," in Proc. 2020 International Youth Conference on Radio Electronics, Electrical and Power Engineering (REEPE), Moscow, Russia, pp. 1-5, Mar. 2020.

[29] A. Osiadacz, Simulation and analysis of gas networks. Houston, TX, USA: Gulf, 1987.

[30] C. Fletcher, Computational Techniques for Fluid Dynamics 2: Specific Techniques for Different Flow Categories. Berlin, Germany: Springer-Verlag, 2012.

[31] S. Mokhatab and W. A. Poe, Handbook of Natural Gas Transmission and Processing. Houston, TX, USA: Gulf, 2012.

[32] J. Fang, Q. Zeng, X. Ai, Z. Chen and J. Wen, "Dynamic optimal energy flow in the integrated natural gas and electrical power systems," IEEE Transactions on Sustainable Energy, vol. 9, no. 1, pp. 188-198, Jan. 2018.

[33] Electricity market liberalisation, European Commission, 2014. [online]. Available: https://ec.europa.eu/energy/content/electricity-market-liberalisation_en

[34] M. Oksanen, R. Karjalainen, S. Viljainen and D. Kuleshov, "Electricity markets in Russia, the US, and Europe," in Proc. 2009 6th International Conference on the European Energy Market, Leuven, Belgium, pp. 1-7, May 2009.

[35] G. Pepermans, "European energy market liberalization: experiences and challenges," International Journal of Economic Policy Studies, vol. 13, no. 1, pp. 3-26, Jan. 2019.

[36] K. J. Shin and S. Managi, "Liberalization of a retail electricity market: Consumer satisfaction and household switching behavior in Japan," Energy Policy, vol. 110, pp. 675-685, Nov. 2017.

[37] Wholesale Gas Price Survey 2021 Edition, International Gas Union (IGU), 2021. [online]. Available: https://www.igu.org/resources/global-wholesale-gas-price-survey-2021/

[38] F. L. Müller, J. Szabó, O. Sundström, and J. Lygeros, "Aggregation and disaggregation of energetic flexibility from distributed energy resources," IEEE Transactions on Smart Grid, vol. 10, no. 2, pp. 1205–1214, Mar. 2019.

[39] Z. Yi, Y. Xu, W. Gu and W. Wu, "A multi-time-scale economic scheduling strategy for virtual power plant based on deferrable loads aggregation and disaggregation," IEEE Transactions on Sustainable Energy, vol. 11, no. 3, pp. 1332-1346, Jul. 2020.

[40] G. E. Asimakopoulou and N. D. Hatziargyriou, "Evaluation of economic benefits of DER aggregation," IEEE Transactions on Sustainable Energy, vol. 9, no. 2, pp. 499–510, Apr. 2018.

[41] A. Zangeneh, A. S.-Rad, and F. Nazari, "Multi-leader-follower game the-ory for modelling interaction between virtual power plants and distribution company," IET generation, transmission & distribution, vol. 12, no. 21, pp. 5747–5752, Nov. 2018..

[42] F. Khavari, A. Badri, and A. Zangeneh, "Energy management in multi-microgrids via an aggregator to override point of common coupling

congestion," IET generation, transmission & distribution, vol. 13, no. 5, pp. 634–642, Dec. 2019.

[43] H. Cui, F. Li, X. Fang, H. Chen, and H. Wang, "Bilevel arbitrage potential evaluation for grid-scale energy storage considering wind power and LMP smoothing effect," IEEE Transactions on Sustainable Energy, vol. 9, no. 2, pp. 707–718, Apr. 2018.

[44] S. Bahramara, M. Y.-Damavandi, J. Contreras, M. S.-Khah, and J. P. S. Catalão, "Modeling the strategic behavior of a distribution company in wholesale energy and reserve markets," IEEE Transactions on Smart Grid,vol.9, no. 4, pp. 3857–3870, Jul. 2018.

[45] G. Zhang, G. Zhang, Y. Gao, and J. Lu, "Competitive strategic bidding optimization in electricity markets using bilevel programming and swarm technique," IEEE Transactions on Industrial Electronics, vol. 58, no. 6, pp. 2138–2146, Jun. 2011.

[46] M. J. Rider, J. M. L.-Lezama, J. Contreras, and A. P.-Feltrin, "Bilevel approach for optimal location and contract pricing of distributed generation in radial distribution systems using mixed-integer linear programming," IET generation, transmission & distribution, vol. 7, no. 7, pp. 724–734, Jul. 2013.

[47] M. Y.-Damavandi, N. Neyestani, M. S.-khah, J. Contreras, and J. P. S. Catalão, "Strategic behavior of multi-energy players in electric-ity markets as aggregators of demand side resources using a bi-level approach," IEEE Transactions on Power Systems, vol. 33, no. 1, pp. 397–411, Jan. 2018..

[48] M. Y.-Damavandi, N. Neyestani, G. Chicco, M. S.-khah, and J. P. S. Catalão, "Aggregation of distributed energy resources under the concept of multienergy players in local energy systems," IEEE Transactions on Sustainable Energy, vol. 8, no. 4, pp. 1679–1693, Oct. 2017.

[49] I. Momber, S. Wogrin, and T. Román, "Retail pricing: a bilevel program for PEV aggregator decisions using indirect load control," IEEE Transactions on Power Systems, vol. 31, no. 1, pp. 464–473, Jan. 2016.

[50] D. T. Nguyen, H. T. Nguyen, and L. B. Le, "Dynamic pricing design for demand response integration in power distribution networks," IEEE Transactions on Power Systems, vol. 31, no. 5, pp. 3457–3472, Sep. 2016.

[51] A. Akrami, M. Doostizadeh and F. Aminifar, "Power system flexibility: an overview of emergence to evolution," in Journal of Modern Power Systems and Clean Energy, vol. 7, no. 5, pp. 987-1007, Sept. 2019.

[52] A. Akrami, M. Doostizadeh and F. Aminifar, "Review of energy system flexibility measures to enable high levels of variable renewable electricity," Renewable and sustainable energy reviews, vol. 45, pp. 785-807, May 2015.

[53] M. I. Alizadeh, M. Parsa Moghaddam, N. Amjady, P. Siano, and M. K. Sheikh-El-Eslami, "Flexibility in future power systems with high renewable penetration: A review," Renewable and sustainable energy reviews, vol. 57, pp. 1186–1193, May 2016.

[54] E. Lannoye, D. Flynn, and M. O'Malley, "Evaluation of power system flexibility," IEEE Transactions on Power System, vol. 27, no. 2, pp. 922–931, Jan. 2012.

[55] K. Studarus and R. D. Christie, "A deterministic metric of stochastic operational flexibility," in Proc. 2013 IEEE Power & Energy Society General Meeting, Vancouver, BC, Canada, pp. 1-4, Jul. 2013.

[56] M. Huber, D. Dimkova and T. Hamacher, "Integration of wind and solar power in Europe: Assessment of flexibility requirements," Energy, vol. 69, pp. 236-246, May 2014.

[57] M. A. Bucher, S. Delikaraoglou, K. Heussen, P. Pinson and G. Andersson, "On quantification of flexibility in power systems," in Proc. 2015 IEEE Eindhoven PowerTech, Eindhoven, Netherlands, pp.1-6, 2015.

[58] R. D. Coninck and L. Helsen, "Quantification of flexibility in buildings by cost curves - methodology and application," Applied Energy, vol. 162, pp. 653–665, Jan. 2016.

[59] X. Zhang, M. Shahidehpour, A. Alabdulwahab and A. Abusorrah, "Hourly electricity demand response in the stochastic day-ahead scheduling of coordinated electricity and natural gas networks," IEEE Transactions on Power Systems, vol. 31, no. 1, pp. 592-601, Jan. 2016.

[60] C. Liu, M. Shahidehpour and J. Wang, "Coordinated scheduling of electricity and natural gas infrastructures with a transient model for natural gas flow," Chaos: An Interdisciplinary Journal of Nonlinear Science, vol. 21, no. 2, pp. 025102, Jun. 2011.

[61] X. Zhang, L. Che, M. Shahidehpour, A. Alabdulwahab and A. Abusorrah, "Electricity-natural gas operation planning with hourly demand response for deployment of flexible ramp," IEEE Transactions on Sustainable Energy, vol. 7, no. 3, pp. 996-1004, Jul. 2016

[62] Q. Zeng et al., "A bi-level programming for multistage co-expansion planning of the integrated gas and electricity system," Applied Energy, vol. 200, pp. 192-203, Aug. 2017.

[63] Q. Zeng et al., "Steady-state analysis of the integrated natural gas and electric power system with bi-directional energy conversion," Applied Energy, vol. 184, pp. 1483-1492, Dec. 2016.

[64] J. Yang, N. Zhang, C. Kang and Q. Xia, "Effect of natural gas flow dynamics in robust generation scheduling under wind uncertainty," IEEE Transactions on Power Systems, vol. 33, no. 2, pp. 2087-2097, Mar. 2018.

[65] K. Shu et al., "Real-time subsidy based robust scheduling of the integrated power and gas system," Applied Energy, vol. 236, pp. 1158-1167, Feb. 2019.

[66] S. Bracco, G. Dentici, and S. Siri, "Economic and environmental optimization model for the design and the operation of a combined heat and power distributed generation system in an urban area," Energy, vol. 55, pp. 1014–1024, Jun. 2013.

[67] X. Liu, J. Wu, N. Jenkins, and A. Bagdanavicius, "Combined analysis of electricity and heat networks,"Applied Energy, vol. 162, pp. 1238-1250, Jan. 2016.

[68] H. Xiao, W. Pei, Z. Dong and L. Kong, "Bi-level planning for integrated energy systems incorporating demand response and energy storage under uncertain environments using novel metamodel," CSEE Journal of Power and Energy Systems, vol. 4, no. 2, pp. 155-167, Jun. 2018.

[69] F. Wang et al., "Multi-objective optimization model of source–load–storage synergetic dispatch for a building energy management system based on tou price demand response," IEEE Transactions on Industry Applications, vol. 54, no. 2, pp. 1017-1028, Mar. 2018.

[70] Y. Zhang et al., "Energy flexibility from the consumer: Integrating local electricity and heat supplies in a building," Applied Energy, vol. 223, pp. 430-442, Aug. 2018.

[71] A. Arteconi, N. J. Hewitt and F. Polonara, "Domestic demand-side management (DSM): Role of heat pumps and thermal energy storage (TES) systems," Applied thermal engineering, vol. 51, no. 1, pp. 155-165, Mar. 2013.

[72] G. Gahleitner, "Hydrogen from renewable electricity: An international review of power-to-gas pilot plants for stationary applications,"

International Journal of Hydrogen Energy, vol. 38, no. 5, pp. 2039-2061, Feb. 2013.

[73] J. Kim and A. Shcherbakova "Common failures of demand response" Energy, vol. 36, no. 2, pp. 873-880, Feb. 2011.

[74] G. Strbac, "Demand side management: Benefits and challenges," Energy Policy, vol. 36, no. 12, pp. 4419-4426, Dec. 2008.

[75] Z. Yi, Y. Xu, J. Zhou, W. Wu and H. Sun, "Bi-level programming for optimal operation of an active distribution network with multiple virtual power plants," IEEE Transactions on Sustainable Energy, vol. 11, no. 4, pp. 2855-2869, Oct. 2020.

[76] F. M. Bhutta, "Application of smart energy technologies in building sector — future prospects," in Proc. 2017 International Conference on Energy Conservation and Efficiency (ICECE), Lahore, Pakistan, pp. 7–10, Nov. 2017.

[77] Y. Sun, H. Song, A. J. Jara and R. Bie, "Internet of things and big data analytics for smart and connected communities," IEEE Access, vol. 4, pp. 766-773, 2016.

[78] D. Koraki and K. Strunz, "Wind and solar power integration in electricity markets and distribution networks through service-centric virtual power plants," IEEE Transactions on Power Systems, vol. 33, no. 1, pp. 473–485, Jan. 2018.

[79] Q. Zhao, Y. Shen, and M. Li, "Control and bidding strategy for virtual power plants with renewable generation and inelastic demand in electric-ity markets," IEEE Transactions on Sustainable Energy, vol. 7, no. 2, pp. 562–575, Apr. 2016.

[80] E. Heydarian-Forushani, M. E. H. Golshan, M. Shafie-khah and P. Siano, "Optimal Operation of Emerging Flexible Resources Considering Sub-Hourly Flexible Ramp Product," IEEE Transactions on Sustainable Energy, vol. 9, no. 2, pp. 916-929, Apr. 2018.

[81] F. Wei, J. Q. Liu, Z. H. Yang and F. Ni, "A game theoretic approach for distributed energy trading in district energy networks," in Proc. 2017 IEEE Conference on Energy Internet and Energy System Integration (EI2), Beijing, China, pp. 1-6, Nov. 2017.

[82] Y. Liang, W. Wei and C. Wang, "A generalized nash equilibrium approach for autonomous energy management of residential energy hubs," IEEE Transactions on Industrial Informatics, vol. 15, no. 11, pp. 5892-5905, Nov. 2019.

[83] G. Mohy-ud-din, K. M. Muttaqi and D. Sutanto, "A Bi-level Energy Management Model for Energy Transactions from VPP based Integrated Energy Systems under System Uncertainties," in Proc. 2020 IEEE International Conference on Power Electronics, Drives and Energy Systems (PEDES), Jaipur, India, pp. 1-6, Dec. 2020.

[84] Y. Gao, X. Hu, W. Yang, H. Liang, and P. Li, "Multi-objective bilevel coordinated planning of distributed generation and distribution network frame based on multiscenario technique considering timing character-istics," IEEE Transactions on Sustainable Energy, vol. 8, no. 4, pp. 1415–1429, Oct. 2017.

[85] Y. Sun, B. Zhang, L. Ge, D. Sidorov, J. Wang and Z. Xu, "Day-ahead optimization schedule for gas-electric integrated energy system based on second-order cone programming," CSEE Journal of Power and Energy Systems, vol. 6, no. 1, pp. 142-151, Mar. 2020.

[86] L. Wan, W. Zhang and Z. Xu, "Optimal scheduling of hydrogen energy storage integrated energy system based on Mixed Integer Second-order Cone," in Proc. 12th IEEE PES Asia-Pacific Power and Energy Engineering Conference (APPEEC), Nanjing, China, pp. 1–5, Sept. 2020.

[87] Y. Gao, X. Hu, W. Yang, H. Liang, and P. Li, "Bilevel transmission expansion planning using second-order cone programming considering wind investment," Energy, vol. 154, pp. 455–465, Jul. 2018.

[88] Innovative Operation of Pumped Hydropower Storage, International Renewable Energy Agency (IRENA), 2020. [online]. Available: https://www.irena.org/-/media/Files/IRENA/Agency/Publication/2020/Jul/IRENA_Innovative_PHS_operation_2020.pdf

[89] R. Lazdins and A. Mutule, "Operational algorithm for natural gas boiler and heat pump system optimization with PV panel," in Proc. 2020 IEEE 61th International Scientific Conference on Power and Electrical Engineering of Riga Technical University (RTUCON), Riga, Latvia, pp.1-4, Nov. 2020.

[90] Søren Møller Thomsen, "INTE-3ES Energy markets and technologies," Ramboll, Copenhagen, Denmark, 2018.

[91] V. Kleinschmidt, T. Hamacher, V. Perić and M. R. Hesamzadeh, "Unlocking flexibility in multi-energy systems: A literature review," in Proc. 17th International Conference on the European Energy Market (EEM), Stockholm, Sweden, Sept. 2020

[92] R. Castro and J. Crispim, "Variability and correlation of renewable energy sources in the Portuguese electrical system," Energy for Sustainable Development, vol. 42, pp. 64-76, Feb. 2018

[93] A. Lee, "Today in Energy: Fewer wind curtailments and negative power prices seen in Texas after major grid expansion," U.S. Energy Information Administration, Washington, D.C, Jun. 2014.

[94] D. J. Trudnowski, A. Gentile, J. M. Khan and E. M. Petritz, "Fixed-speed wind-generator and wind-park modeling for transient stability studies," IEEE Transactions on Power Systems, vol. 19, no. 4, pp. 1911-1917, Nov. 2004.

[95] Solar Integration: Inverters and Grid Services Basics, Solar Energy Technologies Office, 2021. [online]. Available: https://www.energy.gov/eere/solar/solar-integration-inverters-and-grid-services-basics

[96] P. Denholm and R. M. Margolis, "Evaluating the limits of solar photovoltaics (PV) in electric power systems utilizing energy storage and other enabling technologies," Energy Policy, vol. 35, no. 9, pp. 4424-4433, Spet. 2007.

[97] P. Denholm et al., "Role of energy storage with renewable electricity generation" National Renewable Energy Lab.(NREL), Golden, CO (United States), Jan. 2010.

[98] H. L. Ferreira et al., "Characterisation of electrical energy storage technologies," Energy, vol. 53, pp. 288-298, May. 2013.

[99] DOE OE Global Energy Storage Database, U.S. Department of Energy Energy Storage Systems Program, Sandia National Laboratories, 2020. [online]. Available: https://www.sandia.gov/ess-ssl/global-energy-storage-database-home/

[100] N. S. Hasan, M. Y. Hassan, M. S. Majid and H. A. Rahman, "Mathematical model of Compressed Air Energy Storage in smoothing 2MW wind turbine," in Proc. 2012 IEEE International Power Engineering and Optimization Conference Melaka, Malaysia, pp. 339-343, Jun. 2012.

[101] J. B. Greenblatt et al., "Baseload wind energy: modeling the competition between gas turbines and compressed air energy storage for supplemental generation," Energy Policy, vol. 35, no. 3, pp. 1474-1492, Mar. 2007.

[102] P. Sullivan, W. Short, N. Blair, "Modeling the Benefits of Storage Technologies to Wind Power" In Proc. the Am Wind Energy Association Wind-Power. Houston, Texas, Jun. 2008.

[103] G. B. Alliance, "A Vision for a Sustainable Battery Value Chain in 2030: Unlocking the Full Potential to Power Sustainable Development and

Climate Change Mitigation," World Economic Forum, Geneva, Switzerland, Sept. 2019.

[104] F. Hafiz, P. Fajri and I. Husain, "Load regulation of a smart household with PV-storage and electric vehicle by dynamic programming successive algorithm technique,"in Proc. 2016 IEEE Power and Energy Society General Meeting (PESGM), Boston, MA, USA, pp. 1-5, Jul. 2016.

[105] A. Davydova, R. Chakirov, Y. Vagapov, T. Komenda and S. Lupin, "Coordinated in-home charging of plug-in electric vehicles from a household smart microgrid," in Proc. 2013 Africon, Pointe aux Piments, Mauritius, pp. 1-4, 2013.

[106] H. Liu and J. Jiang, "Flywheel energy storage—An upswing technology for energy sustainability," Energy and Buildings, vol. 39, no. 5, pp. 599-604, Aug. 2007.

[107] K. Ramu et al., "Design and static structural analysis of fly wheel using with differnt composite materials," Journal of Resource Management And Technology, vol. 12, no. 1, pp. 42-48, Aug. 2021.

[108] A. Rabiee, H. Khorramdel and J. Aghaei, "Retracted: A review of energy storage systems in microgrids with wind turbines," Renewable and Sustainable Energy Reviews, vol. 18, pp. 42-48, Feb. 2013.

[109] D. Masa-Bote et al., "Improving photovoltaics grid integration through short time forecasting and self-consumption," Applied Energy, vol. 125, pp. 103-113, Jul. 2014.

[110] P. Breeze, Power generation technologies, Newnes, 2019.

[111] S. Mukoyama et al., "Development of Superconducting Magnetic Bearing for 300 kW Flywheel Energy Storage System," IEEE Transactions on Applied Superconductivity, vol. 27, no. 4, pp. 1-4, Jun. 2017.

[112] M. I. Daoud, A. S. Abdel-Khalik, A. Elserougi, S. Ahmed and A. M. Massoud, "DC bus control of an advanced flywheel energy storage kinetic traction system for electrified railway industry," in Proc. IECON 2013 - 39th Annual Conference of the IEEE Industrial Electronics Society, Vienna, Austria, pp. 6596-6601, Nov. 2013.

[113] X. Luo, J. Wang, M. Dooner and J. Clarke, "Overview of current development in electrical energy storage technologies and the application potential in power system operation", Applied Energy, vol. 137, pp. 511-536, Jan. 2015.

[114] M. G. Molina and P. E. Mercado, "Power Flow Stabilization and Control of Microgrid with Wind Generation by Superconducting

Magnetic Energy Storage," IEEE Transactions on Power Electronics, vol. 26, no. 3, pp. 910-922, Mar. 2011.

[115] P. Simon and Y. Gogotsi, "Materials for electrochemical capacitors," Nat Mater, vol. 7, pp. 845–854, 2008.

[116] W. Li, G. Joos and J. Belanger, "Real-Time Simulation of a Wind Turbine Generator Coupled With a Battery Supercapacitor Energy Storage System," IEEE Transactions on Industrial Electronics, vol. 57, no. 4, pp. 1137-1145, Apr. 2010.

[117] M. E. Glavin and W. G. Hurley, "Ultracapacitor/battery hybrid for solar energy storage," in Proc. 2007 42nd International Universities Power Engineering Conference, pp. 791-795, Sept. 2007.

[118] K. Fell et al., "Assessment of plug-in electric vehicle integration with ISO/RTO systems," KEMA, Inc. and ISO/RTO Council, Mar. 2010.

[119] F. Lin, W. Zhang, H. Zhang, Y. Lin, J. Fang and Y. Zhang, "Study on Ultra-high Harmonics Transfer Characteristics of Transformers," in Proc. 2020 5th Asia Conference on Power and Electrical Engineering (ACPEE), pp. 1885-1890, Jun. 2020.

[120] R. Leou, C. Su and C. Lu, "Stochastic Analyses of Electric Vehicle Charging Impacts on Distribution Network," IEEE Transactions on Power Systems, vol. 29, no. 3, pp. 1055-1063, May 2014.

[121] 2020 Official US Government Source for Fuel Economy Information, U.S. Environmental Protection Agency, 2020. [online]. Available: https://www.fueleconomy.gov/feg/download.shtml

[122] M. Yousefi, N. Kianpoor, A. Hajizadeh and M. Soltani, "Smart Energy Management System for Residential Homes Regarding Uncertainties of Photovoltaic Array and Plug-in Electric Vehicle," in Porc. 2019 IEEE 28th International Symposium on Industrial Electronics (ISIE), Vancouver, BC, Canada, pp. 2201-2206, Jun. 2019.

[123] W. Kempton and J. Tomić, "Vehicle-to-grid power implementation: From stabilizing the grid to supporting large-scale renewable energy," Journal of Power Sources, vol. 144, no. 1, pp. 280-294, Jun. 2005.

[124] Y. Li, R. Kaewpuang, P. Wang, D. Niyato and Z. Han, "An energy efficient solution: Integrating Plug-In Hybrid Electric Vehicle in smart grid with renewable energy," in Proc. 2012 Proceedings IEEE INFOCOM Workshops, Orlando, FL, USA, pp. 73-78, Mar. 2012.

[125] Z. Cao, J. Wang, Q. Zhao, Y. Han and Y. Li, "Decarbonization scheduling strategy optimization for electricity-gas system considering

electric vehicles and refined operation model of power-to-gas," IEEE Access, vol. 9, pp. 5716-5733, Jan. 2021.

[126] Y. Tao, J. Qiu, S. Lai and J. Zhao, "Integrated Electricity and Hydrogen Energy Sharing in Coupled Energy Systems," in IEEE Transactions on Smart Grid, vol. 12, no. 2, pp. 1149-1162, March 2021

[127] A. Züttel, "Hydrogen storage methods," Naturwissenschaften, vol. 91, no. 4, pp. 157-722, Apr. 2004.

[128] J. Graetz, "New approaches to hydrogen storage," Chemical Society Reviews, vol. 38, no. 1, pp. 73-82, Oct. 2009.

[129] M. Sevilla and R. Mokaya, "Energy storage applications of activated carbons: supercapacitors and hydrogen storage," Energy & Environmental Science, vol. 7, no. 4, pp. 1250-1280, Jan. 2014.

[130] M. L. Christian and K. F. Aguey-Zinsou, "Core–shell strategy leading to high reversible hydrogen storage capacity for NaBH4," ACS nano, vol. 6, no. 9, pp. 7739-51, Spet. 2012.

[131] K. Thanapalan, F. Zhang, J. Maddy, G. Premier and A. Guwy, "Design and implementation of on-board hydrogen production and storage system for hydrogen fuel cell vehicles," in Proc. 2011 2nd International Conference on Intelligent Control and Information Processing, Harbin, China, pp. 484-488, Jul. 2011.

[132] Y. M. Yang, J. H. Kim, H. S. Seo, K. Lee and I. S. Yoon, "Development of the world's largest above-ground full containment LNG storage tank," in Proc. 23rd World Gas Conference, Amsterdam, pp. 1-14, Jun. 2006.

[133] A. Bernatík, P. Senovsky and M. Pitt M, "LNG as a potential alternative fuel–safety and security of storage facilities," Journal of loss prevention in the process industries, vol. 24, no. 1, pp. 19-24, Jan. 2011.

[134] S. Effendy, M. S. Khan, S. Farooq and I. A. Karimi, "Dynamic modelling and optimization of an LNG storage tank in a regasification terminal with semi-analytical solutions for N2-free LNG," Computers & Chemical Engineering, vol. 99, pp. 40-50, Apr. 2017.

[135] S. Liu, X. Li, Y. Huo and H. Li, "An analysis of the primary energy consumed by the re-liquefaction of boil-off gas of LNG storage tank," Energy Procedia, vol. 75, pp. 3315-3321, Aug. 2015.

[136] S. M. Hasnain, "Review on sustainable thermal energy storage technologies, Part I: heat storage materials and techniques," Energy Conversion And Management, vol. 39, no. 11, pp. 1127-1138, Aug. 1998.

[137] I. Sarbu, C. Sebarchievici, "A comprehensive review of thermal energy storage. Sustainability," Sustainability, vol. 10, no. 1, pp. 191, Jan. 2018.

[138] H. Zhang, J. Baeyens, G. Cáceres, J. Degreve and Y. Lv, "Thermal energy storage: Recent developments and practical aspects," Progress in Energy and Combustion Science, vol. 53, pp. 1-40, Mar. 2016.

[139] E. S. Barbieri, F. Melino and M. Morini M, "Influence of the thermal energy storage on the profitability of micro-CHP systems for residential building applications," Applied Energy, vol. 97, pp. 714-722, Sept. 2012.

[140] W. T. Sommer et al., "Thermal performance and heat transport in aquifer thermal energy storage," Hydrogeology Journal, vol. 22, no. 1, pp. 263-279, Feb. 2014.

[141] Y. Tian and C. Y. Zhao, "A review of solar collectors and thermal energy storage in solar thermal applications," Applied Energy, vol. 104, pp. 538-53, Apr. 2013.

[142] R. H. Milocco, J. E. Thomas and B. E. Castro, "Generic dynamic model of rechargeable batteries," Journal of Power Sources, vol. 246, pp. 609-620, Jan. 2014.

[143] A. S. Collinson and J. W. Neuberg, "Gas storage, transport and pressure changes in an evolving permeable volcanic edifice," Journal of Volcanology and Geothermal Research, vol. 243, pp. 1-3, Oct. 2012.

[144] Q. Y. Zhang, K. Duan, Y. Y. Jiao and W. Xiang, "Physical model test and numerical simulation for the stability analysis of deep gas storage cavern group located in bedded rock salt formation," International Journal of Rock Mechanics and Mining Sciences, vol. 94, pp. 43-54, Apr. 2017.

[145] Y. Dai et al., "A General Model for Thermal Energy Storage in Combined Heat and Power Dispatch Considering Heat Transfer Constraints," IEEE Transactions on Sustainable Energy, vol. 9, no. 4, pp. 1518-1528, Oct. 2018.

[146] M. Chaudry, N. Jenkins, M. Qadrdan and J Wu, "Combined gas and electricity network expansion planning," Applied Energy, vol. 113, pp. 1171-1187, Jan. 2014.

[147] Z. Bao, Q. Zhou, Z. Yang, Q. Yang, L. Xu and T. Wu, "A Multi Time-Scale and Multi Energy-Type Coordinated Microgrid Scheduling Solution—Part I: Model and Methodology," IEEE Transactions on Power Systems, vol. 30, no. 5, pp. 2257-2266, Sept. 2015.

[148] Q. Zeng, J. Fang, Z. Chen and A. J. Conejo, "A two-stage stochastic programming approach for operating multi-energy systems," in Proc.

2017 IEEE Conference on Energy Internet and Energy System Integration (EI2), Beijing, China, pp. 1-6, Nov. 2017.

[149] A. Bloess, W. Schill and A. Zerrahn, "Power-to-heat for renewable energy integration: A review of technologies, modeling approaches, and flexibility potentials," Applied Energy, vol. 212, pp. 1611-1626, Feb. 2018.

[150] P. Lund, "Large-scale urban renewable electricity schemes – Integration and interfacing aspects," Energy Conversion and Management, vol. 63, pp. 162-172, Nov. 2012.

[151] U Bünger et al., "Power-to-gas (PtG) in transport status quo and perspectives for development," German Federal Ministry of Transport and Digital Infrastructure, Tech. Rep., Germany, Jun. 2014.

[152] U. Eberle, B. Müller and R. V. Helmolt, "Fuel cell electric vehicles and hydrogen infrastructure: status 2012," Energy & Environmental Science, vol. 5, no. 10, pp. 8780-8798, Jul. 2012.

[153] J. G. Speight, Natural Gas, Elsevier Inc., 2004.

[154] Combined cycle gas plant, Energy Education, 2020. [online]. Available: https://energyeducation.ca/encyclopedia/Combined_cycle_gas_plant

[155] L. Mongibello et al., "Comparison between two different operation strategies for a heat-driven residential natural gas-fired CHP system: Heat dumping vs. load partialization," Applied Energy, vol. 184, pp. 55-67, Dec. 2016.

[156] M. Alipour, K. Zare, and M. Abapour, "MINLP Probabilistic Scheduling Model for Demand Response Programs Integrated Energy Hubs," IEEE Transactions on Industrial Informatics, vol. 14, no. 1, pp. 79–88, 2018.

[157] C. Shao, Y. Ding, J. Wang, and Y. Song, "Modeling and integration of flexible demand in heat and electricity integrated energy system," IEEE Transactions on Sustainable Energy, vol. 9, no. 1, pp. 361–370, 2018.

[158] H. A. Aalami, M. P. Moghaddam and G. R. Yousefi, "Demand response modeling considering interruptible/curtailable loads and capacity market programs," Applied Energy, vol. 87, no. 1, pp. 243-50, Jan. 2010.

[159] J. G. Roos and I. E. Lane, "Industrial power demand response analysis for one-part real-time pricing," IEEE Transactions on Power Systems, vol. 13, no. 1, pp. 159-164, Feb. 1998.

[160] M. Ghasemifard, M. Fotuhi-Firuzabad, M. Parvania and A. Abbaspour, "Incorporating Two-Part Real-Time Pricing Scheme into Distribution System Operation, in Proc. 2014 IEEE Electrical Power and Energy Conference, Calgary, AB, Canada, pp. 178-183, Nov. 2014.

[161] P. Faria and Z. Vale, "Demand response in electrical energy supply: An optimal real time pricing approach," Energy, vol. 36, no. 8, pp. 5374–5384, Aug. 2011.

[162] A. J. Conejo, J. M. Morales and L. Baringo, "Real-time demand response model," IEEE Transactions on Smart Grid, vol. 1, no. 3, pp. 236-42, Oct. 2010.

[163] P. Mancarella and G. Chicco, "Real-time demand response from energy shifting in distributed multi-generation," IEEE Transactions on Smart Grid, vol. 4, no. 4, pp. 1928-1938, Dec. 2013.

[164] Lawrence Berkeley National Laboratory, "2025 California Demand Response Potential Study - Charting California's Demand Response Future: Final Report on Phase 2 Results," Building Technology and Urban Systems Division, Berkeley, CA, Mar. 2017.

[165] X. Luo, T. Hong, Y. Chen, and M. A. Piette, "Electric load shape benchmarking for small- and medium-sized commercial buildings," Applied Energy, vol. 204, pp. 1371–1390, Oct. 2017.

[166] H. Lund, P. A. Østergaard, T. B. Nielsen, et al, "Perspectives on fourth and fifth generation district heating," Energy, vol. 227, Jul. 2021, Article 120520.

[167] The Hidden Battery, The Brattle Group, 2016. [online]. Available: https://www.electric.coop/wp-content/uploads/2016/07/The-Hidden-Battery-01-25-2016.pdf

[168] B. V. Mathiesen et al. IDA's energy vision 2050: a smart energy system strategy for 100% renewable Denmark, Aalborg University, 2015.

[169] J. Grainger and J. Stevenson William, Power System Analysis. New York: McGraw–Hill, 1994.

[170] K. Behnam-Guilani, "Fast decoupled load flow: the hybrid model," IEEE Transactions on Power Systems, vol. 3, no. 2, pp. 734-742, May 1988.

[171] M. Chaudry, N. Jenkins, and G. Strbac, "Multi-time period combined gas and electricity network optimisation," Electr. Power Syst. Res., vol. 78, no. 7, pp. 1265–1279, Jul. 2008.

[172] M. Abeysekera, J. Wu, N. Jenkins and M. Rees, "Steady state analysis of gas networks with distributed injection of alternative gas,"Applied Energy, vol. 164, pp. 991-1002, Feb. 2016.

[173] Z. Qiao, Q. Guo, H. Sun, Z. Pan, Y. Liu and Xiong W, "An interval gas flow analysis in natural gas and electricity coupled networks considering the uncertainty of wind power," Applied energy, vol. 201, pp. 343-353, Sept. 2017.

[174] C. Wang, W. Wei, J. Wang, L. Bai, Y. Liang and T. Bi, "Convex optimization based distributed optimal gas-power flow calculation," IEEE Transactions on Sustainable Energy, vol. 9, no. 3, pp. 1145-1156, Jul. 2018.

[175] A. Martinez-Mares and C. R. Fuerte-Esquivel, "A unified gas and power flow analysis in natural gas and electricity coupled networks," IEEE Transactions on Power Systems, vol. 27, no. 4, pp. 2156-2166, May 2012.

[176] A. Kabirian and M. R. Hemmati, "A strategic planning model for natural gas transmission networks," Energy Policy, vol. 35, no. 11, pp. 5656–5670, Nov. 2007.

[177] R. G. B. I. Liberalized, "Gas balancing and line-pack flexibility," European University Institute, 2012.

[178] A. Shabanpour-Haghighi and A. R. Seifi, "An integrated steady-state operation assessment of electrical, natural gas, and district heating networks," IEEE Transactions on Power Systems, vol. 31, no. 5, pp. 3636-3647, Sept. 2016.

[179] Y. Xi et al., "Integration and Coordination of Flexible Resources in Multi-energy Systems," 2020 IEEE Power & Energy Society General Meeting (PESGM), Montreal, QC, Canada, pp. 1-5. Aug. 2020.

[180] N. Srinivas and K. Deb, "Muiltiobjective optimization using nondominated sorting in genetic algorithms," Evolutionary Computation, vol. 2, no. 3, pp. 221-248, Sept. 1994.

[181] Energinet.dk, Market data portal, [Online]. Available: http://osp.energinet.dk/_layouts/Markedsdata/framework/integrations/markedsdatatemplate.aspx.

[182] Danish Energy Agency, Technology Catalogs, [Online]. Available: https://ens.dk/service/fremskrivninger-analyser-modeller/teknologikataloger

[183] V. Perić et al., "CoSES laboratory for combined energy systems at TU Munich," IEEE Power & Energy Society General Meeting (PESGM), Montreal, QC, Canada, Aug. 2020.

[184] Y. Xi, T. Hamacher, V. Perić, Z. Chen and Lund H, "Bi-Level Programming for Integrating flexible demand of a Combined Smart Energy System," in Proc. 7th IEEE International Smart Cities Conference (ISC2), Virtual, Jul. 2021.

[185] Z. Q. Luo, J. S. Pang and D. Ralph, Mathematical programs with equilibrium constraints, Cambridge University Press, 1996.

[186] Energinet.dk, Energy data service, [Online]. Available: https://www.energidataservice.dk/collections/production-and-consumption.

[187] Y Xi, J Fang, Z Chen, Q Zeng and H. Lund, "Optimal coordination of flexible resources in the gas-heat-electricity integrated energy system," Energy, vol. 223, May 2021, Article:119729.

[188] J. S. Pang and M. Fukushima, "Quasi-variational inequalities, generalized Nash equilibria, and multi-leader-follower games," Computational Management Science,vol. 2, no. 1, pp. 21-56, Jan. 2005.

[189] C. Ruiz, A. J. Conejo, J. D. Fuller, S. A. Gabriel, and B. F. Hobbs, "A tutorial review of complementarity models for decision-making in energy markets," EURO Journal on Decision Processes, vol. 2, no. 1–2, pp. 91–120, Jun. 2014.

[190] D. Pozo and J. Contreras, "Finding Multiple Nash Equilibria in Pool-Based Markets: A Stochastic EPEC Approach," IEEE Transactions on Power Systems, vol. 26, no. 3, pp. 1744-1752, Aug. 2011.

[191] J. M. Morales, A. J. Conejo, H. Madsen, P. Pinson and M. Zugno, Integrating Renewables in Electricity Markets, vol. 205. Boston, MA: Springer US, 2014.

[192] H. Qiu and F. You, "Decentralized-distributed robust electric power scheduling for multi-microgrid systems," Applied Energy, vol.269, Jul. 2020. Article: 115146.

Appendix A

Tab. I: Input parameters of the model involved in Section 3.3.

Hourly historical data						
Time (h)	G_t^{l} (MW)	P_t^{l}(MW)	H_t^{l}(MW)	P_t^{WT}(MW)	fp_t^{e}(€/MWh)	fp_t^{g}(€/MWh)
1	130	134.77	138.46	82.71	20.96	17.407
2	131	126.26	118.55	74.69	20.9	
3	137	122.28	100.64	77.37	18.13	
4	147	117.83	85.60	77.37	16.03	
5	165	117.50	69.90	79.04	16.43	
6	179	115.56	57.98	76.70	13.75	
7	183	120.57	52.23	79.04	11.1	
8	188	124.14	50.06	79.04	15.47	
9	189	130.03	45.25	83.71	16.88	
10	188	138.42	39.22	81.04	21.81	
11	185	144.39	35.75	78.04	26.24	
12	183	146.66	33.16	73.02	27.48	
13	181	145.48	29.27	68.01	28.04	
14	185	144.71	27.13	66.34	28.7	
15	190	148.56	27.53	65.67	29.66	
16	193	162.60	28.18	65.67	30.38	
17	193	178.96	29.09	68.01	30.8	
18	188	174.64	25.25	70.35	30.93	
19	168	164.76	23.98	75.03	30.78	
20	151	153.67	31.95	79.37	30.51	
21	135	145.03	38.76	78.04	30.19	
22	130	135.13	40.91	78.70	29.94	
23	127	126.07	46.06	79.71	29.65	
24	126	120.78	53.03	82.71	29.36	

Operating parameters for energy facilities								
B^{PL} (€/MW)			B^{GL}(€/MW)			B^{HL}(€/MW)		
30			25			20		
CHP	γ_i^{CHP}	η_i^{e}	$P_{i,t}^{\mathrm{CHP,min}}$	$P_{i,t}^{\mathrm{CHP,max}}$	Gas source	c_i^{SN}	$G_{j,t}^{\mathrm{SN,max}}$	
	4:5	0.9	12	60		17.407	250	
CFP	c_i^{CFP}	$P_{i,t}^{\mathrm{CFP,min}}$	$P_{i,t}^{\mathrm{CFP,max}}$	η_i^{CFP}	GB	η_i^{GB}	$H_{m,t}^{\mathrm{GB,min}}$	$H_{m,t}^{\mathrm{GB,max}}$
	25	50	250	0.5		0.9	4	20
P2G	η_i^{P2G}	$G_{j,t}^{\mathrm{P2G,min}}$	$G_{j,t}^{\mathrm{P2G,max}}$	EB	COP_m^{EB}		$H_{m,t}^{\mathrm{EB,min}}$	$H_{m,t}^{\mathrm{EB,max}}$
	0.4	0	20		0.99		0	35
GS	c_i^{GS}	$G_{j,t}^{\mathrm{GS,min}}$	$G_{j,t}^{\mathrm{GS,max}}$	HS	c_i^{HS}		$H_{m,t}^{\mathrm{HS,min}}$	$H_{m,t}^{\mathrm{HS,max}}$
	12	-5	5		10		-5	5

Tab. II: Input parameters of the model involved in Section 4.3.

Hourly historical data

Time (h)	G_t^{l} (MW)	P_t^{l}(MW)	H_t^{l}(MW)	P_t^{WT}(MW)	P_t^{PV}(MW)
1	264.40	835.70	827.10	19.41	0.00
2	263.70	824.95	740.60	8.38	0.00
3	259.60	838.80	807.09	20.90	0.00
4	259.30	864.50	873.02	46.76	0.00
5	275.30	920.05	881.72	60.76	0.00
6	398.50	1087.35	822.14	202.62	0.00
7	468.60	1269.15	829.28	256.96	0.00
8	477.30	1342.80	836.87	267.61	1.00
9	475.60	1347.00	836.57	296.53	8.00
10	458.30	1356.90	791.24	336.44	16.50
11	483.00	1341.00	697.40	252.53	27.50
12	413.60	1334.10	666.68	193.68	36.00
13	434.50	1320.55	671.75	323.82	31.50
14	446.50	1276.45	614.45	357.12	18.50
15	379.60	1261.05	600.22	369.13	8.00
16	338.30	1320.25	670.14	485.48	2.00
17	383.10	1439.80	773.79	800.21	0.00
18	417.10	1374.40	771.66	975.43	0.00
19	396.10	1272.40	806.26	980.08	0.00
20	386.20	1161.40	870.73	1185.04	0.00
21	328.00	1059.05	868.85	1446.58	0.00
22	315.90	967.80	789.38	1337.25	0.00
23	340.00	886.25	762.73	1605.06	0.00
24	227.00	827.00	678.29	1763.48	0.00

Operating parameters for energy facilities

B PL (€/MW)	B^{GL}(€/MW)	B^{HL}(€/MW)
100	80	60

CHP	γ_i^{CHP}	η_i^{e}	$P_t^{\mathrm{CHP,min}}$	$P_t^{\mathrm{CHP,max}}$		Gas source	c_i^{SN}	$G_t^{\mathrm{SN,max}}$
	4:5	0.8	160	800			67.23	1500
CFP	c_i^{CFP}	$P_t^{\mathrm{CFP,min}}$	$P_t^{\mathrm{CFP,max}}$	η_i^{CFP}	GB	η_i^{GB}	$H_t^{\mathrm{GB,min}}$	$H_t^{\mathrm{GB,max}}$
	80	350	1000	0.5		0.9	48	240
P2G	η_i^{P2G}	$G_t^{\mathrm{P2G,min}}$	$G_t^{\mathrm{P2G,max}}$	EB		COP_m^{HP}	$H_t^{\mathrm{HP,min}}$	$H_t^{\mathrm{HP,max}}$
	0.4	0	60			2	0	480
GS	c_i^{GS}	$G_t^{\mathrm{GS,min}}$	$G_t^{\mathrm{GS,max}}$	HS		c_i^{HS}	$H_t^{\mathrm{HS,min}}$	$H_t^{\mathrm{HS,max}}$
	30	-20	20			10	-20	20
EV&PV	η_i^{PV}	$P_t^{\mathrm{EV,min}}$	$P_t^{\mathrm{EV,min}}$					
	5.88	-0.3	0.3					

Tab. III: Input parameters of the model involved in Section 5.3.

Hourly historical data

Time (h)	G_t^{l} (MW)	P_t^{l}(MW)	H_t^{l}(MW)	P_t^{LWT}(MW)	P_t^{HWT}(MW)
1	104	175.20	82.72	63.35	172
2	104.8	165.54	74.70	57.32	185
3	109.6	161.12	77.37	49.74	180
4	117.6	154.60	77.37	43.2	200
5	132	152.47	79.04	31.78	209
6	143.2	149.99	76.70	23.48	215.5
7	146.4	155.87	79.04	22.19	211.8
8	150.4	160.03	79.04	21.41	206
9	151.2	167.33	83.72	19.06	200
10	150.4	177.43	81.05	16.55	187
11	148	184.80	78.04	15.34	179
12	146.4	186.81	73.03	14.87	172
13	144.8	182.89	68.02	13.31	166
14	148	181.02	66.35	11.76	164
15	152	185.03	65.68	9.55	165
16	154.4	203.53	65.68	9.67	168
17	154.4	224.22	68.02	9.68	173
18	150.4	217.61	70.36	7.2	179
19	134.4	204.92	75.03	7.58	201
20	120.8	191.31	79.38	13.37	212.5
21	108	179.89	78.04	17.64	219
22	104	168.62	78.71	20.07	225
23	101.6	157.53	79.71	22.9	230
24	100.8	151.40	82.72	25.35	225

Operating parameters for energy facilities

B PL (€/MW)	B^{GL}(€/MW)	B^{HL}(€/MW)
30	25	20

CHP	γ_i^{CHP}	η_i^{e}	$P_{i,t}^{\mathrm{CHP,min}}$	$P_{i,t}^{\mathrm{CHP,max}}$		Gas source	c_i^{SN}	$G_{j,t}^{\mathrm{SN,max}}$
	4:5	0.8	15	75			17.407	250
CFP	c_i^{CFP}	$P_{i,t}^{\mathrm{CFP,min}}$	$P_{i,t}^{\mathrm{CFP,max}}$	η_i^{CFP}	GB	η_i^{GB}	$H_{m,t}^{\mathrm{GB,min}}$	$H_{m,t}^{\mathrm{GB,max}}$
	24	50	130	0.5		0.9	9.6	48
P2G	η_i^{P2G}	$G_{j,t}^{\mathrm{P2G,min}}$	$G_{j,t}^{\mathrm{P2G,max}}$	EB		COP_m^{EB}	$H_{m,t}^{\mathrm{EB,min}}$	$H_{m,t}^{\mathrm{EB,max}}$
	0.4	0	16			0.99	0	60
GS	c_i^{GS}	$G_{j,t}^{\mathrm{GS,min}}$	$G_{j,t}^{\mathrm{GS,max}}$	HS		c_i^{HS}	$H_{m,t}^{\mathrm{HS,min}}$	$H_{m,t}^{\mathrm{HS,max}}$
	12	-5	5			10	-5	5

ISSN (online): 2446-1636
ISBN (online): 978-87-7573-995-0

AALBORG UNIVERSITY PRESS